Whitmarsh, R.B., Sawyer, D.S., Klaus, A., and Masson, D.G. (Eds.), 1996
Proceedings of the Ocean Drilling Program, Scientific Results, Vol. 149

4. OLIGOCENE-MIOCENE CALCAREOUS NANNOFOSSIL BIOSTRATIGRAPHY AND PALEOECOLOGY FROM THE IBERIA ABYSSAL PLAIN[1]

Eric de Kaenel[2] and Giuliana Villa[3]

ABSTRACT

During Ocean Drilling Program (ODP) Leg 149, five sites were drilled on the Iberia Abyssal Plain in the northeastern Atlantic Ocean. Both Mesozoic and Cenozoic sediments were recovered. Oligocene to Miocene sediments were cored at deep-water Sites 897, 898, 899, and 900. Except for a few intervals, occurrences of generally abundant and well-preserved calcareous nannofossils suggest that the deposition of the turbidite-type sediments occurred above the calcite compensation depth (CCD). One major unconformity in the middle late Miocene is present.

Detailed quantitative analyses of calcareous nannofossils are used to determine the changes occurring among the nannoflora in relation to sea-level variation. A succession of 89 biohorizons from the early Oligocene to the late Miocene are defined by combining the biostratigraphic results of the four sites studied in the Iberia Abyssal Plain.

One new genus and eight new species are described: *Camuralithus, Camuralithus pelliculatus, Ericsonia detecta, Helicosphaera limasera, Sphenolithus akropodus, Sphenolithus aubryae, Sphenolithus cometa, Reticulofenestra circus,* and *Syracosphaera lamina.* Two new variations and seven new combinations are also introduced.

INTRODUCTION

Previous works from Deep Sea Drilling Program (DSDP) and Ocean Drilling Program (ODP) sites in the North Atlantic and Indian Ocean have shown the relationship of calcareous nannofossil assemblages with sea surface productivity. By using quantitative methods, Olafsson (1989) and Fornaciari et al. (1990) underlined some sharp rise in abundance at the beginning and at the end of the nannofossil ranges. Similar sharp rises and falls in abundance have been observed within the ranges of several species. In addition to these studies on productivity, Gartner (1992) introduced several new biohorizons that are recognized in this study and complemented by the addition of new events.

The objective of this study was to investigate the possible correlations between the calcareous nannofossil events and global sea level variations described by Haq et al. (1987). The first phase of the work consisted of precisely locating the first and last occurrences, noting the distribution patterns, and characterizing the turnovers within the calcareous nannofossil assemblages at each site. The second phase consisted of using precise taxonomic concepts to define a new succession of biohorizons for the Oligocene-Miocene interval for the four sites. Bioevents are reported in summary tables. Most of the taxonomic work was done on Hole 900A. Many taxonomically ambiguous species were observed in Hole 900A. During the study of the three other holes, a better understanding of these ambiguous forms emerged and some of these taxa are considered very useful for the biostratigraphy of the Oligocene-Miocene interval.

The variability of and the different trends in the nannofossil assemblages have been studied in order to identify paleoceanographic influences. We believe that calcareous nannofossil evolution is directly related to paleoceanographic changes. These include changes in the available amount of nutrients, temperature, salinity, position of the calcite compensation depth (CCD), and in dissolved carbonate content. The occurrence and abundance of new species, genera, or families of calcareous nannofossils have been compared to the sedimentary record to determine possible correlations with the sequence stratigraphy and sea level curve defined by Haq et al. (1987).

Hole 900A was chosen as reference site for this study because from it was recovered the most complete and extended Oligocene-Miocene interval (about 391 m).

The Oligocene-Miocene sedimentary succession recovered in Hole 900A consists of a lower contourite-turbidite-pelagic sequence (Unit II, see Comas et al., this volume) and an upper turbidite-pelagic sequence (Unit I). To eliminate the uncertainties caused by the presence of reworked nannofossils, only pelagic intervals represented by nannofossil ooze or nannofossil chalk were collected. The nannofossil assemblages are, therefore, interpreted as indicative of open ocean conditions. From the early Oligocene to the late Miocene, most of the regressive/transgressive periods can be recognized by variations in the calcareous nannofossil assemblages.

METHODS

In order to obtain good-quality slides, all samples used in this study were prepared using a settling technique. Approximately 1000 samples were processed and at least one sample was examined from each section of core. Different settling techniques have been described in published literature mainly to prepare samples used for scanning electron microscope (SEM) studies (e.g., Hay 1977; Knüttel 1986; Backman 1980). The settling techniques are used to eliminate particles sized below 2 µm and above 30 µm. In this study, a special settling technique has been developed to prepare slides for the light microscope (LM).

A constant volume of 25 mm^3 of sediment was put into a graduated 15 mL test tube, which was filled with distilled water to 8 mL. The sample was shaken several times within an hour and then held still for 30 s to let the larger particles sink to the bottom. A capillary tube was used to remove the bottom solution down to 3 mL, and water was added to 15 mL. Next, the sample was shaken several times for 5 min and then held still for 90 s. A graduated capillary tube was used to place 8 mL of solution from the top of the tube on a cover slide. Up to 30 samples could be processed at regular intervals during an hour.

[1]Whitmarsh, R.B., Sawyer, D.S., Klaus, A., and Masson, D.G. (Eds.), 1996. *Proc. ODP, Sci. Results,* 149: College Station, TX (Ocean Drilling Program).

[2]Department of Geology, Florida State University, Tallahassee, FL 32306-3026, U.S.A. dekaenel@geomag.gey.fsu.edu

[3]Istituto di Geologia, Università degli Studi di Parma Viale delle Scienze 78, 43100 Parma, Italy.

The same settling technique was used to prepare a gridded circular cover slide for transferring and observing the same specimen in both LM and SEM. Eight drops on a gridded cover slide usually provided a good concentration of nannofossils for both LM and SEM. Twenty-two transferred specimens are illustrated on the 14 plates. The specimen transfer technique used herein was developed by Dr. Frank H. Wind at the Florida State University.

This settling technique, using a constant volume of sediment and solution, has two important advantages: first, it is a relatively quick method, and, second, the coccolith dispersion is uniform over the slides, which is very important for a quantitative analysis. Also, occurrences of markers or rare species are found more quickly on a settled slide than on an ordinary smear slide. This has helped in this study to improve the biostratigraphic ranges of many species while at the same time improving the resolution of the Oligocene-Miocene zonation.

Abundances of individual species in each sample were counted for each sample using a Zeiss Photomicroscope III under ×1250 magnification and by using cross-polarized and phase-contrast light. With computer assistance using BugWare (BugWare, Inc.), between 300 and 500 specimens were counted on each slide and their frequency converted to the number of specimens per mm^2. Every specimen of the nannofossil assemblage was counted at the species level. Next, two long traverses of the slide were observed for rare taxa excluded from the initial counts; these were added to the counts with a value of one. Backman and Shackleton (1983) detailed different methods to obtain quantitative abundance. They also indicated that similar information is obtained by counting specimens per mm^2 or by counting the number of microfossils per gram of sediment. Following their comments we chose to use a constant volume of sediment instead of sediment weight and to express the abundance relative to the area observed. This approach has the advantage of speed and easy application by other biostratigraphers.

For each site, a table with the absolute number of specimens per mm^2 was generated. These large numeric tables (numeric range charts are not presented in this paper) were transferred into CricketGraph to draw the abundance curves (Figs. 3, 5, 8, 10-17).

The range-charts presented herein in Tables 3, 5, 7, 9 were obtained directly from the numeric tables with the absolute numbers of specimens per mm^2 translated in seven levels of single species abundance according to the following definitions:

P (present) = 1 to 4 specimens/ mm^2;
R (rare) = 5 to 10 specimens/ mm^2;
F (few) = 11 to 50 specimens/ mm^2;
C (common) = 51 to 150 specimens/ mm^2;
A (abundant) = 151 to 1000 specimens/ mm^2;
V (very abundant) = 1001 to 5000 specimens/ mm^2;
O (ooze) = 5001 to 25000 specimens/ mm^2.

The same definitions are used for estimations of total abundance of each sample, with the additional definition of B (barren of nannofossils).

In addition to the abundance of individual species, special attention was focused on the occurrence of reworked Mesozoic and Paleogene (mostly Eocene) species. Except for the early Oligocene Zone NP21, the presence of reworked material did not interfere with the biostratigraphic results. Both groups of reworked specimens were counted separately and presented in the first two columns of the range charts. The absolute number of specimens per mm^2 of Mesozoic species is presented for Hole 900A and correlated with the sequence chronostratigraphy.

Different estimations of calcareous nannofossil preservation have been used and discussed in previous studies. The following estimation are based on the comments of Roth and Thierstein (1972). The qualitative evaluation of calcareous nannofossils preservation was denoted as follows:

P (poor) = severe dissolution, fragmentation and/or overgrowth has occurred; most primary features have been destroyed and many specimens cannot be identified at the species level;
M (moderate) = Dissolution and/or overgrowth are evident; a significant proportion (up to 25%) of the specimens cannot be identified to species level with absolute certainty;
X (mixed) = Dissolution and/or overgrowth are evident among certain taxa, but nearly all specimens (up to 95%) can be identified with certainty;
G (good) = Little dissolution and/or overgrowth is observed; diagnostic characteristics are preserved and all specimens can be identified;
E (excellent) = No dissolution is seen; all specimens can be identified.

RESULTS

Summary of Sites

The Oligocene to Miocene calcareous nannofossil assemblages recovered during Leg 149 are presented in detail on the range charts (Tables 3, 5, 7, 9). A short discussion for each hole gives a synthesis of the age and major problems encountered, followed by a description of Martini's standard zonation (1971) and a description of the succession of biohorizons considered important for biostratigraphic interpretations and paleoenvironmental correlations. Martini's index fossils are used to describe the age and zone assignments of the Oligocene/Miocene interval except two zonal markers: the last occurrence (LO) of *Helicosphaera recta* used to define the Zone NP25/NN1 boundary (LO observed in Zone NN2) and the first occurrence (FO) of *Catinaster coalitus* (not recorded in this study).

Site 897

This site is located on the eastern edge of the Iberia Abyssal Plain (Fig. 1, Table 1). The nannofossil zonal marker events and the important biohorizons are given in Figure 2; the sample intervals and average depths of these events are listed in Table 2 and the stratigraphic distribution of calcareous nannofossil are indicated in Table 3. Nannofossils are rare to very abundant and moderately well-preserved throughout the Oligocene-Miocene sequence. Two intervals barren of calcareous nannofossils were observed: a short one in the lower Miocene Zone NN2, and a longer interval (425-443 m), intercalated with samples yielding poorly preserved nannofossils. We place the Zone NP25/NN1 boundary at the LO of *Sphenolithus ciperoensis* (Fig. 3), which was observed in Sample 149-897C-37R-5, 27-28 cm; in the same sample the LO of *Reticulofenestra bisecta* was detected. The barren samples did not allow a better resolution of Zone NP25. Nevertheless, we placed the Zone NP25/NP24 boundary at Sample 149-897C-42R-1, 41-42 cm, based on the LO of *Sphenolithus predistentus,* just below the barren interval, although the LO of *Sphenolithus distentus* was observed one sample below, in Sample 149-897C-42R-3, 61-62 cm. This assignment was inferred assuming that *S. predistentus,* as described for Site 900, is considered a good alternative marker for the top of Zone NP24, as it was never found in Zone NP25. The FO of *S. ciperoensis,* detected in Sample 149-897C-45R-5, 4-5 cm, marks the base of Zone NP 24. The Zone NP23/NP22 boundary was identified in Sample 149-897C-49R-1, 128-129 cm with the LO of *Reticulofenestra umbilicus* and the LO of *Isthmolithus recurvus.* The LO of *Ericsonia formosa* detected in the same sample is considered unreliable and is ascribed to reworking. Yet the presence of a short Zone NP21 is arguable: the Zone NP21/NP22 boundary could be inferred to be at the drop in abundance of *E. formosa,*

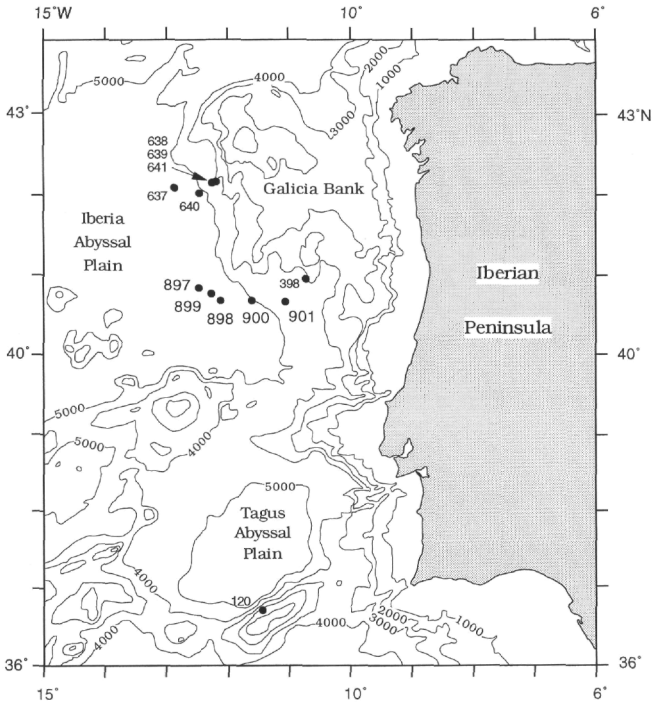

Figure 1. Location map of the Iberia Abyssal Plain showing Leg 149 Sites 897 to 901. Site 398 (DSDP Leg 47) and Sites 637 to 641 (ODP Leg 103) are shown for reference.

between Sample 149-897C-49R-3, 123-124 cm and Sample 149-897C-49R-5, 16-17 cm (Fig. 3). The FO *of Sphenolithus akropodus* in Sample 149-897C-49R-3, 123-124 cm could confirm this hypothesis (see "Site 900").

Site 898

Site 898 is located on the eastern edge of the Iberia Abyssal Plain (Fig. 1, Table 1). The purpose of drilling this site was to elucidate the nature of the basement at the ocean/continent transition. About 870 m of sediment overlie the basement that has been defined by seismic interpretation. Hole 898A recovered the upper 340 m of sediment, consisting of turbidite and contourite sequences. The nannofossil zonal marker events and the important biohorizons are given in Figure 4. The sample intervals and average depths of these events are listed in Table 4. The stratigraphic distribution of calcareous nannofossil are indicated in Table 5.

The Oligocene-Miocene interval extends from Samples 149-898A-18X-4, 105-106 cm, to 36X-CC and ranges from the middle Miocene Zone NN7 to the late Oligocene Zone NP25. Medium to well-preserved, common to very abundant nannofossils are found in most of the samples. Only the hemipelagic or pelagic intervals were sampled in order to have better material and avoid as much as possible reworking problems. Nevertheless, in the pelagic intervals, consistent, rare reworked Cretaceous species were found, as well as rare, reworked Cenozoic species. The stratigraphic distribution of the main *Helicosphaera* and *Sphenolithus* species across the Oligocene/Miocene boundary is given in Figure 5.

The upper Miocene Zones NN8 to NN12 are not present and a major unconformity is placed between Samples 149-898A-18X-4, 58-59 cm (Pliocene), and Samples 149-898A-18X-4, 134 cm. Samples 149-898A-18X-4, 105-106 cm and 149-898A-18X-4, 142 cm are red clay layers barren of nannofossils, which may be related to a temporary drop of the CCD. The presence *of Discoaster kugleri* and the absence of *Cyclicargolithus abisectus* (>10 µm) in Sample 149-898A-

Table 1. Locations of ODP Leg 149 Sites with Oligocene-Miocene sediments.

Hole	Latitude (°N)	Longitude (°W)	Water depth (m)
897C	40°50.32′	12°28.44′	5320
898A	41°41.10′	12°07.37′	5279
899A	40°46.33′	12°12.15′	5291
899B	40°46.34′	12°16.06′	5291
900A	46°40.99′	11°36.25′	5048

18X-4, 134 cm indicate middle Miocene age in the upper part of Zone NN7. The Miocene interval extends down to Sample 149-898A-28X-2, 49-50 cm based on the LO of *S. ciperoensis* in Sample 149-898A-28X-3, 145-146 cm (Fig. 5). The Oligocene interval extends down to Sample 149-898A-36X-CC. The presence *of S. ciperoensis* and the absence of *S. distentus* indicate that the Oligocene interval recovered is represented only by Zone NP25. On the presence *of Helicosphaera obliqua* in Sample 149-898A-36R-1, 108-109 cm, we assume an age not younger than lower part of Zone NP25 for the base of Hole 898A. Zones NN2 and NP25 appear to be very thick. In the Martini's zonal scheme, Zone NN2 represents 4.0 Ma based on the *Discoaster druggii* FO at the top of chronozone C6C (23.3 Ma) Gartner (1992). It is one of the longest Cenozoic nannofossil zones, and sixteen biohorizons are recognized in Zone NN2 in Hole 898A (see discussion of biohorizons).

Site 899

This site is located on the eastern edge of the Iberia Abyssal Plain (Fig. 1, Table 1). The nannofossil zonal marker events and the important biohorizons are given in Figure 6; the sample intervals and average depths of these events are listed in Table 6; and the stratigraphic distribution of calcareous nannofossil are indicated in Table 7. Two holes were drilled. Miocene sediments were recovered from Hole 899A to the lower Miocene Zone NN2, where drilling was stopped by an abrupt lithological change. Lower Miocene to lower Oligocene sediments were recovered from Hole 899B.

The Zone NN1/NP25 boundary was detected in Sample 149-899B-4R-CC, at the same level the LO of *R. bisecta* was observed; within Zone NP25 the drop in abundance of *S. ciperoensis,* indicated as *S. ciperoensis* last common occurrence (LCO) (Table 6), occurs in Sample 149-899B-6R-1, 68-69 cm. The LO of *S. distentus* marks the base of Zone NP25 in Sample 149-899B-10R-2, 147-148 cm, revealing an expanded thickness for the latter biozone.

The base of Zone NP24 is placed at Sample 149-899B-11R-3, 90-91 cm, but common *S. ciperoensis* occur only from Sample 149-899B-10R-2, 147-148 cm, up hole. Since the FCO of *S. ciperoensis* coincides with the base of Zone NP25, the result is a reduced thickness for Zone NP24 at Site 899 compared to the other sites studied. Therefore, we assume the presence of a hiatus involving the upper part of Zone NP24. The LO *of R. umbilicus* was observed in Sample 149-899B-14R-2, 15-16 cm, together with the *I. recurvus* LO. Therefore the Zone NP23/NP22 boundary was positioned at 347.28 m.

Site 900

This site is located on the eastern edge of the Iberia Abyssal Plain (Fig. 1, Table 1). The nannofossil zonal marker events and the important biohorizons are given in Figure 7; the sample intervals and average depths of these events are listed in Table 8. The Oligocene-Miocene nannofossil assemblages are abundant, well-preserved, and highly diverse, having numerous species of *Discoaster, Helicosphaera, Sphenolithus,* and holococcoliths. A detailed range chart

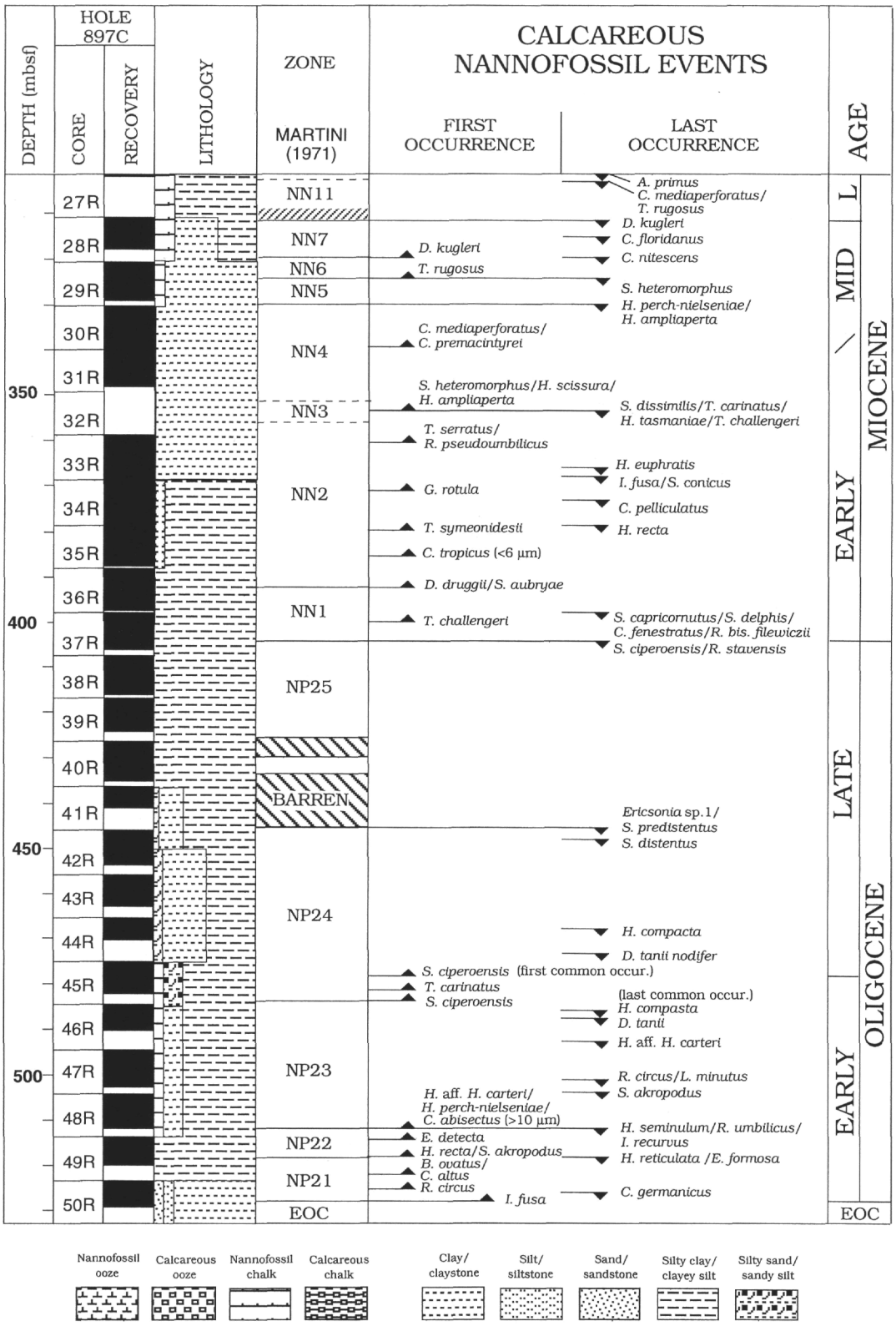

Figure 2. Calcareous nannofossil biostratigraphic summary of the Oligocene-Miocene interval of Hole 897C. Indicated are the sub-bottom depths (mbsf), core recovery, lithology, zonal units of Martini (1971), zonal and important bioevents organized by first and last occurrences, and age. The graphic lithology has been compiled by the Leg 149 Shipboard Scientific Party (1994). Graphic symbols depict intervals exceeding 20 cm in thickness. For comparison, similar symbols are used in the *Initial Reports* volume (Sawyer, Whitmarsh, Klaus, et al., 1994).

Table 2. Summary of the key nannofossil biohorizons in Hole 897C.

Calcareous Nannofossil Event	Interval (cm)	Depth (mbsf)
Hole 897C		
A. primus LO	27R-1, 1/27R-1, 5	301.23
C. mediaperforatus LO	27R-1, 5/27R-CC	302.10
T. rugosus LO	27R-1, 5/27R-CC	302.10
Unconformity (TB 3.1)		
D. kugleri LO	28R-1, 26/28R-2, 120	312.38
C. floridanus LCO	28R-2, 120/28R-4, 138	315.19
D. kugleri FO	28R-CC/29R-1, 126	319.78
C. nitescens LO	29R-1, 126/28R-CC	319.78
T. rugosus FO	29R-1, 126/29R-4, 26	323.51
S. heteromorphus LO	29R-1, 126/29R-4, 26	323.51
H. perch-nielseniae LO	29R-CC/30R-1, 48	329.91
H. ampliaperta LO	29R-CC/30R-1, 48	329.91
C. mediaperforatus FO	30R-6, 118/31R-1, 22	339.50
C. premacintyrei FO	30R-6, 118/31R-1, 22	339.50
S. dissimilis LO	31R-6, 102/33R-1, 12	353.82
S. heteromorphus FO	31R-6, 102/33R-1, 12	353.82
H. scissura FO	31R-6, 102/33R-1, 12	353.82
H. mediterranea LO	31R-6, 102/33R-1, 12	353.82
T. carinatus LO	31R-6, 102/33R-1, 12	353.82
H. tasmaniae LO	31R-6, 102/33R-1, 12	353.82
H. ampliaperta FO	31R-6, 102/33R-1, 12	353.82
T. challengerei LO	31R-6, 102/33R-1, 12	353.82
R. pseudoumbilicus FO	33R-1, 12/33R-1, 98	359.65
T. serratus FO	33R-1, 12/33R-1, 98	359.65
H. euphratis LO	33R-5, 145/33R-6, 132	367.23
C. leptoporus FO	33R-6, 132/33R-5, 145	367.23
S. conicus LO	33R-7, 45/34R-1, 96	369.15
I. fusa LO	33R-7, 45/34R-1, 96	369.15
G. rotula FO	34R-1, 96/34R-3, 10	370.73
O. aureus LO	34R-3, 10/34R-4, 31	372.55
C. pelliculatus LO	34R-3, 10/34R-4, 31	372.55
H. recta LO	34R-7, 46/34R-8, 17	378.19
T. symeonidesii FO	34R-8, 17/35R-1, 106	378.89
C. tropicus (<6 µm) FO	35R-3, 44/35R-4, 46	382.60
D. druggii FO	36R-3, 92/36R-4, 109	392.85
S. aubryae FO	36R-3, 92/36R-4, 109	392.85
S. capricornutus LO	36R-7, 42/37R-1, 43	397.87
S. delphix LO	36R-7, 42/37R-1, 43	397.87
C. fenestratus LO	36R-7, 42/37R-1, 43	397.87
R. bisecta filewiczii LO	36R-7, 42/37R-1, 43	397.87
T. challengerei FO	37R-1, 43/37R-2, 91	399.22
S. ciperoensis LO	37R-4, 10/37R-5, 27	403.23
R. bisecta bisecta LO	37R-4, 10/37R-5, 27	403.23
Ericsonia sp. 1 LO	41CC/42R-1, 41	446.00
S. predistentus LO	41CC/42R-1, 41	446.00
S. distentus LO	42R-1, 41/42R-3, 61	448.01
H. compacta LO	44R-2, 59/44R-4, 14	468.67
D. tanii nodifer LO	44R-4, 14/45R-2, 89	473.66
S. ciperoensis FCO	45R-2, 88/45R-4, 109	478.98
T. carinatus FO	45R-4, 109/46R-1, 117	483.18
S. ciperoensis FO	45R-5, 4/46R-1, 117	483.76
H. compacta LCO	46R-1, 117/46R-3, 89	487.13
D. tanii LO	46R-2, 41/46R-4, 12	487.81
H. aff. *H. carteri* LO	46R-4, 1/47R-2, 85	492.83
R. circus LO	47R-4, 68/47R-6, 6	500.57
L. minutus LO	47R-4, 68/47R-6, 6	500.57
S. akropodus LO	47R-6, 6/48R-3, 60	504.63
H. seminulum LO	48R-3, 60/49R-1, 128	511.19
H. aff. *H. carteri* FO	48R-3, 60/49R-1, 128	511.19
R. umbilicus LO	48R-3, 60/49R-1, 128	511.19
I. recurvus LO	48R-3, 60/49R-1, 128	511.19
H. perch-nielseniae FO	48R-3, 60/49R-1, 128	511.19
C. abisectus (>10 µm) FO	48R-3, 60/49R-1, 128	511.19
E. detecta FO	49R-1, 128/49R-3, 123	516.35
E. formosa LO	49R-3, 123/49R-5, 16	518.80
H. reticulata LO	49R-3, 123/49R-5, 16	518.80
H. recta FO	49R-3, 123/49R-5, 16	518.80
S. akropodus FO	49R-3, 123/49R-5, 16	518.80
C. altus FO	49R-5, 16/50R-1, 85	521.91
R. circus FO	50R-1, 85/50R-2, 124	524.99
C. germanicus LO	50R-2, 124/50R-3, 71	526.43
I. fusa FO	50R-3, 71/50R-4, 26	527.20

Note: Indicated is the average depth between two samples; LO = last occurrence, FO = first occurrence; LCO = last common occurrence; FCO = first common occurrence.

(Table 9, back pocket, this volume), including more than 220 species, is presented. The LO of *Cryptococcolithus mediaperforatus* is used to define the uppermost Miocene zone (lower part of Zone NN12) in Sample 149-900A-11R-CC. Part of the lower upper Miocene, Zones NN9 and NN10, is missing. The interval around 120 m includes some numerous thin silt layers and an interval barren of calcareous nannofossils between 113.65 and 112.70 mbsf. The Oligocene/Miocene boundary (top of Zone NP25) is placed at the LO of *S. ciperoensis* in Sample 149-900A-35R-1, 125-126 cm. Recently Fornaciari et al. (1993) proposed a redefinition of the Zone NP25/NN1 boundary using the LO of *S. ciperoensis,* because the original definition using the LO of *H. recta* has not proven reliable in many areas (e.g., Fornaciari et al. 1990; see discussion below in biohorizon description). Just below, at Sample 149-900A-35R-2, 121-122 cm, the LO of *R. bisecta* was observed. The LCO of *S. ciperoensis* is easily recognizable in Sample 149-900A-37R-5, 53-54 cm. Its sporadic occurrence above this level is not believed to be due to reworking, since the same distribution pattern has been found at Sites 898 and 899.

The LO of *S. distentus* was observed in Sample 149-900A-45R-4, 112-113 cm. *S. predistentus* LO was observed 1 m below, in Sample 149-900A-45R-5, 82-83 cm, and was used to approximate the Zone NP24/NP25 boundary. The FO of *S. ciperoensis,* detected in Sample 149-900A-49R-3, 113-114 cm, marks the base of Zone NP 24. In its lower range, *S. ciperoensis* is rare, but becomes more abundant upward within Zone NP24 (Fig. 8). This zone is characterized, in terms of sphenoliths, by peaks in abundance of *S. distentus.* The interval between Sample 149-900A-49R-3, 113-114 cm, and Sample 149-900A-51R-2, 124-125 cm was assigned to Zone NP23. In the latter Sample, *R. umbilicus* LO was recognized. The LO of *I. recurvus* is 1 m below, in Sample 149-900A- 51R-3, 50-51 cm. This form is widely recognized as a useful marker in approximating the top of Zone NP22. *S. distentus* is present below the LO *of R. umbilicus,* thus demonstrating that the first occurrence of this taxon is not a reliable marker for the CP17/CP18 boundary (middle of Zone NP23), as already suggested by many authors (e.g., Backman, 1987; Fornaciari et al. 1990; Olafsson and Villa, 1992). In Zone NP23 high abundances of *S. predistentus* were found in association with *S. akropodus. E. formosa* underwent a marked decrease in abundance, which we use to tentatively place the Zone NP21/NP22 boundary at the horizon in Sample 149-900A-52R-4, 143-144 cm. The persistence of this taxon above *R. umbilicus* LO is due to reworking. The lower Oligocene interval at Site 900 is marked by the presence of more reworked species. On the basis of the FO of *Ilselithina fusa* in Sample 149-900A-52R-3, 65-66 cm (483.99 mbsf), known to occur in the early Oligocene, and the juxtaposition of the FO of *S. akropodus* (481.50 mbsf) to the LO of *E. formosa* (481.50 mbsf), we infer the presence of a short Zone NP21 in the interval between these two bioevents; nevertheless it is uncertain if the presence of *E. formosa* could be ascribed to reworking. In fact in this interval few *Discoaster saipanensis* and *Discoaster barbadiensis* are found reworked. Below the *Ilselithina fusa* FO, the succession is assigned to latest part of the Eocene. This determination is based on the common occurrence of *D. barbadiensis* and *D. saipanensis* and the absence of *Reticulofenstra reticulata.* The Eocene/Oligocene boundary interval is incomplete in this section, as evidenced by the reduced thickness of Zone NP21.

The stratigraphic correlations among Leg 149 sites are presented in Figure 9. Epoch boundaries are drawn from site to site with a major biostratigraphic marker.

BIOSTRATIGRAPHY: APPLICATION OF THE MARTINI (1971) ZONATION AND ADDITIONAL BIOEVENTS

Two Miocene calcareous nannofossil zonations, Martini (1971) and Okada and Bukry (1980), have been widely adopted for biostratigraphic studies in the North Atlantic. The Okada-Bukry zonal scheme is based on the initial work of Bukry (1971). Using several low-latitude DSDP sites from the Pacific Ocean, Bukry presented a Cenozoic scheme including 10 Miocene zones subdivided into 15 subzones. Bukry (1973, 1975) presented a low-latitude zonal scheme for the Venezuela Basin in the Caribbean Sea that has been applied to most equatorial and subtropical DSDP and ODP sites in the North Atlantic Ocean (e.g., Gartner, 1992: Site 608, 42°N; Olafsson, 1989: Site 667, 4°N; Muza et al., 1987: Site 603, 36°N; Parker et al., 1985: Sites 558, 37°N, 563, 33°N).

It is interesting to note that Jiang and Gartner (1984) used the Martini zonal scheme (for Sites 525-529, 28°S), but introduced some modifications to the original zonal scheme of the early Miocene that follow the zonation of Bukry (1973, 1975).

Table 3. Stratigraphic distribution of calcareous nannofossil taxa in Hole 897C (Cores 149-897C-33R through 50R).

Age	Zone	Core, section, interval (cm)	Depth (mbsf)	Abundance	Preservation	Reworked Cretaceous	Reworking	*Bicolumnus ovatus*	*Blackites spinosus*	*Blackites tenuis*	*Braarudosphaera bigelowii*	*Branletteius serraculoides*	*Calcidiscus fuscus*	*Calcidiscus leptoporus*	*Calcidiscus pataecus*	*Calcidiscus radiatus*	*Calcidiscus tropicus* (< 6 µm)	*Calcidiscus tropicus* (> 6 µm)	*Camuralithus pelliculatus*	*Chiasmolithus altus*	*Chiasmolithus oamaruensis*	*Chiasmolithus* spp.	*Clausicoccus fenestratus*	*Clausicoccus obrutus*	*Clausicoccus subdisticha*	*Coccolithus miopelagicus*	*Coccolithus pelagicus*	*Coccolithus* sp. 1	*Coccolithus streckeri*	*Coronalithus germanicus*
early Miocene	NN2	33R-1,12-13	359.22	O	M	C	.	.	.	.	.	.	.	.	C	C	.	.	C	.	.	.	.	.	.	A	O	.	C	.
		33R-1,98-99	360.08	B	.	.	.	.	.	.	.	.	.	.	.	.	.	.	.	.	.	.	.	.	.	.	.	.	.	.
		33R-3,129-130	363.39	B	.	.	.	.	.	.	.	.	.	.	.	.	.	.	.	.	.	.	.	.	.	.	.	.	.	.
		33R-4,91-92	364.51	B	.	.	.	.	.	.	.	.	.	.	.	.	.	.	.	.	.	.	.	.	.	.	.	.	.	.
		33R-5,145-146	366.55	V	P	F	.	.	.	.	.	.	.	.	F	F	.	.	.	.	.	.	.	.	.	A	A	.	.	.
		33R-6,132-133	367.92	O	M	F	.	.	.	.	.	.	.	.	.	.	F	F	.	.	.	.	.	.	.	C	V	.	F	.
		33R-7,45-46	368.55	A	P	.	.	.	.	.	.	.	.	.	.	.	.	.	.	.	.	.	.	.	.	P	F	.	.	.
		34R-1,96-97	369.76	O	X	A	.	.	.	.	.	.	.	.	A	.	C	C	.	.	.	.	.	.	.	A	V	C	.	.
		34R-3,10-11	371.70	O	X	C	.	.	.	.	.	.	.	.	A	.	C	.	.	.	.	.	.	.	.	C	V	.	C	.
		34R-4,31-32	373.41	O	X	C	.	.	.	.	.	.	.	.	C	.	A	C	C	.	.	.	.	.	.	C	A	.	C	.
		34R-7,46-47	378.06	O	M	.	.	.	.	.	.	.	.	.	C	.	F	.	.	.	.	.	.	.	.	F	A	.	.	.
		34R-8,17-18	378.33	O	X	F	.	.	.	.	.	.	.	.	F	.	C	F	F	.	.	.	.	.	.	F	A	.	.	.
		35R-1,106-107	379.46	V	M	F	.	.	.	.	.	.	.	.	F	.	.	.	.	.	.	.	.	.	.	F	A	.	.	.
		35R-2,71-72	380.61	O	X	F	.	.	.	.	.	.	.	.	C	.	F	F	F	.	.	.	.	F	.	F	A	.	.	.
		35R-3,44-45	381.84	O	X	F	.	.	.	.	.	.	.	.	F	.	F	F	F	.	.	.	.	.	.	F	A	.	.	.
		35R-4,46-47	383.36	O	G	A	.	.	.	.	.	.	.	.	A	.	A	.	A	.	.	.	.	.	.	A	V	.	.	.
		35R-5,83-84	385.23	O	G	C	.	.	.	.	.	.	.	.	C	C	.	.	C	.	.	.	.	.	.	C	V	.	.	.
		35R-6,1-2	385.91	O	G	C	.	.	.	.	.	.	.	.	C	C	C	.	C	.	.	.	.	.	.	F	C	.	.	.
		35R-6,138-139	387.28	O	G	C	.	.	.	.	C	.	.	.	C	C	C	.	C	.	.	.	.	C	.	C	A	.	.	.
		36R-1,106-107	389.16	O	X	C	.	.	.	.	.	.	.	.	C	C	C	.	C	.	.	.	.	.	.	C	A	C	.	.
		36R-3,92-93	392.02	O	G	A	.	.	.	.	.	.	.	.	A	.	.	.	A	.	.	.	.	.	.	C	A	.	.	.
	NN1	36R-4,109-110	393.69	V	M	R	.	.	.	.	.	.	.	.	R	.	.	.	.	.	.	.	.	.	.	F	A	.	.	.
		36R-6,13-14	395.73	B	.	.	.	.	.	.	.	.	.	.	.	.	.	.	.	.	.	.	.	.	.	.	.	.	.	.
		36R-7,42-43	397.52	B	.	.	.	.	.	.	.	.	.	.	.	.	.	.	.	.	.	.	.	.	.	.	.	.	.	.
		37R-1,43-44	398.23	O	X	F	.	.	.	.	.	.	F	.	.	.	.	.	.	.	.	.	F	F	.	F	A	.	.	.
		37R-2,91-92	400.21	V	M	F	.	.	.	.	.	.	.	.	.	.	.	.	.	.	.	.	P	.	.	F	A	.	.	.
		37R-3,31-32	401.11	O	X	F	.	.	.	.	.	.	.	.	.	.	.	.	.	F	.	.	F	.	.	C	A	F	.	.
		37R-4,10-11	402.40	O	X	C	.	.	.	.	.	.	.	.	.	C	.	.	C	.	.	.	C	C	.	C	A	.	.	.
late Oligocene	NP25	37R-5,27-28	404.07	O	X	F	.	.	.	.	.	.	.	.	.	F	.	.	F	.	.	F	F	A	.	C	A	.	.	.
		37R-6,34-35	405.14	O	G	A	.	.	.	.	A	.	.	.	A	A	.	.	A	.	.	.	V	V	.	A	O	.	.	.
		38R-1,35-36	407.75	V	P	C	.	.	.	.	R	.	.	.	.	.	.	.	.	.	.	.	F	.	.	.	A	.	.	.
		38R-4,121-122	413.11	V	P	.	.	.	.	.	.	.	.	.	.	.	.	.	.	.	.	.	.	.	.	.	A	.	.	.
		39R-1,59-60	417.69	V	P	.	.	.	.	.	.	.	.	.	.	.	.	.	.	.	.	.	.	.	.	.	C	.	.	.
		39R-3,129-130	421.39	V	M	R	F	.	.	.	R	.	.	.	.	.	.	.	.	.	.	.	R	.	.	.	A	.	.	.
		39R-5,33-34	423.43	V	M	.	R	R	.	.	.	.	.	.	.	.	.	.	.	.	.	.	F	F	.	.	A	.	.	.
		40R-1,24-25	426.94	B	.	.	.	.	.	.	.	.	.	.	.	.	.	.	.	.	.	.	.	.	.	.	.	.	.	.
		40R-1,88-89	427.58	B	.	.	.	.	.	.	.	.	.	.	.	.	.	.	.	.	.	.	.	.	.	.	.	.	.	.
		40R-2,41-42	428.61	B	.	.	.	.	.	.	.	.	.	.	.	.	.	.	.	.	.	.	.	.	.	.	.	.	.	.
		40R-2,128-129	429.48	B	.	.	.	.	.	.	.	.	.	.	.	.	.	.	.	.	.	.	.	.	.	.	.	.	.	.
		40R-3,59-60	430.29	V	M	.	R	.	.	.	.	.	.	.	.	.	.	.	.	.	.	.	R	.	.	.	A	.	.	.
		40R-4,22-23	431.42	A	P	.	.	.	.	.	.	.	.	.	.	.	.	.	.	.	.	.	.	.	.	.	F	.	.	.
		40R-4,128-129	432.48	V	P	.	.	P	.	.	.	.	.	.	.	.	.	.	.	.	.	.	P	.	.	.	C	.	.	.
		40R-5,132-133	434.02	B	.	.	.	.	.	.	.	.	.	.	.	.	.	.	.	.	.	.	.	.	.	.	.	.	.	.
		40R-5,47-48	433.17	B	.	.	.	.	.	.	.	.	.	.	.	.	.	.	.	.	.	.	.	.	.	.	.	.	.	.
		40R-7,12-13	435.33	B	.	.	.	.	.	.	.	.	.	.	.	.	.	.	.	.	.	.	.	.	.	.	.	.	.	.
		41R-1,36-37	436.76	B	.	.	.	.	.	.	.	.	.	.	.	.	.	.	.	.	.	.	.	.	.	.	.	.	.	.
		41R-1,99-100	437.39	B	.	.	.	.	.	.	.	.	.	.	.	.	.	.	.	.	.	.	.	.	.	.	.	.	.	.
		41R-2,103-104	438.93	B	.	.	.	.	.	.	.	.	.	.	.	.	.	.	.	.	.	.	.	.	.	.	.	.	.	.
		41R-3,34-35	439.74	B	.	.	.	.	.	.	.	.	.	.	.	.	.	.	.	.	.	.	.	.	.	.	.	.	.	.
		41R-4,15-16	440.55	B	.	.	.	.	.	.	.	.	.	.	.	.	.	.	.	.	.	.	.	.	.	.	.	.	.	.
	NP24	42R-1,41-42	446.41	V	M	.	.	R	.	.	R	.	.	.	.	.	.	.	.	.	.	.	R	.	.	F	A	.	.	.
		42R-3,61-62	449.61	V	P	.	.	.	.	.	.	.	.	.	.	.	.	.	.	R	.	.	R	.	.	.	A	.	.	.
		42R-4,106-107	451.58	V	P	P	P	.	.	.	.	.	.	.	.	.	.	.	.	.	.	.	.	P	.	.	A	.	.	.
		42R-5,109-110	453.11	V	M	.	.	R	.	.	.	.	.	.	.	.	.	.	.	.	.	.	R	.	.	F	A	.	.	.
		43R-1,89-90	456.49	O	P	.	.	.	.	.	.	.	.	.	.	.	.	.	.	.	.	.	R	F	.	R	A	.	.	.
		43R-2,100-101	458.10	V	P	.	R	.	.	.	F	.	.	.	.	.	.	.	.	R	.	.	R	.	.	F	A	.	.	.
		43R-3,123-124	459.83	V	M	.	.	.	.	.	.	.	.	.	.	.	.	.	.	F	.	.	F	.	.	.	A	.	.	.
		43R-4,80-81	460.90	V	M	R	.	R	.	.	.	R	.	.	.	.	.	.	.	.	.	.	R	.	.	R	A	.	.	.
		43R-5,84-85	462.44	V	M	R	R	R	.	.	F	.	.	.	.	.	.	.	.	.	.	.	R	R	.	F	A	.	.	.
		44R-2,59-60	467.39	V	M	.	.	R	.	.	.	.	.	.	.	.	.	.	.	F	.	.	F	F	.	.	A	.	.	.
		44R-4,14-15	469.95	V	M	P	P	R	.	.	.	.	.	.	.	.	.	.	.	.	.	.	P	.	.	F	C	.	.	.
		45R-2,88-89	477.38	V	M	R	.	R	.	.	.	.	.	.	.	.	.	.	.	F	.	.	F	R	.	R	A	.	.	.
		45R-4,109-110	480.59	V	M	P	R	.	.	.	P	.	.	.	.	.	.	.	.	.	.	.	P	.	.	.	C	.	.	.
early Oligocene	NP23	46R-1,117-118	485.77	V	P	.	.	.	.	.	.	.	.	.	.	.	.	.	.	.	.	.	F	.	.	C	A	.	.	.
		46R-2,8-9	486.18	O	P	.	.	.	.	.	.	.	.	.	.	.	.	.	.	.	.	.	C	.	.	F	A	.	.	.
		46R-2,41-42	486.51	O	M	F	A	F	.	.	F	.	.	.	.	.	.	.	.	F	.	.	F	F	.	F	V	.	.	.
		46R-4,1-2	489.11	V	M	R	R	R	.	.	R	.	.	.	.	.	.	.	.	.	.	.	F	F	.	F	A	.	.	.
		47R-2,1-2	496.55	O	M	R	.	F	.	.	R	.	.	.	.	.	.	.	.	R	.	.	C	F	.	.	A	.	.	.
		47R-4,68-69	499.38	O	M	F	F	F	F	.	.	.	.	.	.	.	.	.	.	.	.	.	F	F	.	F	A	.	.	.
		47R-6,6-7	501.76	O	M	.	.	F	.	.	F	.	.	.	.	.	.	.	.	F	.	.	F	.	.	.	A	.	.	.
		48R-3,60-61	507.50	O	M	.	.	.	.	F	.	.	.	.	.	.	.	.	.	F	.	F	.	.	F	.	V	.	.	.
	NP 22	49R-1,128-129	514.88	O	M	F	.	.	C	.	F	.	.	.	.	.	.	.	.	.	.	.	A	.	.	F	V	.	.	.
		49R-3,123-124	517.83	V	M	C	R	.	.	.	.	.	.	.	.	.	.	.	.	F	.	.	A	.	.	R	A	.	.	.
		49R-5,16-17	519.78	V	M	R	.	F	F	.	R	.	.	.	.	.	.	.	.	R	.	R	F	F	.	F	A	.	.	.
		50R-1,85-86	524.05	V	M	.	.	.	.	.	.	R	.	.	.	.	.	.	.	.	.	.	.	F	.	F	A	.	.	.
		50R-2,124-125	525.94	A	P	.	.	.	.	.	.	.	.	.	.	.	.	.	.	.	R	.	.	.	.	.	A	.	.	.
		50R-3,71-72	526.92	V	M	R	.	.	P	.	P	R	.	.	.	.	.	.	.	.	.	.	.	.	R	R	A	.	.	R

Table 3 (continued).

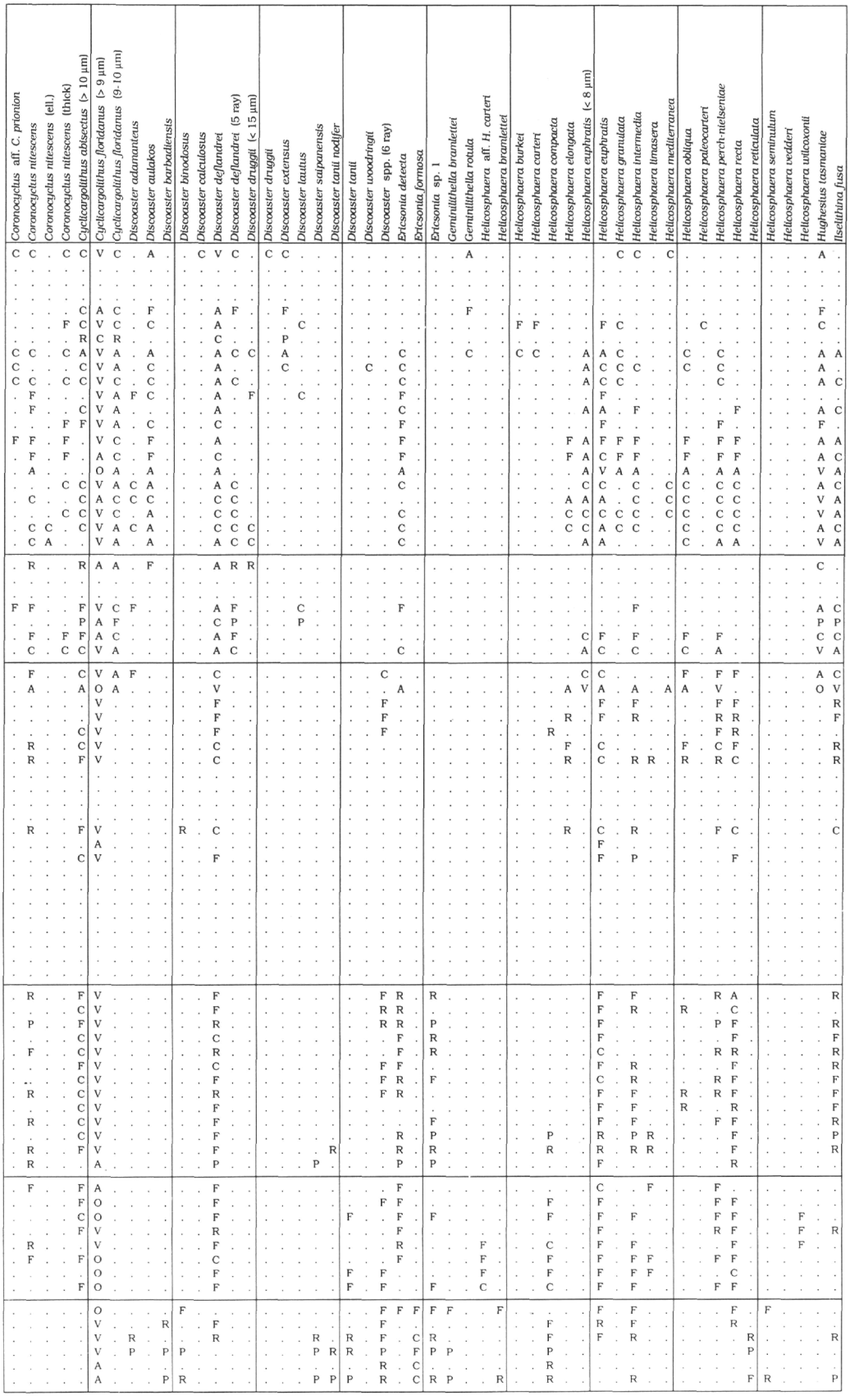

Table 3 (continued).

Age	Zone	Core, section, interval (cm)	Depth (mbsf)	Abundance	Preservation	*Isthmolithus recurvus*	*Lanternithus minutus*	*Lithostromation simplex*	*Micrantholithus aequalis*	*Orthozygus aureus*	*Pedinocyclus larvalis*	*Pemma papillata*	*Pontosphaera antisotrema*	*Pontosphaera callosa*	*Pontosphaera enormis*	*Pontosphaera logiforaminis*	*Pontosphaera multipora*	*Pontosphaera* spp.	*Pyrocyclus hermosus*	*Pyrocyclus inversus*	*Pyrocyclus orangensis*	*Reticulofenestra bisecta bisecta*	*Reticulofenestra bisecta fileuticzii*	*Reticulofenestra circus*	*Reticulofenestra daviesi*	*Reticulofenestra hampdenensis*	*Reticulofenestra haqii*	*Reticulofenestra* cf. *R. haqii*	*Reticulofenestra hesslandii*	*Reticulofenestra hillae*
early Miocene	NN2	33R-1,12-13	359.22	O	M	.	.	.	.	.	.	.	.	.	.	.	C	.	C	.	.	.	.	.	.	.	A	.	.	.
		33R-1,98-99	360.08	B		.	.	.	.	.	.	.	.	.	.	.	.	.	.	.	.	.	.	.	.	.	.	.	.	.
		33R-3,129-130	363.39	B		.	.	.	.	.	.	.	.	.	.	.	.	.	.	.	.	.	.	.	.	.	.	.	.	.
		33R-4,91-92	364.51	B		.	.	.	.	.	.	.	.	.	.	.	.	.	.	.	.	.	.	.	.	.	.	.	.	.
		33R-5,145-146	366.55	V	P	.	.	.	.	.	.	.	.	.	.	.	F	.	.	.	.	.	.	.	.	.	C	.	.	.
		33R-6,132-133	367.92	O	M	.	.	.	.	.	.	.	.	.	.	.	F	.	F	.	C	.	.	.	.	.	A	.	.	.
		33R-7,45-46	368.55	A	P	.	.	.	.	.	.	.	.	.	.	.	.	.	.	.	.	.	.	.	.	.	F	.	.	.
		34R-1,96-97	369.76	O	X	.	.	.	.	.	.	.	.	.	.	.	A	.	C	.	C	.	.	.	.	.	V	.	.	.
		34R-3,10-11	371.70	O	X	.	.	.	.	.	.	.	.	.	.	.	C	.	C	.	C	.	.	.	.	.	V	.	.	.
		34R-4,31-32	373.41	O	X	.	.	.	.	C	.	.	C	.	.	.	A	.	.	.	C	.	.	.	.	.	V	.	.	.
		34R-7,46-47	378.06	O	M	.	.	.	.	.	.	.	.	.	.	.	C	.	.	.	F	.	.	.	.	.	V	.	.	.
		34R-8,17-18	378.33	O	X	.	.	.	.	.	.	.	.	.	.	.	C	.	.	.	.	.	.	.	.	.	A	.	.	.
		35R-1,106-107	379.46	V	M	.	.	.	.	.	.	.	.	.	.	.	F	.	F	.	F	.	.	.	.	.	V	.	.	.
		35R-2,71-72	380.61	O	X	.	.	.	.	.	.	.	.	F	.	.	A	.	.	.	F	.	F	.	.	.	V	.	.	.
		35R-3,44-45	381.84	O	X	.	.	.	.	.	.	.	.	F	.	.	C	.	.	.	F	.	.	.	.	.	A	.	.	.
		35R-4,46-47	383.36	O	G	.	.	.	.	.	.	.	.	.	.	.	V	.	A	.	A	.	.	.	.	.	O	.	.	.
		35R-5,83-84	385.23	O	G	.	.	.	.	.	.	.	.	.	.	.	C	.	C	.	C	.	.	.	.	.	O	.	.	.
		35R-6,1-2	385.91	O	G	.	.	.	.	.	.	.	.	.	.	.	A	.	.	.	C	.	.	.	.	.	V	.	.	.
		35R-6,138-139	387.28	O	G	.	.	.	.	.	.	.	.	.	.	.	A	.	.	.	C	.	.	.	.	.	V	.	.	.
		36R-1,106-107	389.16	O	X	.	.	.	.	.	.	.	.	.	.	.	C	.	.	.	C	C	.	.	.	.	O	.	C	.
		36R-3,92-93	392.02	O	G	.	.	.	.	.	.	.	.	.	.	.	A	.	.	.	.	.	C	.	.	.	O	.	.	.
	NN1	36R-4,109-110	393.69	V	M	.	.	.	.	.	.	.	.	.	.	.	.	.	.	.	R	.	.	.	.	.	V	.	.	.
		36R-6,13-14	395.73	B		.	.	.	.	.	.	.	.	.	.	.	.	.	.	.	.	.	.	.	.	.	.	.	.	.
		36R-7,42-43	397.52	B		.	.	.	.	.	.	.	.	.	.	.	.	.	.	.	.	.	.	.	.	.	.	.	.	.
		37R-1,43-44	398.23	O	X	.	.	.	.	.	.	.	.	.	.	.	F	.	.	.	F	.	F	.	.	.	V	.	C	.
		37R-2,91-92	400.21	V	M	.	.	.	.	.	.	.	.	.	.	.	.	.	.	.	.	.	R	.	.	.	A	.	.	.
		37R-3,31-32	401.11	O	X	.	.	.	.	.	.	.	.	.	.	.	.	.	.	F	.	.	C	.	.	.	V	.	.	.
		37R-4,10-11	402.40	O	X	.	.	.	.	C	.	.	.	.	.	.	C	.	.	.	C	.	C	.	.	.	V	.	.	.
late Oligocene	NP25	37R-5,27-28	404.07	O	X	.	.	.	.	C	.	.	.	.	F	.	C	.	.	.	F	F	F	.	F	.	V	.	C	.
		37R-6,34-35	405.14	O	G	.	.	.	.	A	.	.	.	.	A	A	A	.	.	A	A	A	A	.	A	.	O	.	V	.
		38R-1,35-36	407.75	V	P	.	.	.	.	R	.	.	.	.	.	.	.	F	.	.	.	.	F	.	R	.	.	.	.	.
		38R-4,121-122	413.11	V	P	.	.	.	.	R	.	.	.	.	.	.	.	F	.	.	R	.	.	.	R	.	.	.	.	.
		39R-1,59-60	417.69	V	P	.	.	.	.	.	.	R	.	.	.	.	.	.	.	.	.	.	.	.	C	.	.	.	.	.
		39R-3,129-130	421.39	V	M	.	.	.	.	R	.	.	.	.	.	.	.	C	.	.	.	.	F	.	F	.	.	.	.	.
		39R-5,33-34	423.43	V	M	.	.	.	.	.	.	.	.	.	.	.	.	C	.	.	.	.	F	.	F	.	.	.	.	.
		40R-1,24-25	426.94	B		.	.	.	.	.	.	.	.	.	.	.	.	.	.	.	.	.	.	.	.	.	.	.	.	.
		40R-1,88-89	427.58	B		.	.	.	.	.	.	.	.	.	.	.	.	.	.	.	.	.	.	.	.	.	.	.	.	.
		40R-2,41-42	428.61	B		.	.	.	.	.	.	.	.	.	.	.	.	.	.	.	.	.	.	.	.	.	.	.	.	.
		40R-2,128-129	429.48	B		.	.	.	.	.	.	.	.	.	.	.	.	.	.	.	.	.	.	.	.	.	.	.	.	.
		40R-3,59-60	430.29	V	M	.	.	.	.	R	.	.	.	.	.	.	.	C	.	.	F	.	.	.	R	R	.	.	.	.
		40R-4,22-23	431.42	A	P	.	.	.	.	.	.	.	.	.	.	.	.	.	.	.	.	.	.	.	.	.	.	.	.	.
		40R-4,128-129	432.48	V	P	.	.	.	.	.	.	.	.	.	.	.	.	R	.	.	.	.	R	.	F	.	.	.	.	.
		40R-5,132-133	434.02	B		.	.	.	.	.	.	.	.	.	.	.	.	.	.	.	.	.	.	.	.	.	.	.	.	.
		40R-5,47-48	433.17	B		.	.	.	.	.	.	.	.	.	.	.	.	.	.	.	.	.	.	.	.	.	.	.	.	.
		40R-7,12-13	435.33	B		.	.	.	.	.	.	.	.	.	.	.	.	.	.	.	.	.	.	.	.	.	.	.	.	.
		41R-1,36-37	436.76	B		.	.	.	.	.	.	.	.	.	.	.	.	.	.	.	.	.	.	.	.	.	.	.	.	.
		41R-1,99-100	437.39	B		.	.	.	.	.	.	.	.	.	.	.	.	.	.	.	.	.	.	.	.	.	.	.	.	.
		41R-2,103-104	438.93	B		.	.	.	.	.	.	.	.	.	.	.	.	.	.	.	.	.	.	.	.	.	.	.	.	.
		41R-3,34-35	439.74	B		.	.	.	.	.	.	.	.	.	.	.	.	.	.	.	.	.	.	.	.	.	.	.	.	.
		41R-4,15-16	440.55	B		.	.	.	.	.	.	.	.	.	.	.	.	.	.	.	.	.	.	.	.	.	.	.	.	.
	NP24	42R-1,41-42	446.41	V	P	.	.	.	.	.	.	.	.	.	.	.	.	C	.	.	.	.	R	.	F	.	.	.	.	.
		42R-3,61-62	449.61	V	P	.	.	.	.	.	.	.	.	.	.	.	.	F	.	.	R	.	F	.	F	.	.	.	.	.
		42R-4,106-107	451.58	V	M	.	.	.	.	.	.	.	.	.	.	.	.	F	.	.	P	.	F	.	F	.	.	.	.	.
		42R-5,109-110	453.11	V	M	.	.	.	.	.	.	.	.	.	.	.	.	F	.	.	R	.	.	.	F	.	.	.	.	.
		43R-1,89-90	456.49	O	M	.	.	.	.	.	.	.	.	.	.	.	.	F	.	.	.	.	.	.	F	.	.	F	.	.
		43R-2,100-101	458.10	V	M	.	.	.	.	R	.	.	.	.	.	.	.	F	.	.	R	.	F	.	F	.	.	.	.	.
		43R-3,123-124	459.83	V	M	.	.	.	.	.	.	.	.	.	.	.	.	F	.	.	R	.	.	.	F	.	.	.	.	.
		43R-4,80-81	460.90	V	M	.	.	.	.	.	.	.	.	.	.	.	.	F	.	.	R	.	F	.	F	.	.	.	.	.
		43R-5,84-85	462.44	V	M	.	.	.	R	.	.	.	.	.	.	.	.	F	.	.	R	.	F	.	F	.	.	.	.	.
		44R-2,59-60	467.39	V	M	.	.	.	.	.	.	.	.	.	.	.	.	F	.	.	.	.	.	.	.	.	.	.	.	.
		44R-4,14-15	469.95	V	M	.	.	.	.	P	.	.	.	.	.	.	.	R	.	.	P	.	.	.	P	.	.	.	.	.
		45R-2,88-89	477.38	V	M	.	.	.	.	.	.	.	.	.	.	.	.	.	.	.	R	R	.	.	R	F	.	R	.	.
		45R-4,109-110	480.59	V	M	.	.	.	.	P	.	.	.	.	.	.	.	F	.	.	.	.	.	.	F	.	.	.	.	.
early Oligocene	NP23	46R-1,117-118	485.77	V	P	.	.	.	.	.	.	.	.	.	.	.	.	.	.	.	.	.	.	.	C	F	.	F	.	.
		46R-2,8-9	486.18	O	P	.	.	.	.	.	F	.	.	.	.	.	.	F	.	.	.	F	C	.	F	F	.	.	.	.
		46R-2,41-42	486.51	O	M	.	.	.	.	.	.	.	.	.	.	.	.	.	.	.	.	F	.	.	F	.	.	.	.	.
		46R-4,1-2	489.11	V	M	.	.	.	R	.	.	.	.	.	.	.	.	F	.	.	R	F	.	.	F	.	.	R	.	.
		47R-2,1-2	496.55	O	M	.	.	.	.	F	.	.	.	.	.	.	.	R	.	.	.	R	R	.	F	F	.	.	.	.
		47R-4,68-69	499.38	O	M	.	.	.	.	F	.	.	.	.	.	.	.	.	.	.	.	F	.	.	C	.	.	.	.	.
		47R-6,6-7	501.76	O	M	.	F	.	F	.	.	.	.	.	.	.	.	F	.	.	F	.	.	F	F	F	.	.	.	.
		48R-3,60-61	507.50	O	M	.	F	.	.	F	.	.	.	.	.	.	.	F	.	.	.	F	.	F	F	F	.	.	.	.
	NP 22	49R-1,128-129	514.88	O	M	F	C	.	.	.	F	.	.	.	.	.	.	F	.	.	.	.	.	.	.	.	.	.	.	.
		49R-3,123-124	517.83	V	M	.	C	.	R	.	R	.	.	.	.	.	.	.	.	.	.	C	.	.	.	.	.	.	.	.
		49R-5,16-17	519.78	V	M	F	F	.	R	.	.	.	.	.	.	.	.	R	.	.	.	C	.	.	.	.	.	.	.	.
		50R-1,85-86	524.05	V	M	.	F	.	.	P	P	.	.	.	.	.	.	P	.	.	.	F	.	R	.	R	.	.	.	.
		50R-2,124-125	525.94	A	P	.	F	.	.	.	.	.	.	.	.	.	.	R	.	.	.	F	.	.	.	.	.	.	.	.
		50R-3,71-72	526.92	V	M	F	C	R	.	.	P	P	.	.	.	.	.	P	.	.	.	R	.	.	.	R	.	P	.	P

Table 3 (continued).

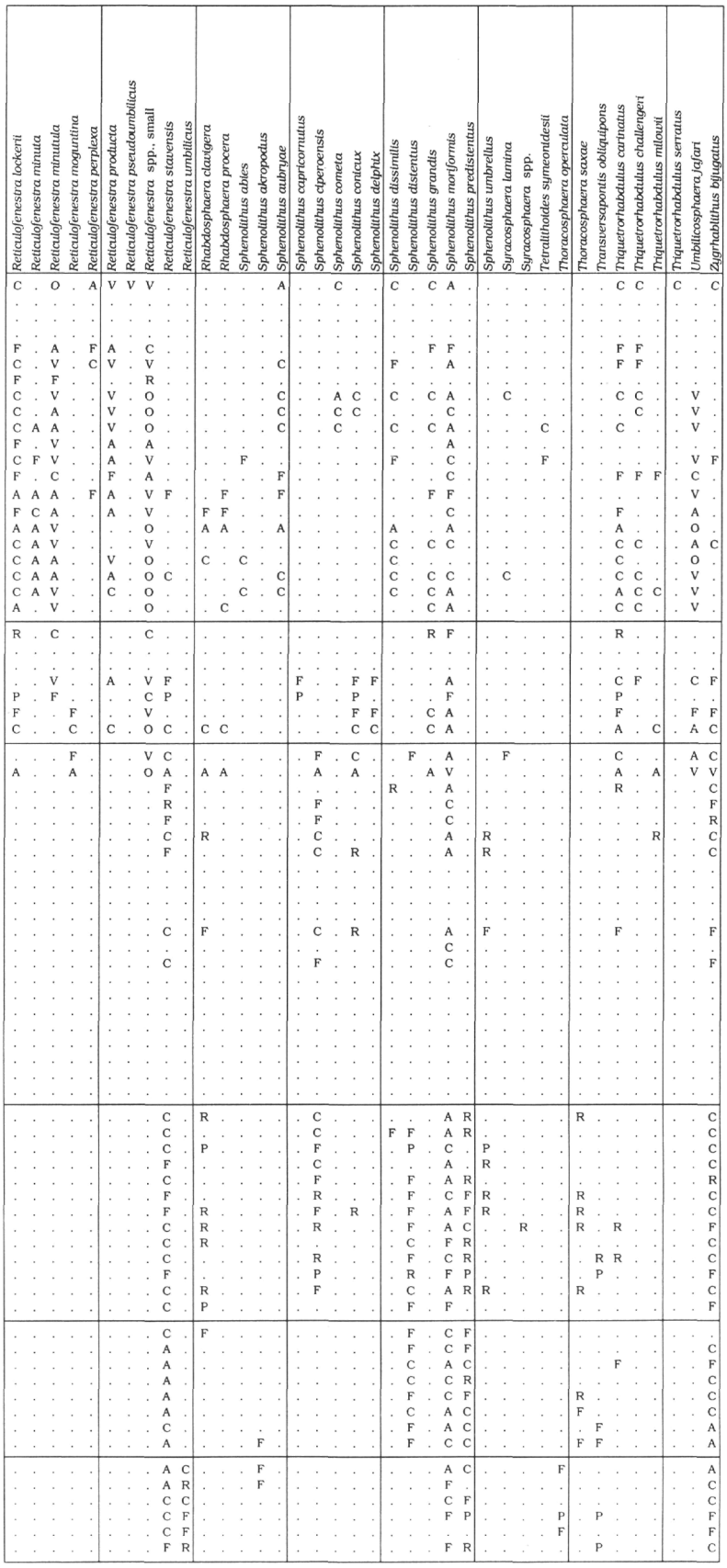

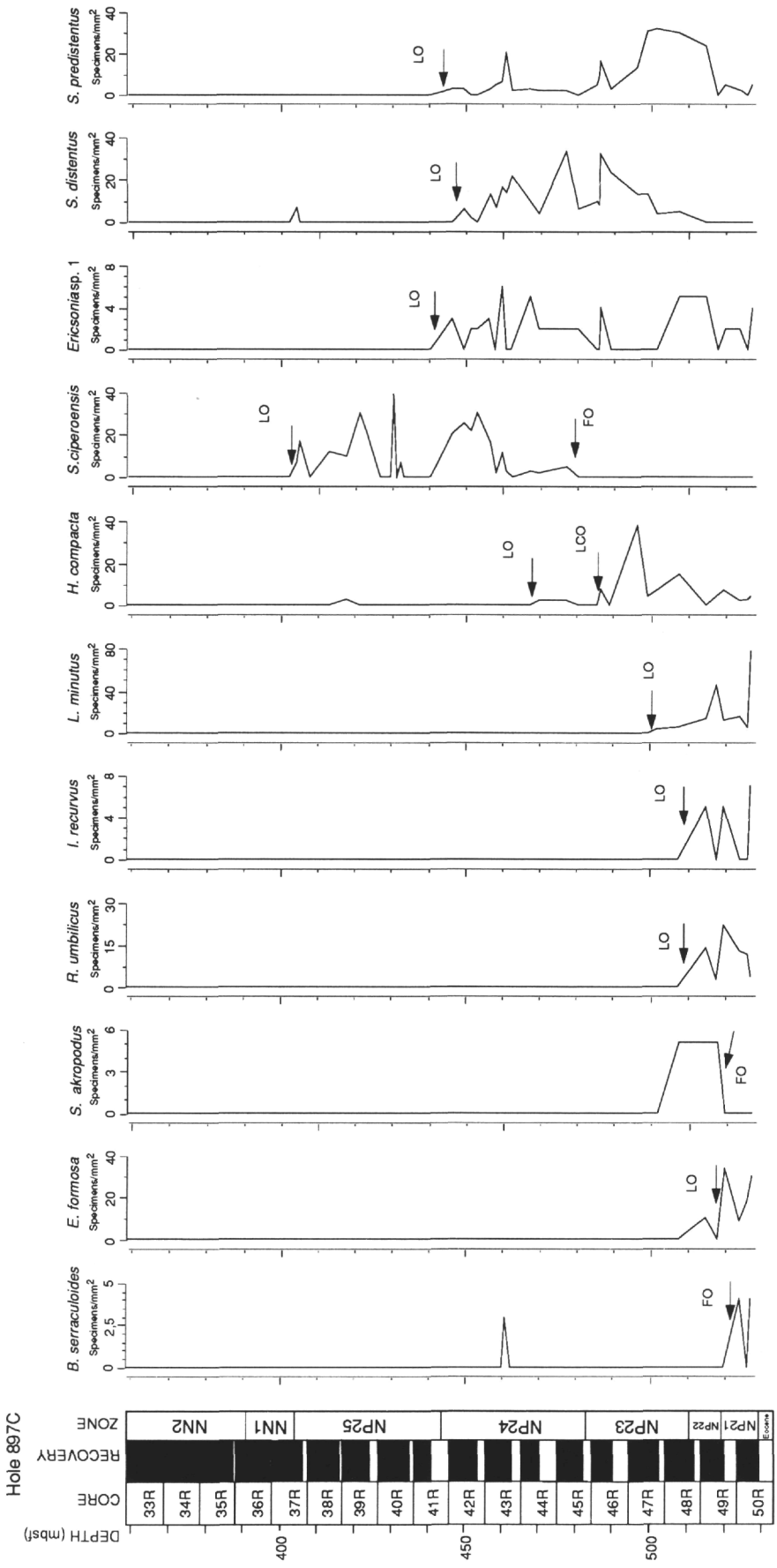

Figure 3. Abundance plot of the main Oligocene taxa in Hole 897C.

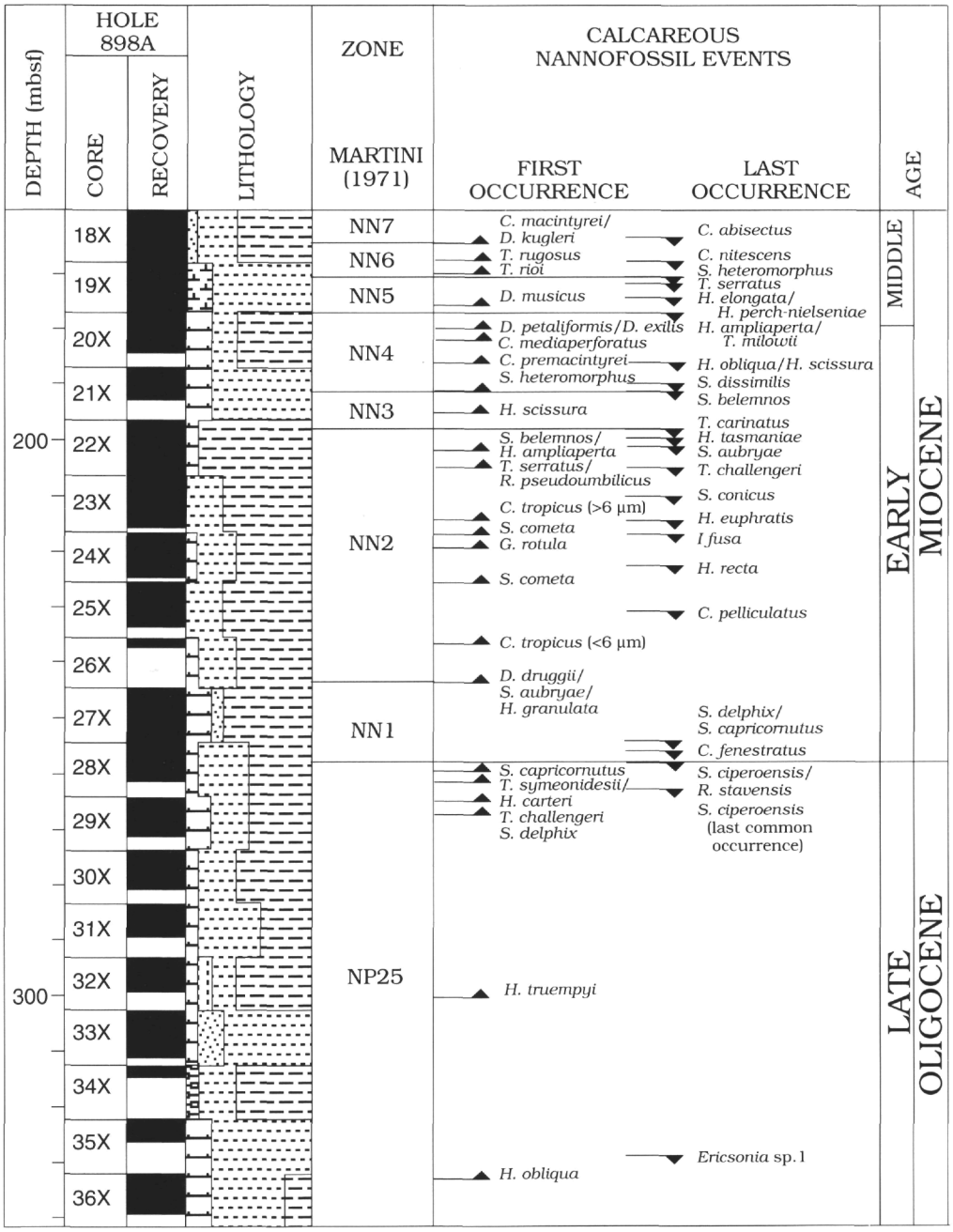

Figure 4. Calcareous nannofossil biostratigraphic summary of the Oligocene-Miocene interval of Hole 898A. See Figure 2 for symbol explanations.

Most DSDP-ODP biostratigraphic studies from low- to mid-latitude sites (0° to 40°N) have been well dated by using the zonation of Okada and Bukry (1980) or a slightly modified version of the Martini zonation (1971). The general trend for mid-latitude studies is to integrate both zonal schemes. High-latitude studies are usually based on the Martini (1971) zonal units.

Sites from Leg 149 can be zoned using both zonal schemes with some exceptions or modifications, primarily for the lower part of the Miocene. The zonation of Martini (1971) has been selected as the standard for this study. The zonation of Okada and Bukry (1980) is less applicable for both Oligocene (CP17/18) and Miocene (CN 1/2; CN3/4). For the Miocene/Pliocene boundary, the FO of *Ceratolithus* (zonal marker of CN10a/10b) was applied according to Okada and Bukry's zonal scheme.

Oligocene/Miocene Boundary

The Oligocene/Miocene boundary is placed between the Chattian Stage (late Oligocene) and the Aquitanian Stage (early Miocene). The definition of this boundary using calcareous nannofossils has been long discussed (see IUGS working group on the Paleogene/Neogene boundary, Steininger, 1994). Several calcareous nannofossils from the Chattian-type locality (Doberg, Germany) described by Martini and Muller (1975) are not observed in the Aquitanian sediments (Saint Jean d'Etampes, France). *Pontosphaera enormis* is present in the last sample from the Chattian-type section, but has not been reported in the Aquitanian sediment. *P. enormis* may be useful in determining the Chattian/Aquitanian boundary using calcareous nannofossils. In this study, the LO of this species is correlated with

Table 4. Summary of the key nannofossil biohorizons in Hole 898A.

Calcareous Nannofossil Event	Interval (cm)	Depth (mbsf)
Hole 898A		
C. abisectus (>10 µm) LO	18X-4, 142/18X-5, 53	164.30
C. macintyrei (>11 µm) FO	18X-5, 53/18X-5, 75	164.76
D. kugleri FO	18X-5, 53/18X-5, 75	164.76
T. rioi LO	18X-6, 103/18X-7, 42	167.09
C. premacintyrei LO	18X-7, 42/19X-1, 33	167.83
T. rugosus FO	19X-1, 33/19X-1, 106	168.36
C. nitescens LO	19X-1, 33/19X-1, 106	168.36
T. rioi FO	19X-1, 106/19X-2, 24	169.20
D. braarudii FO	19X-2, 24/19X-2, 116	170.00
S. heteromorphus LO	19X-2, 116/19X-3, 27	170.76
T. serratus LO	19X-3, 27/19X-3, 138	171.62
H. elongata LO	19X-5, 72/19X-6, 80	175.31
H. perch-nielseniae LO	19X-5, 72/19X-6, 80	175.31
D. musicus FO	19X-6, 80/19X-6, 112	176.16
T. milowii LO	19X-7, 1/20X-1, 72	177.46
H. ampliaperta LO	19X-7, 1/20X-1, 72	177.46
D. moorei FO	20X-1, 72/20X-2, 25	178.63
D. petaliformis FO	20X-2, 25/20X-3, 43	180.00
D. exilis FO	20X-2, 25/20X-3, 43	180.00
D. calculosus LO	20X-3, 43/20X-4, 9	181.41
C. mediaperforatus FO	20X-4, 9/20X-5, 9	182.74
C. premacintyrei FO	20X-5, 9/21X-1, 66	185.57
H. scissura LO	20X-5, 9/21X-1, 66	185.57
H. obliqua LO	20X-5, 9/21X-1, 66	185.57
S. dissimilis LO	21X-2, 5/21X-3, 96	189.97
S. heteromorphus FO	21X-4, 64/21X-CC	192.54
S. belemnos LO	21X-4, 64/21X-CC	192.54
H. scissura FO	21X-CC/22X-1, 37	195.01
H. mediterranea LO	22X-1, 37/22X-2, 73	198.00
T. carinatus LO	22X-1, 37/22X-2, 73	198.00
H. tasmaniae LO	22X-2, 73/22X-3, 100	199.81
S. aubryae LO	22X-3, 100/22X-4, 35	201.12
S. belemnos FO	22X-4, 35/22X-4, 89	201.77
H. ampliaperta FO	22X-4, 35/22X-4, 89	201.77
T. serratus FO	22X-5, 86/23X-1, 80	205.38
R. pseudoumbilicus FO	22X-5, 86/23X-1, 80	205.38
T. challengeri LO	22X-5, 86/23X-1, 80	205.38
S. conicus LO	23X-2, 45/23X-4, 51	209.88
H. euphratis LO	23X-4, 51/23X-5, 70	212.26
C. tropicus (>6.0 µm) FO	23X-4, 51/23X-5, 70	212.26
Z. bijugatus LO	24X-1, 11/24X-2, 28	217.16
S. cometa LO	24X-1, 11/24X-2, 28	217.16
I. fusa LO	24X-1, 11/24X-2, 28	217.16
G. rotula FO	24X-2, 28/24X-3, 65	219.11
H. recta LO	24X-3, 65/24X-4, 121	221.08
O. aureus LO	24X-4, 121/24X-5, 24	222.38
S. cometa FO	24X-5, 24/25X-1, 105	224.66
C. pelliculatus LO	25X-3, 35/26X-1, 102	232.60
C. tropicus (<6.0 µm) FO	26X-1, 102/26X-2, 62	236.77
D. druggii FO	26X-2, 62/27X-1, 132	241.72
S. aubryae FO	26X-2, 62/27X-1, 132	241.72
H. granulata FO	26X-2, 62/27X-1, 132	241.72
S. capricornutus LO	27X-7, 18/28X-1, 99	254.76
S. delphix LO	27X-7, 18/28X-1, 99	254.76
S. conicus LO	27X-7, 18/28X-1, 99	254.76
C. fenestratus LO	28X-1, 99/28X-2, 49	255.99
R. bisecta filewiczii LCO	28X-2, 49/28X-3, 145	257.73
S. ciperoensis LO	28X-2, 49/28X-3, 145	257.73
R. stavensis LCO	28X-2, 49/28X-3, 145	257.73
S. capricornutus FO	28X-3, 145/28X-4, 114	259.56
T. symeonidesii FO	28X-4, 114/28X-5, 28	260.48
H. carteri FO	28X-4, 114/28X-5, 28	260.48
S. ciperoensis LCO	29X-1, 52/29X-1, 103	264.97
T. challengeri FO	29X-1, 103/29X-2, 26	266.05
S. delphix FO	29X-2, 117/29X-3, 46	267.37
H. truempyi FO	32X-3, 34/32X-4, 44	297.34
Ericsonia sp. 1 LO	35X-2, 108/36X-1, 108	329.38
H. obliqua FO	36X-1, 108/36X-2, 17	333.27

Note: See Table 2 for explanation.

the LOs of *S. ciperoensis* and *R. bisecta bisecta* at the top of Zone NP25. According to Steininger (1994), the FO of *Sphenolithus capricornutus* is the event closest to the boundary and is placed at the top of chronozone C6Cn2r. In Site 898 *S. capricornutus* is observed in one sample together with *S. ciperoensis* and *P. enormis.* The Oligocene/Miocene boundary is defined in Sites 897, 898, 899, and 900 by the LO of *S. ciperoensis* and secondarily by the LO of *P. enormis,* and therefore the FO of *S. capricornutus* is placed in the uppermost Oligocene.

Biohorizons

A succession of bioevents is observed from the upper part of Zone NP21 to the uppermost Miocene Zone NN12. One major hiatus in the lower part of the upper Miocene interrupts the sedimentary record and the sequence of bioevents. Using data from Sites 897, 898, 899, and 900, we propose a synthesis of the major biohorizons based on the earliest/latest occurrence of each taxon. Hole and sample numbers are indicated only for the events used to establish this synthesis. Most of the events described below are listed with sample interval and depth in Tables 2, 4, 6, 8. The following succession of biohorizons has been identified:

FO of *Ilselithina fusa*

This event is observed at Sites 897, 899, and 900 near the base of the Oligocene. At the beginning of its range, *I. fusa* is rare, but its characteristic distal spines make this species easily identifiable. The abundance pattern and the range of *I. fusa* in Hole 900A is shown on Figure 10, together with *Z. bijugatus.*

Hole 900A: Sample 149-900A-52R-3, 65-66 cm.

LO of *Bramletteius serraculoides*

The LO of *B. serraculoides* is observed at Site 897 and at Site 900. At both sites it occurs at the top of Zone NP21, at the extinction level of *Ericsonia formosa,* and is in good agreement with the distribution given by Backman (1987). The plots of the abundance pattern of the range of *B. serraculoides* are shown for Sites 897 and 900 (Figs. 3 and 8).

Hole 900A: Sample 149-900A-52R-4, 143-144 cm.

LO *of Ericsonia formosa*

The decrease in abundance of *E. formosa* at Sites 897 and 900 (Figs. 3 and 8) is tentatively interpreted as its last true occurrence; this interpretation could be supported by the position of the FO of *S. akropodus* (see below) and the LO of *B. serraculoides,* relative to this event.

Hole 900A: Sample 149-900A-52R-4, 143-144 cm.

FO of *Sphenolithus akropodus*

This species is likely to be similar to the form illustrated by Okada (1990) as *Sphenolithus* aff. *distentus,* which range is reported from the top of CP16b to the middle of CP17. According to the distribution of Okada (1990), we use this event to approximate the Zone NP21/NP22 boundary, both at Sites 897 and 900 (Figs. 3 and 8).

Hole 900A: Sample 149-900A-51R-6, 47-48 cm.

FO *of Helicosphaera recta*

This helicolith is found to have its FO in the early Oligocene at Sites 899, 897, and 900. In the two latter sites, it occurs together with the FO of *S. akropodus,* its distribution overlaps the final part of the *Reticulofenestra umbilicus* range. Previous studies report *H. recta* from the lower part of Zone NP23 (e.g., Wei and Wise, 1989; Okada, 1990), but it has not been reported in the upper part of Zone NP22. The abundance pattern of the range of *H. recta* for Hole 900A is shown on Figure 11 with other important helicolith species.

Hole 900A: Sample 149-900A-51R-6, 47-48 cm.

FO of *Chiasmolithus altus*

This chiasmolith, which is the youngest representative of the genus, has its FO in the early Oligocene at Sites 897, 899, and 900.

Hole 900A: Sample 149-900A-51R-5, 120-121 cm.

FO of *Cyclicargolithus abisectus* (>10 µm)

This large form of *Cyclicargolithus* (see Appendix A) is found to occur in the lower Oligocene at Sites 897, 899, and 900. Rio et al. (1990) distinguished *C. abisectus* by its size larger than 10 µm and they observed its LO close to the LO of *S. ciperoensis.* The abundance pattern of the range of *C. abisectus* (>10 µm) for Hole 900A is shown on Figure 12. As reported by Olafsson (1992), large speci-

mens are very rare in the Miocene. The LO of *C. abisectus* (>10 µm) occurs in Zone NN7, but its last consistent occurrence is recorded at the top of Zone NP25 (end of the regressive phase).

Hole 900A: Sample 149-900A-51-4, 9-10 cm.

FO of *Helicosphaera perch-nielseniae*

The FO *of Helicosphaera perch-nielseniae* is observed in the early Oligocene Zone NP22 at Sites 897, 899, and 900. The abundance pattern of the range of *H. perch-nielseniae* in Hole 900A is shown on Figure 11, along with other helicoliths species.

Hole 900A: Sample 149-900A-51R-4, 9-10 cm.

FO of *Reticulofenestra circus*

The FO of this new taxon is observed in the lower Oligocene Zone NP22 in Hole 897C.

Hole 897C: Sample 149-897C-50R-1, 85-86 cm.

LO *of Isthmolithus recurvus*

The LO of this holococcolith occurs at Sites 897, 899, and 900 at the same level or just below the LO of *R. umbilicus* (Figs. 3 and 8), which is in agreement with the placement of this datum by Premoli Silva et al. (1988) in mid-latitude sections. At the low-latitude Site 522, Backman (1987) reported this event below the LO of *E. formosa,* but concluded it is a diachronous event. This diachroneity could be explained by a preference of this species for cool water (Wei and Wise, 1990). The abundance pattern of the range of *I. recurvus* for Hole 900A is shown on Figure 10.

Hole 900A: Sample 149-900A-51R-3, 50-51 cm.

LO *of Reticulofenestra umbilicus*

It was found in Sites 897, 899, and 900 and marks the Zone NP22/NP23 boundary (Figs. 3 and 8).

Hole 900A: Sample 149-900A-51R-2, 24-25 cm.

FO of *Helicosphaera* aff. *H. carteri*

This medium-sized helicolith (see Appendix A) has its FO in lower Zone NP23, and it is discontinuously distributed up to lower Zone NP24. It is observed at Sites 897 and 900.

Hole 900A: Sample 149-900A-50R-5, 16-17 cm.

LO of *Lanternithus minutus*

The LO *of Lanternithus minutus* is observed at Sites 897 and 900 (Figs. 3 and 8) and occurs within Zone NP23.

Hole 900A: Sample 149-900A-50R-3, 129-130 cm.

LO of *Reticulofenestra circus*

This subcircular *Reticulofenestra* has a range restricted to the lower Oligocene. Its LO occurs at the same level or close (at Site 897) to that of *L. minutus.*

Hole 900A: Sample 149-900A-50R-2, 120-121 cm.

LO of *Sphenolithus akropodus*

This bioevent is observed within Zone NP23 at Sites 897 and 900 (Figs. 3, 8 and 13). The abundance pattern of the range of *S. akropodus* for Hole 900A is shown on Figure 13 with other *Sphenolithus* markers.

Hole 900A: Sample 149-900A-50R-2, 63-64 cm.

LCO of *Helicosphaera compacta*

The LCO of *H. compacta* is more easily detectable than its LO. At Sites 897 and 900 (Figs. 3 and 8), this bioevent is observed below the FO of S. *ciperoensis.* The sharp decrease in abundance *of H. compacta* for Hole 900A is shown on Figure 10.

Hole 900A: Sample 149-900A-49R-4, 99-100 cm.

FO of *Sphenolithus ciperoensis*

S. ciperoensis is rare and somewhat discontinuous at its first range. Its FO observed at Sites 897, 899, and 900 defines the base of Zone NP24 (Figs. 3 and 8). The abundance pattern of the range of *S. ciperoensis* for Hole 900A is shown on Figure 13.

Hole 900A: Sample 149-900A-49R-4, 99-100 cm.

FO of *Triquetrorhabdulus carinatus*

The FO of *T. carinatus* occurs in the lower part of Zone NP24 at Sites 897, 899, and 900. *T. carinatus* has a rare and sporadic occurrence from Zones NP24 to NP25, and is more abundant in Miocene sediments.

Hole 900A: Sample 149-900A-48R-4, 142-143 cm.

LO of *Helicosphaera compacta*

The LO of *Helicosphaera compacta* is found in Zone NP24 at Sites 897, 899, and 900 and this data is in accordance with the assignment of *H. compacta* proposed by Perch-Nielsen (1985). The discrepancy with the LO of this form, reported by Fornaciari et al. (1990) to occur in Zone NP23, could be related to both mid-latitude preference and the difficulty of pinpointing the LO, because of rare abundance of this taxon in its upper range (abundance pattern shown on Figs. 3, 8, 10).

Hole 900A: Sample 149-900A-48R-2, 131-132 cm.

FCO of *S. ciperoensis*

The FCO of *S. ciperoensis* (shown on Figs. 3, 8 and 13) is more easily detected than the FO, and is recorded at Sites 897, 899, and 900.

Hole 900A: Sample 149-900A-47R-3, 64-65 cm.

LO of *Sphenolithus predistentus*

Though the distribution of *S. predistentus* in its upper range decreases, its LO seems a good alternative marker to approximate the Zone NP24/NP25 boundary (Figs. 3, 8 and 13) in the eastern Atlantic Ocean, as already suggested for the western Indian Ocean (Fornaciari et al., 1990).

Hole 900A: Sample 149-900A-45R-5, 82-83 cm.

LO of *Sphenolithus distentus*

At the top of its range, the abundance of *S. distentus* decreases sharply, and occurrences above this level (Figs. 3, 8 and 13) are considered reworked.

Hole 900A: Sample 149-900A-45R-4, 112-133 cm.

FO *of Helicosphaera obliqua*

The FO of *Helicosphaera obliqua* is observed in Zone NP25 in Holes 898A, 899B and 900A, and can be useful to recognize the lower part of this Zone. The abundance pattern of the range *of H. obliqua* for Hole 900A is shown on Figure 11.

Hole 900A: Sample 149-900A-44R-1, 131-132 cm.

Table 5. Stratigraphic distribution of calcareous nannofossil taxa in Hole 898A (Cores 149-898A-18X through 36X).

Age	Zone	Core,section, interval (cm)	Depth (mbsf)	Abundance	Preservation	Reworked Cretaceous	Reworking	*Bicolumnus ovatus*	*Blackites tenuis*	*Braarudosphaera bigelowii*	*Braarudosphaera discula*	*Braarudosphaera regularis*	*Bramletteius serraculoides*	*Calcidiscus fusca*	*Calcidiscus leptoporus*	*Calcidiscus macintyrei*	*Calcidiscus pataecus*	*Calcidiscus premacintyrei* (< 9 µm)	*Calcidiscus premacintyrei* (> 9 µm)	*Calcidiscus radiatus*	*Calcidiscus tropicus* (< 6 µm)	*Calcidiscus tropicus* (> 6 µm)	*Camaralithus pellucidatus*	*Chiasmolithus altus*	*Chiasmolithus oamaruensis*	*Clausicoccus fenestratus*	*Clausicoccus obrutus*	*Coccolithus miopelagicus*	*Coccolithus pelagicus*	*Coccolithus streckeri*	*Coccolithus* sp. 1	*Coronocyclus* aff. *C. prionion*
middle Miocene	NN7	18X-4,105-106	163.67	B																											
		18X-4,134	163.96	V	P	P									R	P					R	R					C	A		R	
		18X-4,142	164.04	B																											
		18X-5,53	164.65	V	M	P									P	R	R				F	C					F	A		R	
	NN6	18X-5,75	164.87	B																											
		18X-5,110	165.22	A	P																P	R					F	C		P	
		18X-6,103-104	166.65	A	M																	R					C	C		R	
		18X-7,42-43	167.54	A	M										F						P	F					C	C		P	
		19X-1,33-34	168.13	V	M										R		R		R		R	R					C	A		R	
		19X-1,106-107	168.86	V	M										R		R		R		R						F	A		F	
		19X-2,24-25	169.54	V	M										R		R		F		R	F					C	A			
		19X-2,116-117	170.46	A	P										P		P				P	P					P	F			
	NN5	19X-3,27-28	171.07	A	M	P												P	R			P					F	C		P	
		19X-3,133-139	172.18	V	M	R									F			R	R			R					C	A	R	R	R
		19X-4,1-2	172.31	A	P																						R	F			
		19X-5,72-73	174.62	V	M	R									F		F	R	R			R					R	A		R	
		19X-6,80-81	176.10	A	M	P									P		F		P		P	P					F	C		P	P
		19X-6,112-113	176.42	C	P																						P	F			
		19X-7,1-2	176.81	V	M	P									F		F		P		P	P					C	A	R	P	P
early Miocene	NN4	20X-1,72-73	178.12	V	X	F									F		F	R	F		F	F					F	A		R	R
		20X-2,25-26	179.15	A	M	P									R		P	P	P		P						F	A		P	
		20X-3,43-44	180.83	V	M										P		R	P	F		P	R					F	A		P	
		20X-4,9-10	181.99	V	M	P											P		R		F						C	A		P	P
		20X-5,9-10	183.49	V	M										R		R	R			F						F	A	R		
		21X-1,66-67	187.66	V	G	R								R	R		F				R						F	C			
		21X-2,5-6	188.55	V	X	R									R		C				R						R	A	R		R
		21X-3,96-97	190.96	V	M										R							R					F	C	R		
		21X-4,63-64	192.13	V	G	P									P		F					P					F	A	P		
	NN3	21X-CC	192.95	V	X	F									R							R					R	A	R		
		22X-1,37-38	197.07	V	M	R									R												R	A	R		
	NN2	22X-2,37-38	198.93	V	X									R	R		R					R					R	A	R	R	
		22X-3,100-101	200.70	V	X	R									R		R										F	A			
		22X-4,35-36	201.55	V	X	F									R		R					R					F	A	R	R	
		22X-4,89	201.99	V	M	R								R	F												F	A		R	
		22X-5,86-87	203.56	A	M										R												P	A	P		
		23X-1,80-81	207.20	V	M	P								P	P					P		P					F	A	P		P
		23X-2,45-46	208.35	A	M	P														R							F	C	P		
		23X-4,51	211.41	V	X	F														R		R					R	C			
		23X-5,70-71	213.12	V	X	R								R			R			R							F	A	R	R	
		23X-6,9-10	214.01	B																											
		24X-1,11-12	216.15	V	G	R								F			R			R	F						F	A			R
		24X-2,28-29	218.18	O	G	F								C			A			F	F							A		F	
		24X-3,65-66	220.05	V	G	F				F				C			F			F	F						F	A	F	F	
		24X-4,121	222.11	V	X	R											R			R	R						R	C		F	
		24X-5,24-25	222.66	V	G	F											F			F	F						F	A	F	F	
		25X-1,105-106	226.65	V	M	R								R			F			F							R	C			
		25X-2,77-78	227.89	O	X									F			A			F								A	F	F	
		25X-3,35-36	228.98	V	X	R								R			C			R							R	C		R	
		26X-1,102-103	236.22	V	X	R											F				R		R			R	R	F		R	
		26X-2,62-63	237.32	V	X	R											F			R							F	C			
	NN1	27X-1,132-133	246.12	V	X	P														P						P	P	F			
		27X-3,5-6	247.85	V	G	F																	F			F	F	C			
		27X-5,26-27	251.08	V	E	F				F													F				F	C	F		
		27X-6,50-51	252.85	O	E	C				F							C						C			C	F	C	F	F	
		27X-7,18-19	254.03	V	G	R				R										R			F				R	F			
		28X-1,41-42	254.91	V	M																					F	R	F			
		28X-1,99-100	255.49	V	G	F								R						R			F			R	R	F			
		28X-2,23-24	256.23	V	M																					P		R			
		28X-2,49-50	256.49	V	E	F																	R			R	F	F			
late Oligocene	NP 25	28X-3,145-146	258.97	V	G	F														R			F			R	R	R	C			
		28X-34,114-115	260.16	O	E	F				F				F						F			F				F	C			
		28X-5,28-29	160.80	V	G	F				F										F			F			F	F	C	C			
		29X-1,52-53	264.72	V	X	P														P			P			P	P	P	C		P	
		29X-1,103-104	265.23	V	G	F														F			F			R	F	F	C			
		29X-2,26-27	265.96	A	M				P																	P	P	P	F			
		29X-2,117-118	266.87	V	G	P				P			P	P						P			F			P	P	P	F			
		29X-3,46-47	267.66	A	M	P									F												P	P	F			
		29X-4,70-71	269.40	V	G	F		F	F											F			F			F	C	F	A			
		30X-2,9-10	275.39	A	P			P		P																P	R		C			
		30X-4,30-31	278.64	A	M	P		P	P																		R		F			
		31X-1,138-139	284.88	A	M	P		P																		R	F		F			
		31X-3,65-66	287.15	V	M		P		P	P																P		C			
		31X-4,101-102	289.01	V	M	R	R																		R	F	F	F	A			
		32X-2,33-34	295.03	A	P	P	P	P	P	P																R	P		F			
		32X-3,34-35	296.54	A	M	R																				F	F		C			
		32X-4,44-45	298.14	A	P			P																		F			C			
		33X-2,18-19	304.48	A	M			R																		R	P	R	C			
		33X-4,67-68	307.97	A	M	P				P																P	P		F			
		33X-6,52-53	310.82	A	M			R																		R			F			
		34X-2,17-18	314.17	V	M	P																				P	P		C			
		35X-1,84-85	323.04	V	M																					F	C	R	A			
		35X-2,108-109	324.78	A	M																					P	P		C			
		36X-1,108-109	332.98	A	M		P																	P		R	R		C			
		36X-2,17-18	333.57	V	M																			P		P	R		C			
		36X-4,91-92	337.31	A	M				P																		F		C			
		36X-4,132-133	337.72	A	P			P																		R	P		C			
		36X-5,114-115	339.04	A	M		P		R																		R		F			

Table 5 (continued).

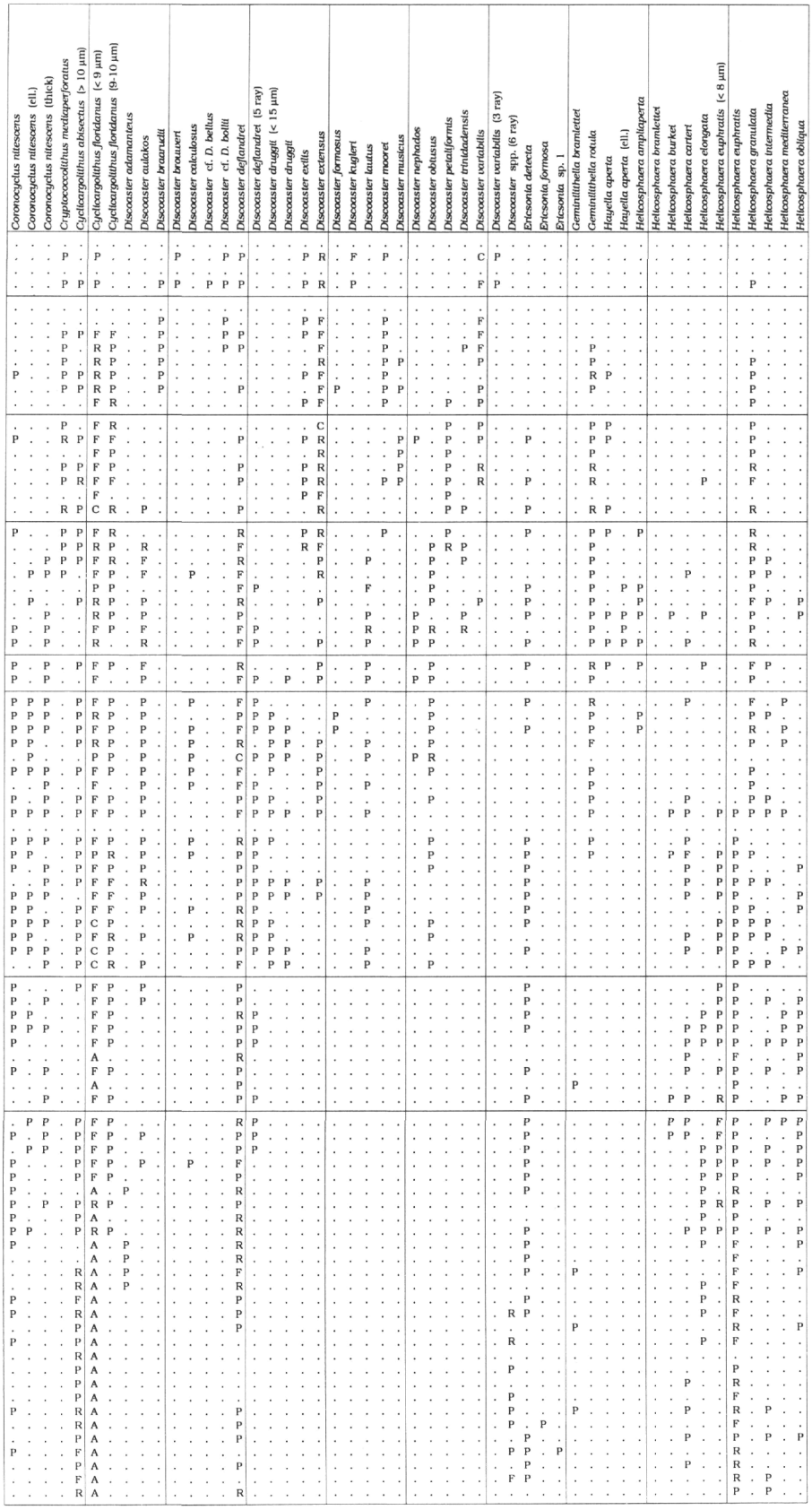

Table 5 (continued).

Age	Zone	Core,section, interval (cm)	Depth (mbsf)	Abundance	Preservation	*Helicosphaera paleocarteri*	*Helicosphaera perch-nielseniae*	*Helicosphaera recta*	*Helicosphaera rhomba*	*Helicosphaera scissura*	*Helicosphaera truempyi*	*Helicosphaera vedderi*	*Hughesius tasmaniae*	*Umbilithina fusa*	*Micrantholithus aequalis*	*Orthozygus aureus*	*Pontosphaera antisotrema*	*Pontosphaera callosa*	*Pontosphaera enormis*	*Pontosphaera longiforaminis*	*Pontosphaera multipora*	*Pontosphaera* spp.	*Pyrocyclus hermosus*	*Pyrocyclus inversus*	*Pyrocyclus orangensis*	*Reticulofenestra amplumbilicus*	*Reticulofenestra bisecta bisecta*	*Reticulofenestra bisecta, filewiczii*	*Reticulofenestra circus*	*Reticulofenestra daviesi*
middle Miocene	NN7	18X-4,105-106	163.67	B		.	.	.	.	.	.	.	.	.	.	.	.	.	.	.	.	.	.	.	.	.	.	.	.	.
		18X-4,134	163.96	V	P	.	.	.	.	.	.	.	.	.	.	.	.	.	.	.	P	.	.	.	.	R	.	.	.	.
		18X-4,142	164.04	B		.	.	.	.	.	.	.	.	.	.	.	.	.	.	.	.	.	.	.	.	.	.	.	.	.
		18X-5,53	164.65	V	M	.	.	.	.	.	.	.	.	.	.	.	.	.	.	.	P	.	.	.	.	.	.	.	.	.
	NN6	18X-5,75	164.87	B		.	.	.	.	.	.	.	.	.	.	.	.	.	.	.	.	.	.	.	.	.	.	.	.	.
		18X-5,110	165.22	A	P	.	.	.	.	.	.	.	.	.	.	.	.	.	.	.	.	.	.	.	.	P	.	.	.	.
		18X-6,103-104	166.65	A	M	.	.	.	.	.	.	.	.	.	.	.	.	.	.	.	.	.	.	.	.	.	.	.	.	.
		18X-7,42-43	167.54	A	M	.	.	.	.	.	.	.	.	.	.	.	.	.	.	.	.	.	.	.	.	.	.	.	.	.
		19X-1,33-34	168.13	V	M	.	.	.	.	.	.	.	.	.	.	.	.	.	.	.	.	.	.	.	.	R	.	.	.	.
		19X-1,106-107	168.86	V	M	.	.	.	.	.	.	.	.	.	.	.	.	.	.	.	R	.	.	.	.	F	.	.	.	.
		19X-2,24-25	169.54	V	M	.	.	.	.	.	.	.	.	.	.	.	.	.	.	.	R	.	.	.	.	.	.	.	.	.
		19X-2,116-117	170.46	A	P	.	.	.	.	.	.	.	.	.	.	.	.	.	.	.	.	.	.	.	.	.	.	.	.	.
	NN5	19X-3,27-28	171.07	A	M	.	.	.	.	.	.	.	.	.	.	.	.	.	.	.	.	.	.	.	.	.	.	.	.	.
		19X-3,133-139	172.18	V	M	.	.	.	.	.	.	.	.	.	.	.	.	.	.	.	R	.	.	.	.	.	.	.	.	.
		19X-4,1-2	172.31	A	P	.	.	.	.	.	.	.	.	.	.	.	.	.	.	.	.	.	.	.	.	.	.	.	.	.
		19X-5,72-73	174.52	V	M	.	.	.	.	.	.	.	.	.	.	.	.	.	.	.	R	.	.	.	.	.	.	.	.	.
		19X-6,80-81	176.10	A	M	.	P	.	.	.	.	.	.	.	.	.	R	.	.	.	P	.	.	.	P	.	.	.	.	.
		19X-6,112-113	176.42	C	P	.	.	.	.	.	.	.	.	.	.	.	.	.	.	.	.	.	.	.	.	.	.	.	.	.
		19X-7,1-2	176.81	V	M	F	.	.	.	.	.	.	.	.	.	.	.	.	.	.	.	.	.	.	.	.	.	.	.	.
early Miocene	NN4	20X-1,72-73	178.12	V	X	F	R	.	.	.	.	.	.	.	.	.	.	.	.	.	F	.	R	.	.	.	.	.	.	.
		20X-2,25-26	179.15	A	M	.	P	.	.	.	.	.	.	.	.	.	.	.	.	.	R	.	P	.	.	.	.	.	.	.
		20X-3,43-44	180.83	V	M	.	.	.	.	.	.	.	.	.	.	.	.	.	.	.	.	.	P	.	P	.	.	.	.	.
		20X-4,9-10	181.99	V	M	.	.	.	.	.	.	.	.	.	.	.	.	.	.	.	.	.	P	.	.	P	.	.	.	.
		20X-5,9-10	183.49	V	M	.	.	.	R	.	.	.	.	.	.	.	.	.	.	.	.	.	R	.	R	.	.	.	.	.
		21X-1,66-67	187.66	V	G	.	R	.	R	R	.	.	.	.	.	.	.	.	.	R	R	.	.	.	.	.	.	.	.	.
		21X-2,5-6	188.55	V	X	.	.	.	R	R	.	.	.	.	.	.	.	.	.	R	.	.	F	.	.	.	.	.	.	.
		21X-3,96-97	190.96	V	M	.	.	.	.	.	.	.	.	.	.	.	R	.	.	.	R	.	R	.	.	R	.	.	.	.
		21X-4,63-64	192.13	V	G	.	.	.	.	P	.	P	.	.	.	.	.	.	.	.	R	.	P	.	.	P	.	.	.	.
	NN3	21X-CC	192.95	V	X	.	.	.	R	R	.	R	.	.	.	.	.	.	.	.	R	.	.	.	.	R	.	.	.	.
		22X-1,37-38	197.07	V	M	.	.	.	.	.	.	.	.	.	.	.	.	.	.	.	.	.	.	.	.	R	.	.	.	.
	NN2	22X-2,37-38	198.93	V	X	.	.	.	.	.	.	.	.	.	.	.	.	.	.	.	.	.	F	.	R	.	.	.	.	.
		22X-3,100-101	200.70	V	X	.	R	.	.	.	.	.	R	.	.	.	R	.	.	.	R	.	F	.	.	.	.	.	.	.
		22X-4,35-36	201.55	V	X	.	.	.	.	.	.	.	F	.	.	.	R	.	.	.	F	.	R	.	.	.	.	.	.	.
		22X-4,89	201.99	V	M	.	.	.	.	.	.	.	F	.	.	.	.	.	.	.	.	.	R	.	.	.	.	.	.	.
		22X-5,86-87	203.56	A	M	.	.	.	.	.	.	.	.	.	.	.	.	.	.	.	.	.	P	.	.	R	.	.	.	.
		23X-1,80-81	207.20	V	M	.	.	.	.	.	.	.	.	.	.	.	.	.	.	.	.	.	.	.	P	.	.	.	.	.
		23X-2,45-46	208.35	A	M	.	.	.	.	.	.	.	.	.	.	.	.	.	.	.	.	.	.	.	.	.	.	.	.	.
		23X-4,51	211.41	V	X	.	R	.	.	.	R	R	.	.	.	.	.	.	.	.	R	.	R	.	R	.	.	.	.	.
		23X-5,70-71	213.12	V	X	.	R	.	.	.	.	.	R	.	.	.	.	.	.	.	R	.	R	.	R	.	.	R	.	.
		23X-6,9-10	214.01	B		.	.	.	.	.	.	.	.	.	.	.	.	.	.	.	.	.	.	.	.	.	.	.	.	.
		24X-1,11-12	216.15	V	G	.	R	.	.	.	.	.	F	.	.	.	.	.	.	.	R	.	.	.	.	.	.	R	.	.
		24X-2,28-29	218.18	O	G	.	F	.	.	.	.	.	F	C	.	.	F	.	.	.	F	.	.	.	F	.	.	F	.	.
		24X-3,65-66	220.05	V	G	.	F	.	.	.	.	.	F	F	F	.	F	.	.	.	C	.	.	.	.	.	.	.	.	.
		24X-4,121	222.11	V	X	.	R	R	.	.	.	.	F	R	.	.	R	.	.	.	R	.	R	.	R	.	.	.	.	.
		24X-5,24-25	222.66	V	G	.	F	.	.	.	.	F	A	F	.	F	.	F	.	.	C	.	.	.	F	.	.	.	.	.
		25X-1,105-106	226.65	V	M	.	R	R	.	.	.	.	C	F	.	.	.	.	.	.	.	.	.	.	R	.	.	.	.	.
		25X-2,77-78	227.89	O	X	.	.	F	.	.	.	.	A	F	.	.	.	.	.	.	F	.	.	.	F	.	.	.	.	.
		25X-3,35-36	228.98	V	X	.	.	R	R	.	.	.	C	R	.	.	.	.	.	.	R	.	R	.	F	.	.	.	.	.
		26X-1,102-103	236.22	V	X	.	R	R	R	.	.	.	A	F	.	.	.	R	.	.	R	.	.	.	R	.	.	R	.	.
		26X-2,62-63	237.32	V	X	.	F	R	.	.	.	.	F	F	.	.	.	.	.	.	R	.	.	.	.	.	.	R	.	.
	NN1	27X-1,132-133	246.12	V	X	.	R	P	.	.	.	.	C	F	.	.	.	.	.	.	.	.	.	.	P	.	.	.	.	.
		27X-3,5-6	247.85	V	G	.	F	F	.	.	.	.	A	F	.	.	.	.	.	.	F	.	.	.	F	.	F	F	.	.
		27X-5,26-27	251.08	V	E	.	F	F	.	.	.	.	A	C	.	.	.	.	.	.	F	.	.	.	F	.	.	.	.	.
		27X-6,50-51	252.85	O	E	.	C	F	.	.	.	.	A	A	F	C	.	.	.	.	C	.	.	.	F	.	.	F	.	.
		27X-7,18-19	254.03	V	G	.	R	R	.	.	.	.	C	F	R	F	.	R	.	R	F	.	.	.	R	.	.	R	.	.
		28X-1,41-42	254.91	V	M	.	.	P	.	.	.	.	.	R	.	R	.	.	.	.	R	.	.	.	.	.	.	.	.	.
		28X-1,99-100	255.49	V	G	.	R	.	.	.	.	.	C	F	.	F	.	R	.	F	R	.	.	.	.	.	.	R	.	R
		28X-2,23-24	256.23	V	M	.	P	.	.	.	.	.	.	.	.	.	.	.	.	.	P	.	.	.	.	.	.	.	.	P
		28X-2,49-50	256.49	V	E	.	R	R	.	.	.	.	A	R	.	F	.	R	.	R	R	.	.	.	.	.	.	R	.	.
late Oligocene	NP 25	28X-3,145-146	258.97	V	G	.	R	R	.	.	.	.	C	F	.	.	R	R	R	R	R	.	.	.	.	.	R	F	.	.
		28X-34,114-115	260.16	O	E	.	F	F	.	.	.	.	A	F	F	F	.	F	F	F	F	.	.	.	F	.	.	C	.	F
		28X-5,28-29	160.80	V	G	.	F	.	.	.	.	.	A	C	F	F	.	.	F	F	F	.	F	.	F	.	.	F	.	.
		29X-1,52-53	264.72	V	X	.	R	P	.	.	P	.	C	F	.	R	.	.	P	P	P	.	.	P	P	.	P	R	.	P
		29X-1,103-104	265.23	V	G	.	F	.	.	.	.	.	A	F	.	F	.	.	R	R	F	.	.	.	R	.	R	R	.	.
		29X-2,26-27	265.96	A	M	.	R	.	.	.	.	.	.	.	.	P	.	.	.	.	P	.	.	.	.	.	.	.	.	.
		29X-2,117-118	266.87	V	G	.	R	.	.	.	.	.	C	R	.	R	.	.	P	P	R	.	.	.	.	.	P	R	.	.
		29X-3,46-47	267.66	A	M	.	P	.	.	.	.	.	.	P	.	P	.	.	.	.	P	.	.	.	P	.	.	P	.	P
		29X-4,70-71	269.40	V	G	.	F	F	.	.	.	.	A	F	.	C	.	.	F	F	F	.	.	.	F	.	F	F	F	F
		30X-2,9-10	275.39	A	P	.	R	P	.	.	.	.	.	.	.	.	.	.	.	.	.	P	.	.	.	.	.	R	.	R
		30X-4,30-31	278.64	A	M	.	R	P	.	.	P	.	.	P	.	P	.	.	.	.	R	.	.	.	P	.	.	R	.	P
		31X-1,138-139	284.88	A	M	.	R	P	.	.	P	.	.	.	.	P	.	.	.	.	P	R	.	.	P	.	.	P	P	R
		31X-3,65-66	287.15	V	M	.	F	R	.	.	.	.	.	.	.	P	.	.	.	.	.	F	.	.	.	.	.	P	.	R
		31X-4,101-102	289.01	V	M	.	R	R	.	.	R	.	.	R	.	.	.	.	.	.	F	.	.	.	F	.	.	F	.	F
		32X-2,33-34	295.03	A	P	.	R	P	.	.	.	.	.	P	.	.	.	.	.	.	.	F	.	.	.	.	.	P	.	P
		32X-3,34-35	296.54	A	M	.	P	P	.	.	P	.	.	R	.	P	.	.	.	.	P	P	.	.	P	.	R	.	P	.
		32X-4,44-45	298.14	A	P	.	F	P	.	.	.	.	.	P	.	.	.	.	.	.	.	F	.	.	.	.	.	P	.	P
		33X-2,18-19	304.48	A	M	.	R	.	.	.	.	.	.	.	.	.	.	.	.	.	.	P	.	.	F	.	F	P	.	R
		33X-4,67-68	307.97	A	M	.	P	P	.	.	.	.	.	.	.	.	.	.	.	.	.	.	.	.	.	.	.	.	.	P
		33X-6,52-53	310.82	A	M	.	P	.	.	.	.	.	.	.	.	.	.	.	.	.	.	P	.	.	P	.	R	.	.	R
		34X-2,17-18	314.17	V	M	.	.	F	.	.	.	.	.	P	.	.	.	.	.	.	.	F	.	.	P	.	.	.	.	R
		35X-1,84-85	323.04	V	M	.	F	P	.	.	.	.	.	.	.	.	.	.	.	.	P	.	.	.	F	.	F	R	P	F
		35X-2,108-109	324.78	A	M	.	R	F	.	.	.	.	.	R	.	.	.	.	.	.	.	F	.	.	.	.	.	P	.	R
		36X-1,108-109	332.98	A	M	.	F	R	.	.	.	.	.	.	.	P	.	.	.	.	F	.	.	.	F	.	P	R	.	F
		36X-2,17-18	333.57	V	M	.	P	F	.	.	P	.	.	P	.	.	.	.	.	.	.	R	.	.	P	.	.	P	.	P
		36X-4,91-92	337.31	A	M	.	P	R	.	.	.	.	.	.	.	.	.	.	.	.	.	P	.	.	P	.	P	P	.	P
		36X-4,132-133	337.72	A	P	.	F	F	.	.	.	.	.	P	.	.	.	.	.	.	.	P	.	.	.	.	.	P	.	F
		36X-5,114-115	339.04	A	M	.	P	R	.	.	P	.	.	.	.	.	.	.	.	.	P	P	.	.	P	.	.	R	.	R

Table 5 (continued).

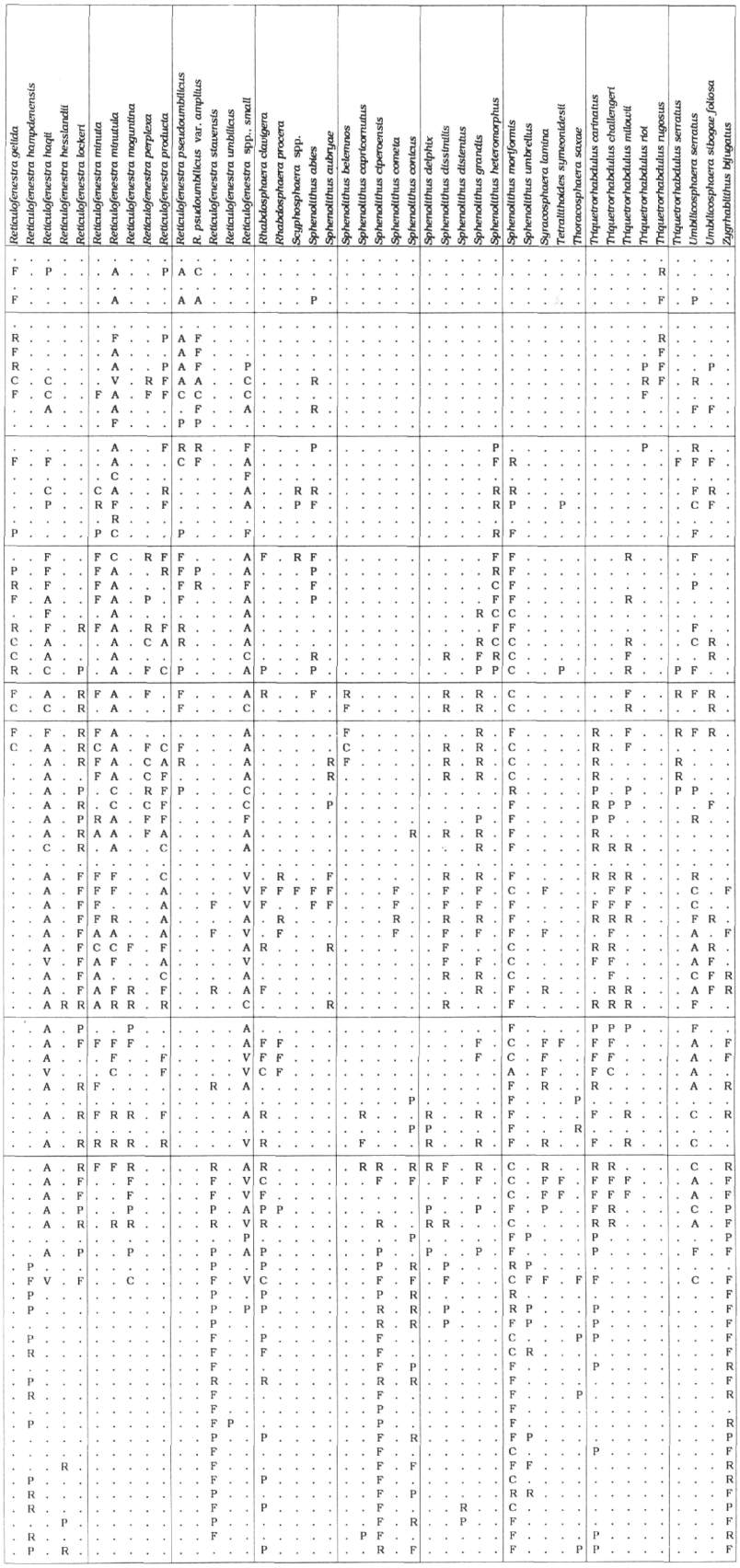

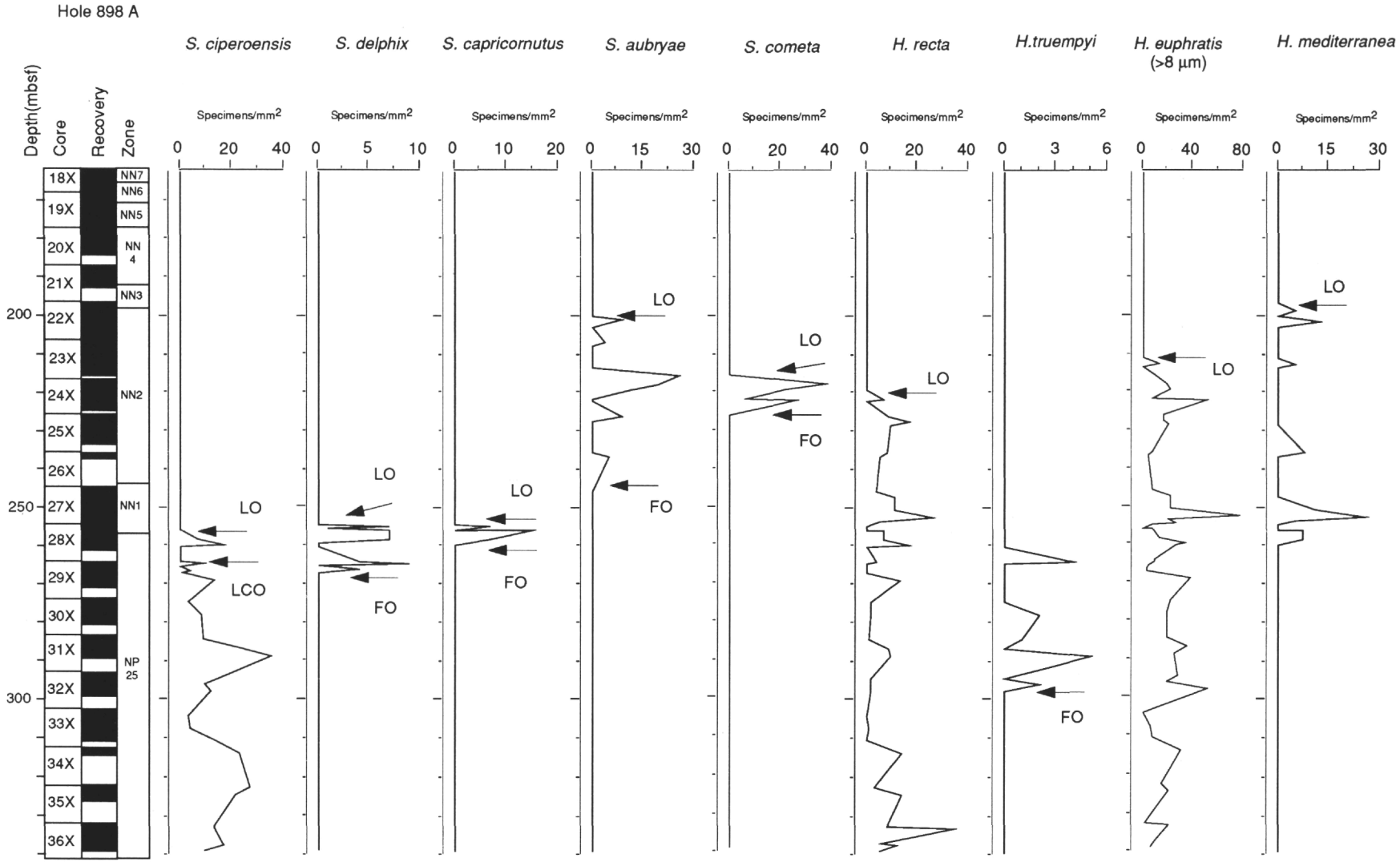

Figure 5. Plot of abundance of some sphenolith and helicolith marker species in Hole 898A.

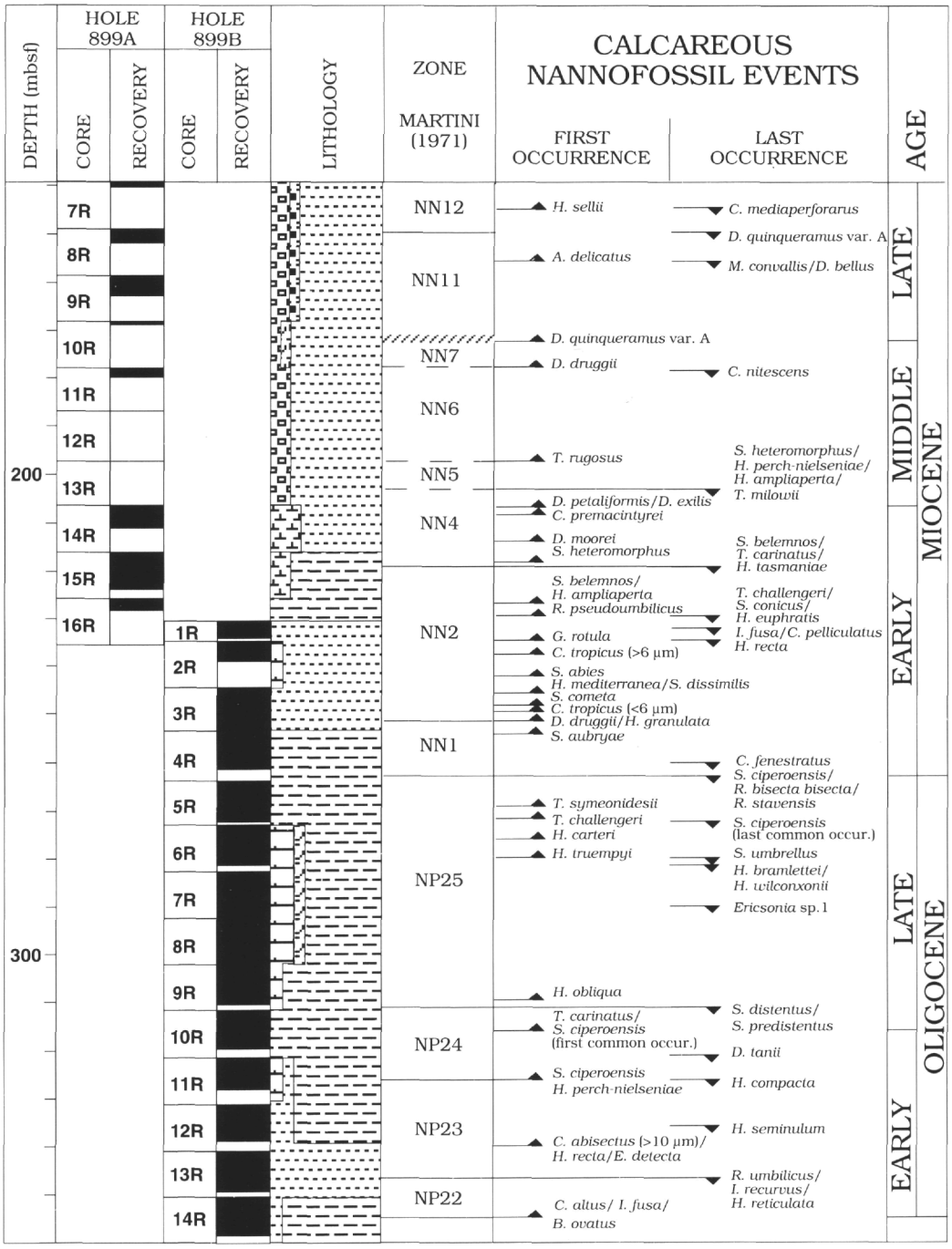

Figure 6. Calcareous nannofossil biostratigraphic summary of the Oligocene-Miocene interval of Holes 899A and 899B. See Figure 2 for symbol explanations.

LO of *Ericsonia* sp. 1

This round species of *Ericsonia* (see Appendix A) is restricted to the Oligocene interval (Figs. 3, 8 and 10). Its LO is placed between the FOs of *H. obliqua* and *H. truempyi* in Zone NP25 and is correlated among Sites 898, 899, and 900. At Site 897, an interval barren of calcareous nannofossils lies above the LO of *Ericsonia* sp. 1, which precludes precise location of this event.

Hole 900A: Sample 149-900A-43R-2, 80-81 cm.

FO of *Sphenolithus delphix*

This characteristic form is found only in Holes 897C and 898A. At Site 897 its FO occurs above the LO of *S. ciperoensis,* whereas at Site 898, it takes place just below the LCO of *S. ciperoensis.* The latter finding is somewhat in contrast with previous assignment; in Rio et al. (1990), and Gartner (1992), these two sphenoliths do not overlap, which could be explained as a consequence of different methods used to pick out the LO of *S. ciperoensis,* because, as described above, it is very rare in its upper range.

Hole 898A: Sample 149-898A-29X-2, 117-118 cm.

FO of *Helicosphaera truempyi*

This helicolith is rare to few in Leg 149 sediments. The FO was observed in the middle part of Zone NP25 (Fig. 5), close to the FO of *Sphenolithus umbrellus* and the LO of *H. bramlettei,* and above the LO *of Ericsonia* sp. 1.

Table 6. Summary of the key nannofossil biohorizons in Holes 899A and 899B.

Calcareous Nannofossil Event	Interval (cm)	Depth (mbsf)
Hole 899A		
A. primus LO	6R-4, 40/7R1, 40	136.92
A. amplificus LO	6R-4, 40/7R1, 40	136.92
C. mediaperforatus LO	7R-1, 81/8R-1, 37	144.44
T. rugosus LO	7R-1, 81/8R-1, 37	144.44
H. sellii FO	7R-1, 81/8R-1, 37	144.44
D. quinqueramus var. A LO	8R-1, 37/8R-1,84	149.23
A. delicatus FO	8R-2, 54/9R-1, 95	155.00
M. convallis LO	8R-2, 54/9R-1, 95	155.00
D. bellus LO	8R-2, 54/9R-1, 95	155.00
D. quinqueramus var. A FO	10R-CC/11R-1, 118	173.22
Hiatus		
D. braarudii FO	11R-1, 118/11R-2, 11	179.00
C. macintyrei (>11 µm) FO	11R-1, 118/11R-2, 11	179.00
D. kugleri FO	11R-1, 118/11R-2, 11	179.00
C. nitescens LO	11R-2, 11/11R-2, 47	179.39
T. rugosus FO	13R-CC, 7/13R-CC, 40	197.16
S. heteromorphus LO	13R-CC, 40/14R-1, 40	202.20
H. perch-nielseniae LO	13R-CC, 40/14R-1, 40	202.20
T. milowii LO	13R-CC, 40/14R-1, 40	202.20
H. ampliaperta LO	13R-CC, 40/14R-1, 40	202.20
D. calculosus LO	13R-CC, 40/14R-1, 40	202.20
D. petaliformis FO	14R-1, 40/14R-1, 110	207.35
D. exilis FO	14R-1, 40/14R-1, 110	207.35
C. premacintyrei FO	14R-1, 110/14R-2, 35	208.75
D. moorei FO	14R-3, 117/15R-2, 6	214.31
S. heteromorphus FO	15R-2, 6/15R-3, 124	219.20
S. belemnos LO	15R-2, 6/15R-3, 124	219.20
H. mediterranea LO	15R-2, 6/15R-3, 124	219.20
T. carinatus LO	15R-2, 6/15R-3, 124	219.20
H. tasmaniae LO	15R-2, 6/15R-3, 124	219.20
S. belemnos FO	16R-1, 42/16R-2, 104	227.38
H. ampliaperta FO	16R-1, 42/16R-2, 104	227.38
R. pseudoumbilicus FO	16R-2, 104/1R-1, 138	230.16
T. challengeri LO	16R-2, 104/1R-1, 138	230.16
S. conicus LO	16R-2, 104/1R-1, 138	230.16
H. euphratis LO	16R-2, 104/1R-1, 138	230.16
Z. bijugatus LO	16R-2, 104/1R-1, 138	230.16
Hole 899B		
I. fusa LO	1R-1, 138/1R-2, 104	232.45
C. altus LO	1R-2, 104/1R-3, 32	233.42
C. pelliculatus LO	1R-3, 32/2R-1, 35	234.48
H. recta LO	1R-3, 32/2R-1, 35	234.48
C. tropicus (>6.0 µm) FO	2R-1, 35/2R-2, 88	236.16
D. calculosus FO	2R-2, 88/2R-3, 148	238.23
S. abies FO	2R-3, 148/3R-1, 16	241.92
S. dissimilis FO	3R-1, 50/3R-2, 103	245.91
H. mediterranea FO	3R-1, 50/3R-2, 103	245.91
S. cometa FO	3R-2, 103/3R-4, 30	248.06
C. tropicus (<6.0 µm) FO	3R-4, 30/3R-4, 124	249.47
H. granulata FO	3R-5, 114/3R-6, 59	252.01
D. druggii FO	3R-5, 114/3R-6, 59	252.01
S. aubryae FO	3R-6, 59/4R-2, 70	254.34
O. aureus LO	4R-5, 54/4R-6, 18	261.11
C. fenestratus LO	4R-5, 54/4R-6, 18	261.11
R. bisecta filewiczii LO	4R-5, 54/4R-6, 18	261.11
R. stavensis LO	4R-5, 54/4R-6, 18	261.11
S. ciperoensis LO	4R-6, 18/4R-CC	261.81
P. enormis LO	5R-2, 63/5R-3, 134	266.93
T. symeonidesii FO	5R-3, 134/5R-4, 128	268.76
T. challengeri FO	5R-5, 130/5R-6, 15	271.17
S. ciperoensis LCO	5R-6, 15/6R-1, 68	272.71
H. carteri FO	6R-2, 75/6R-3, 124	276.64
S. umbrellus LO	6R-4, 145/6R-5, 65	279.70
H. truempyi FO	7R-4, 72/7R-5, 92	279.70
Ericsonia sp. 1 LO	7R-5, 92/7R-6, 126	289.07
H. bramlettei LO	6R-4, 145/6R-5, 65	290.84
H. obliqua FO	9R-5, 21/9R-6, 15	309.23
S. distentus LO	9R-6, 15/10R-2, 147	312.46
S. predistentus LO	9R-6, 15/10R-2, 147	312.46
T. carinatus FO	10R-2, 147/10R-5, 23	316.60
S. ciperoensis FCO	10R-2, 147/10R-5, 23	316.60
D. tanii LO	10R-5, 23/11R-3, 90	321.71
H. compacta LO	11R-3, 90/11R-5, 29	326.69
S. ciperoensis FO	11R-3, 90/11R-5, 29	326.69
H. perch-nielseniae FO	11R-3, 90/11R-5, 29	326.69
H. seminulum LO	12R-2, 139/12R-5, 43	335.86
E. detecta FO	12R-5, 43/13R-1, 141	339.97
C. abisectus (>10 µm) FO	12R-5, 43/13R-1, 141	339.97
H. recta FO	12R-5, 43/13R-1, 141	339.97
R. umbilicus LO	13R-1, 141/14R-2, 15	347.28
I. recurvus LO	13R-1, 141/14R-2, 15	347.28
H. reticulata LO	13R-1, 141/14R-2, 15	347.28
C. altus FO	14R-2, 15/14R-2, 24	352.30
B. ovatus FO	14R-2, 15/14R-2, 24	352.30
I. fusa FO	14R-2, 15/14R-2, 24	352.30

Note: See Table 2 for explanation.

Hole 900A: Sample 149-900A-40R-2, 116-117 cm.

LO of *Sphenolithus umbrellus*

It was recognized in Holes 898A, 899B, and 900A below the LCO of *S. ciperoensis,* in the upper part of Zone NP25.

Hole 900A: Sample 149-900A-39R-3, 109-110 cm.

FO of *Triquetrorhabdulus challengeri*

An early morphotype of *T. challengeri* with three bright ridges first occurs in the upper part of Zone NP25. Though rare at the beginning of its range, *T. challengeri* becomes more abundant in Zones NN1 and NN2. Specimens observed are well preserved and easily distinguishable from *Triquetrorhabdulus carinatus* and *Triquetrorhabdulus millowii.* Its FO is found in Hole 898A at the same level as the LCO of *S. ciperoensis.*

Hole 898A: Sample 149-898A-29X-1, 103 cm.

LCO of *Sphenolithus ciperoensis*

This event corresponds to the last consistent occurrence and represents a drop in abundance (Figs. 3, 8 and 13). It is recognized at Sites 898, 899, and 900. At Site 897 the decrease in abundance is sharp (from 20 to 0 specimens/mm^2) and coincides with the LO of S. *ciperoensis.* At the other sites, the drop in abundance is from about 15 to less than 5 specimens/mm^2.

Hole 900A: Sample 149-900A-37R-5, 53-54 cm.

FO of *Helicosphaera carteri*

H. carteri has a discontinuous, rare occurrence in the upper Oligocene Zone NP25 and its FO is placed above the FO *of H. truempyi.*

Hole 898A: Sample 149-899B-6X-2, 75 cm.

FO of *Tetralithoides symeonidesii*

T. symeonidesii has been identified by Theodoridis (1984) in sediments recovered at ODP Sites 219, 231, 372, and 369. Sites 219 and 231 are located in the Indian Ocean, Site 372 is in the Mediterranean Sea, and Site 369 is situated on the continental slope off the Northwest Africa Margin, south of Leg 149 sites. Theodoridis (1984) reported a range from Zones NN2 to NN11. Its earliest occurrence is found in the upper part of Zone NP25 in Hole 898A and 899B. *T. symeonidesii* occurs rarely and sporadically from Zones NP25 through NN11. Its unique structure, easily identifiable, and its cosmopolitan distribution provide an additional useful marker for the upper part of Zone NP25.

Hole 898A: Sample 149-898A-28X-4, 114cm.

LOs of *Sphenolithus ciperoensis, Reticulofenestra bisecta bisecta,* and *Pontosphaera enormis*

S. ciperoensis occurs rarely in the uppermost part of its range, but its LO is consistent within the four sites investigated. The sharp decrease in abundance recorded lower in Zone NP25 has been frequently used in other studies to place the top of Zone NP25. Rare occurrences of *S. ciperoensis* above this level were frequently attributed to reworked specimens. According to the pattern observed in the Iberia Abyssal Plain, we exclude any possible reworking explanations for the presence of *S. ciperoensis* up to the LO of *R. bisecta bisecta.* Martini and Muller (1986) also indicated the reoccurrence of *S. ciperoensis* in the uppermost Oligocene Zone NP25, and suggested that climatic fluctuations may control the occurrence of *S. ciperoensis.*

The LO of *R. bisecta bisecta* is usually at the same level as the LO of *S. ciperoensis. Reticulofenestra stavensis* and *Reticulofenestra bisecta filewiczii* are present in the lower Miocene Zone NN1. The LO *of P. enormis* occurs with the LOs of *S. ciperoensis* and *R. bisecta bisecta* at the top of Zone NP25. At the Chattian-type section, Martini and Muller (1975) reported the presence of *P. enormis* up to the top of the Chattian, and Martini and Muller (1986) place the LO of *Pontosphaera enormis* at the level of the last reoccurrence of *S. ciperoensis.*

In accordance with Fornaciari et al. (1993) we use the LO of *S. ciperoensis* to place the Zone NP25/NN1 boundary, because the LO of *H. recta,* the original zonal marker of Martini (1971), is recorded in Zone NN2.

Hole 898A: Sample 149-898A-28X-3, 145 cm.

LO *of Clausicoccus fenestratus*

C. fenestratus occurs throughout the Oligocene and its LO is consistently above the LO of *S. ciperoensis.* Only forms with an inner bright cycle and a large central area, similar to the drawing of Prins (1979), have their LO in lowermost part of Zone NN1. *Clausicoccus obruta,* a form with only four perforations, has its LO in Zone NN2. Forms without an inner bright cycle belong to the genus *Hughesius* (Varol, 1989b), and are found throughout the lower Miocene. The abundance pattern of the ranges of *C. fenestratus* and *Hughesius tasmaniae* for Hole 900A are shown on Figure 14, but with different horizontal scales.

Hole 898A: Sample 149-898A-28X-2, 49 cm.

LOs of *Sphenolithus delphix* and *Sphenolithus capricornutus*

These two distinct sphenoliths have short ranges from the uppermost Oligocene Zone NP25 to the middle of Zone NN1 (Fig. 5). Although rare and sporadic in their occurrences, these two events are very reliable. Moreover, a very short, characteristic interval contains abundant forms of large *S. delphix.* This "triradiated" form possesses a very long apical spine and two extremely elongated proximal elements, and it occurs near the top of the range of *S. delphix,* together with frequent *T. carinatus.*

Hole 898A: "long triradiated" *S. delphix:* Sample 149-898A-28X-2, 49 cm

Hole 898A: Sample 149-898A-28X-1, 99 cm.

FO of *Sphenolithus aubryae*

S. aubryae is observed from the uppermost part of Zone NN1 to Zone NN3 (Fig. 5) and it first occurs with small forms *of Discoaster druggii* (<15 µm). According to the original description, *D. druggii* is a large discoaster (larger than 15 µm). In this study, the base of Zone NN1 is drawn at the first occurrence of *D. druggii* (>15 µm). Forms similar to *S. aubryae* were reported, by Rio et al. (1990) from Leg 115 in the Indian Ocean *(S. dissimilis-S. belemnos* intergrade), ranging from the basal part of Zone NN2 and overlapping the range of *S. belemnos. S. aubryae* is not considered herein as being an intergrade *Sphenolithus,* since this form possesses some unique features (see "Appendix A"). *S. aubryae* was also observed, but not described by M.-P. Aubry (pers. comm., 1994)

Hole 899B: Sample 149-899B-3R-6, 59 cm.

FOs *Discoaster druggii* and *Helicosphaera granulata*

The abundance pattern, for Hole 900A, of the ranges *of D. druggii* (larger and smaller than 15 µm) is shown on Figure 15. *D. druggii* small is about 12 to 15 µm. At Hole 898A and 900A, small and large *D. druggii* occur together. At these two latter sites, the sampling resolution at this level is between two to three meters. In Hole 897C and 899B samples are closer, and small specimens of *D. druggii* are observed one meter below the occurrence of the large form. The FO of *H. granulata* is recorded with the FO of D. *druggii* at Hole 898A, and 899B, and few meters above, in the lower basal part of Zone NN2 at Holes 897C and 900A.

Hole 899B: Sample 149-899B-9R-5, 114cm.

FO of *Calcidiscus tropicus* (<6 µm)

The abundance pattern of the range of *C. tropicus* (<6 µm) for Hole 900A is shown on Figure 16. This form, easily distinguished by its relative large central opening, has a consistent FO in the lower part of Zone NN2. The FO of this small form of *Calcidiscus* is a reliable biohorizon, that has been found at the same level at the four sites.

Hole 898A: Sample 149-898A-26X-1, 102cm.

FO of *Sphenolithus cometa*

This species, easily distinguished from other *Sphenolithus* (see Appendix A), occurs in the middle part of Zone NN2, and may be helpful to precise the position of the LO of *Helicosphaera recta.*

Hole 899B: Sample 149-899B-3R-2, 103 cm.

LO of *Helicosphaera recta*

The abundance pattern of the range of *H. recta* for Hole 900A is shown on Figure 11. This species, which first occurs in the upper part of Zone NP22, has a consistent range throughout the early Miocene Zone NN1 to the middle of Zone NN2 and its LO is situated at the same level at the four Sites (Fig. 5). Martini and Worsley (1971) reported *H. recta (= H. truncata)* together with *D. druggii* in Zone NN2 from sediment recovered from the western equatorial Pacific (DSDP Hole 63-1), but use this taxon as the zonal marker for the top of Zone NP25 (defined in the same publication). Several authors also reported this species in the early Miocene Zones NN1 to NN2 (e.g., Perch-Nielsen, 1977). Gartner (1992) was probably the first to point out the important potential of this marker, and correlate the LO of *H. recta* with the chronozone C6Bn at DSDP Site 608 in the North Atlantic.

Near the top of its range, the two central openings *of H. recta* possess a slightly oblique bar, which may make the identification of the LO of *H. recta* difficult.

Hole 898A: Sample 149-898B-24X-4, 121 cm.

FO of *Geminilithella rotula*

The abundance pattern of the range of *G. rotula* for Hole 900A is shown on Figure 16 together with the range of *Umbilicosphaera jafari.* The FO of *G. rotula* was used by Theodoridis (1984) as a zonal marker in his Mediterranean biozonal schemes. Theodoridis (1984) defines a *Triquetrorhabdulus milowii* Zone from the first occurrence of *G. rotula* to the FO of *Sphenolithus heteromorphus* (or LO of *S. belemnos),* and *Triquetrorhabdulus martinii* Subzone from the FO of *G. rotula* to the LO of *Triquetrorhabdulus carinatus* (or FO of *Sphenolithus belemnos).* At the four Sites from Leg 149, the FO of G. *rotula* has been found very useful. The distinction of this biohorizon may be difficult because of the presence of large specimens of *Umbilicosphaera jafari (= Geminilithella jafari* Backman, 1980). Only specimens of *G. rotula* larger than 5 µm were considered.

Hole 898A: Sample 149-898A-24X-2, 28 cm.

LO of *Camuralithus pelliculatus*

This species has a consistent occurrence from the upper Oligocene to the upper part of Zone NN2. Its characteristic rim and central area make this marker easily identifiable, and its LO appears to be a good biohorizon. The slightly different position of the LO of *C. pelliculatus* in the four sites is caused by unfamiliarity in recognizing this new species.

Hole 899B: Sample 149-899B-2R-1, 35 cm.

Table 7. Stratigraphic distribution of calcareous nannofossil taxa in Hole 899B (Cores 149-899B-1R through 14R).

Age	Zone	Core, section, interval (cm)	Depth (mbsf)	Abundance	Preservation	Reworked Cretaceous	Reworking	*Bicolumnus ovatus*	*Blackites spinosus*	*Blackites tenuis*	*Braarudosphaera bigelowii*	*Branletteius serraculoides*	*Calcidiscus fuscus*	*Calcidiscus leptoporus*	*Calcidiscus pataecus*	*Calcidiscus radiatus*	*Calcidiscus tropicus* (< 6 µm)	*Calcidiscus tropicus* (> 6 µm)	*Camuralithus pelliculatus*	*Chiasmolithus altus*	*Chiasmolithus medius*	*Chiasmolithus oamaruensis*	*Chiasmolithus* spp.	*Clausicoccus fenestratus*	*Clausicoccus obrutus*	*Clausicoccus subdistichus*	*Coccolithus miopelagicus*	*Coccolithus pelagicus*	*Coccolithus streckeri*	*Coccolithus* sp. 1
early Miocene	NN2	1R-1, 138-139	231.88	C	M	P	.	.	.	.	.	.	.	.	P	.	P	P	.	.	.	.	.	.	.	.	P	F	.	.
		1R-2, 103-104	233.03	A	X	P	.	.	.	.	.	.	.	P	P	.	P	.	.	.	.	.	.	.	.	.	P	F	.	.
		1R-3, 32-33	233.82	A	X	P	.	.	.	.	.	.	.	P	R	.	R	P	P	.	.	.	.	.	.	.	P	F	P	.
		2R-1, 35-36	235.15	A	X	P	.	.	.	.	.	.	.	.	P	.	P	P	P	.	.	.	.	.	.	.	P	F	P	.
		2R-2, 88	237.18	A	X	P	.	.	.	.	.	.	.	.	P	.	P	.	P	.	.	.	.	.	.	.	P	F	.	.
		2R-3, 148-149	239.28	A	M	P	.	.	.	.	.	.	.	.	P	.	P	.	.	.	.	.	.	.	.	.	P	F	.	.
		23R-1, 16	244.56	A	X	P	.	.	.	.	.	.	.	.	.	P	P	.	P	.	.	.	.	.	.	.	P	R	.	.
		3R-1, 50-51	244.90	A	X	P	.	.	.	.	.	.	.	.	.	R	P	.	P	.	.	.	.	.	.	.	P	R	.	.
		3R-2, 103-104	246.93	A	X	P	.	.	.	.	.	.	.	.	.	.	P	.	P	.	.	.	.	.	.	.	P	R	.	.
		3R-4, 30	249.20	C	G	P	.	.	.	.	.	.	.	.	.	.	P	.	P	.	.	.	.	.	.	.	.	R	.	.
		3R-4, 124-125	250.14	A	X	P	.	.	.	.	.	.	.	.	.	.	.	.	.	.	.	.	.	.	.	.	P	F	.	.
		3R-5, 114-115	251.54	A	X	.	.	.	.	.	.	.	.	.	P	.	.	.	P	.	.	.	.	.	P	.	P	R	.	P
	NN1	3R-6, 59-60	252.49	A	X	P	.	.	.	.	.	.	.	.	P	P	.	.	P	.	.	.	.	.	.	.	P	R	.	P
		4R-2, 70-71	256.20	A	X	P	.	.	.	.	P	.	.	.	.	.	.	.	P	.	.	.	.	P	.	.	P	F	.	.
		4R-5, 54-55	260.54	A	X	P	.	.	.	.	.	.	.	.	.	.	.	.	R	.	.	.	.	.	.	.	P	F	.	.
		4R-6, 18	261.68	A	G	P	.	.	.	.	.	.	.	.	P	P	.	.	P	.	.	.	.	P	P	.	P	P	.	.
early Oligocene	NP25	5R-1, 16-17	263.86	A	G	P	.	.	.	.	P	.	.	.	P	.	.	.	P	.	.	.	.	P	P	.	P	P	.	P
		5R-1, 95-96	264.65	A	X	P	.	.	.	.	.	.	P	.	.	P	.	.	P	.	.	.	.	.	.	.	P	R	.	.
		5R-2, 62-63	265.82	A	X	P	.	.	.	.	.	.	P	.	.	P	.	.	P	.	.	.	.	.	.	.	R	C	.	.
		5R-3, 134-135	268.04	A	G	P	.	.	.	.	.	.	.	.	.	P	.	.	P	.	.	.	.	P	P	.	P	R	P	.
		5R-4, 128-129	269.48	A	G	P	.	.	.	.	.	.	P	.	.	R	.	.	P	.	.	.	.	R	R	.	P	F	.	.
		5R-5, 130-131	271.00	A	X	P	.	.	.	.	.	.	.	.	.	.	.	.	R	.	.	.	.	P	P	.	P	F	.	.
		5R-6, 15-16	271.35	A	E	.	.	.	.	.	.	.	.	.	.	P	.	.	.	.	.	.	.	P	F	.	P	F	.	.
		6R-1, 68-69	274.08	A	M	.	.	.	.	.	.	.	.	.	.	.	.	.	.	.	.	.	.	P	R	.	P	F	.	.
		6R-2, 75-76	275.65	V	P	.	.	.	.	.	.	.	.	.	.	.	.	.	.	.	.	.	.	R	.	R	.	C	.	.
		6R-3, 124-125	277.64	A	M	P	.	.	.	P	.	.	.	.	.	.	.	.	.	.	.	.	.	P	F	.	.	F	.	.
		6R-4, 145-146	279.35	V	M	P	P	P	.	.	.	.	.	.	.	.	.	.	.	.	.	.	.	P	.	P	.	C	.	.
		6R-5, 65-66	280.05	V	M	P	P	.	.	F	.	.	.	.	.	.	.	.	.	.	.	.	.	F	F	.	.	C	.	.
		7R-1, 34-35	283.34	A	M	P	P	P	.	.	.	.	.	.	.	.	.	.	.	.	.	.	.	R	R	.	.	F	.	.
		7R-2, 29-30	284.79	A	M	P	.	.	R	.	.	.	.	.	.	.	.	.	.	P	.	.	.	R	R	.	.	F	.	.
		7R-2, 122-123	285.72	V	M	P	.	P	.	.	.	.	.	.	.	.	.	.	.	.	.	.	.	R	.	R	.	F	.	.
		7R-3, 145-146	287.45	A	M	.	P	.	.	P	.	.	.	.	.	.	.	.	.	.	.	.	.	P	R	.	.	F	.	.
		7R-4, 72-73	288.22	V	M	P	.	P	.	.	.	.	.	.	.	.	.	.	.	.	.	.	.	R	.	.	.	C	.	.
		7R-5, 92-93	289.92	A	M	P	P	.	P	.	.	.	.	.	.	.	.	.	.	P	.	.	.	P	P	.	.	F	.	.
		7R-6, 126-127	291.76	A	M	F	P	.	.	.	.	.	.	.	.	.	.	.	.	.	.	.	.	R	.	.	.	C	.	.
		8R-1, 16-17	292.76	A	M	P	.	.	.	P	.	.	.	.	.	.	.	.	.	.	.	.	.	R	P	.	.	C	.	.
		8R-2, 23-24	294.33	V	M	P	F	P	.	.	.	.	.	.	.	.	.	.	.	.	.	.	.	P	.	P	.	C	.	.
		8R-2, 67-68	294.77	A	M	P	P	.	.	P	.	.	.	.	.	.	.	.	.	P	.	.	.	P	P	.	.	F	.	.
		8R-3, 44-45	296.04	A	V	P	.	.	.	.	P	.	.	.	.	.	.	.	.	.	.	.	.	R	.	.	.	C	.	.
		8R-4, 97-98	298.07	A	M	P	P	.	.	.	.	.	.	.	.	.	.	.	.	P	.	.	.	P	P	.	.	F	.	.
		8R-5, 21-22	298.81	A	V	.	.	P	.	.	.	.	.	.	.	.	.	.	.	.	.	.	.	P	.	.	.	F	.	.
		8R-6, 122-123	301.32	A	M	P	P	.	.	P	.	.	.	.	.	.	.	.	.	P	P	.	.	P	R	.	.	C	.	.
		9R-1, 19-20	302.49	A	P	P	.	.	.	.	.	.	.	.	.	.	.	.	.	.	.	.	.	P	.	P	.	F	.	.
		9R-2, 72-73	304.52	A	P	P	P	P	.	.	.	.	.	.	.	.	.	.	.	P	.	.	.	P	F	.	.	C	.	.
		9R-3, 83-84	306.13	A	P	.	.	P	.	.	.	.	.	.	.	.	.	.	.	P	.	.	.	R	.	.	P	F	.	.
		9R-4, 60-61	307.40	A	M	.	.	.	P	.	P	.	.	.	.	.	.	.	.	P	P	.	.	P	C	.	.	C	.	.
		9R-5, 21-22	308.51	A	P	R	.	.	.	.	.	.	.	.	.	.	.	.	.	P	.	.	.	P	R	P	P	C	.	.
		9R-6, 15-16	309.95	A	M	.	.	.	.	.	.	P	.	.	.	.	.	.	.	P	P	P	.	F	F	.	.	F	.	.
	NP24	10R-2, 147-148	314.97	V	P	P	.	.	.	.	.	.	.	.	.	.	.	.	.	P	.	.	.	P	.	.	R	C	.	.
		10R-5, 23-24	318.23	V	P	P	P	.	F	.	.	.	.	.	.	.	.	.	.	.	R	P	.	R	F	.	.	C	.	.
		11R-3, 90-91	325.50	V	M	R	P	.	P	.	.	.	.	.	.	.	.	.	.	P	.	.	.	R	C	.	.	A	.	.
	NP23	11R-5, 29-30	327.89	A	M	P	.	P	.	.	.	.	.	.	.	.	.	.	.	P	.	.	P	P	.	.	.	C	.	.
		12R-2, 139-140	334.09	A	M	.	.	.	.	.	.	P	.	.	.	.	.	.	.	.	P	.	P	P	R	.	.	C	.	.
		12R-5, 43-44	337.63	V	M	P	.	.	.	.	.	.	.	.	.	.	.	.	.	.	.	.	.	.	R	R	P	C	.	.
		13R-1, 141-142	342.31	A	M	.	.	.	.	.	.	.	.	.	.	.	.	.	.	.	.	.	.	.	R	R	.	C	.	.
	NP 22	14R-2, 15-16	352.25	A	M	P	.	P	.	P	.	P	.	.	.	.	.	.	P	.	.	.	.	.	F	F	.	C	.	.
		14R-4, 105-106	356.15	V	M	.	.	.	.	.	.	R	.	.	.	.	.	.	.	.	.	.	.	.	P	.	.	A	.	.

LO of *Ilselithina fusa*

The abundance pattern range of *I. fusa* at Hole 900A is shown on Figure 10. This species has a consistent occurrence from the upper part of Zone NP21 to the upper part of Zone NN2. This biohorizon is used on Figure 9 to correlate the four sites. The LO of *I. fusa* is recorded above the LO of *H. recta,* at the level of the FO of *G. rotula* or slightly above. Gartner (1992) used *I. fusa* as a marker, and mentions the presence of two morphotypes in lower Miocene sediments from ODP Site 608: one morphotype, present from the Oligocene, with 12 to 14 petals in the basal cycle of elements, and a second one, restricted to the lower Miocene with six elements. The specimens recovered from lower Miocene sediments from Leg 149 have 10 to 14 proximal elements, and are clearly identifiable by their robust distal spine (crown), which has only 5 to 7 elements (see transferred specimen Pl. 12, figs. 22-26).

Hole 899B: Sample 149-899B-1R-2, 104cm.

LO of *Helicosphaera euphratis*

This large, distinctive helicolith has a consistent LO between the LO of *I. fusa* and the FO of *Reticulofenestra pseudoumbilicus* at the four Sites from Leg 149. Although rare near the top of its range, the LO *of H. euphratis* (large morphotype) is a useful biohorizon in the upper Zone NN2. The abundance pattern range of *H. euphratis* is shown on Figure 11.

Table 7 (continued).

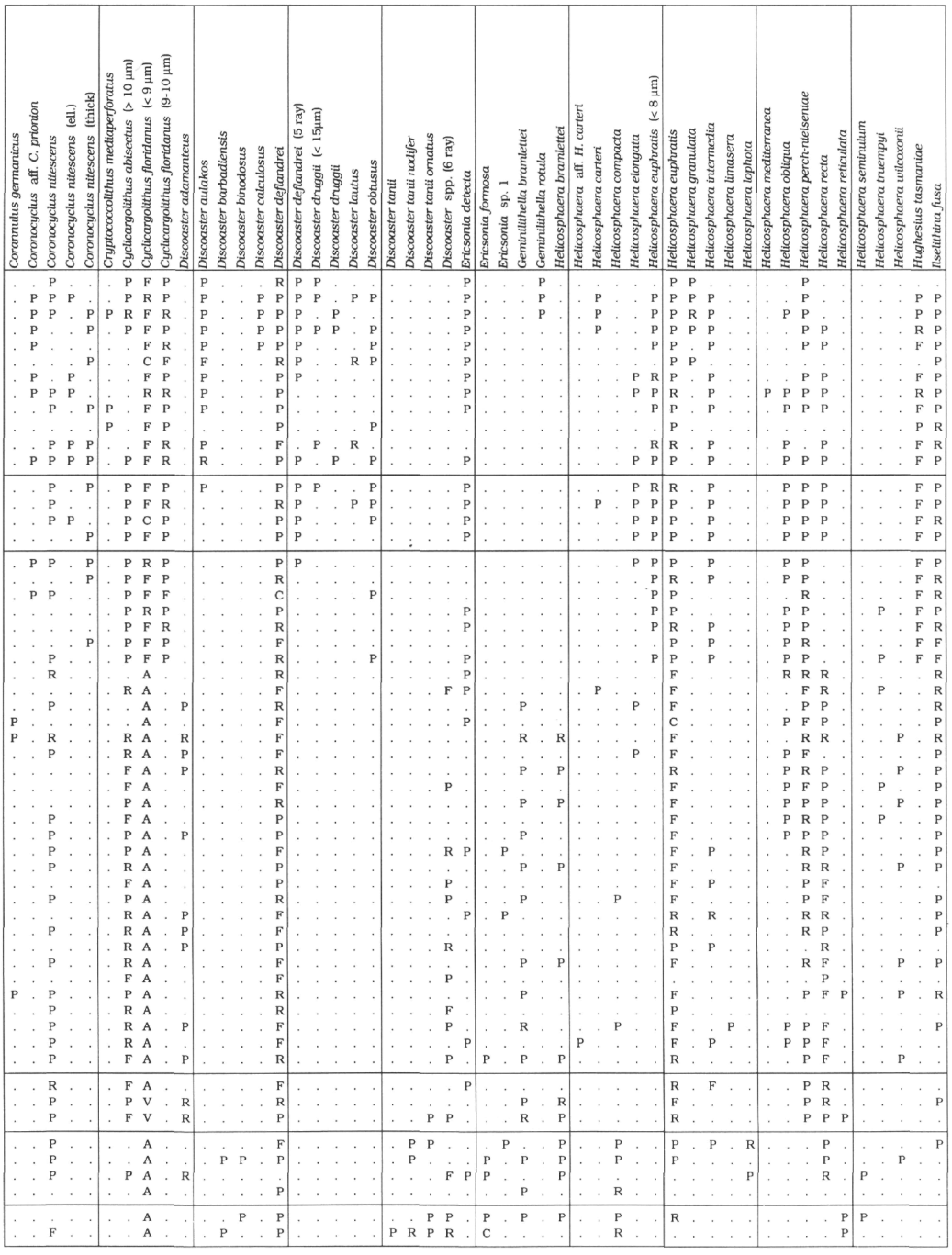

Hole 898A: Sample 149-898A-23X-5, 70 cm.

LO of *Sphenolithus conicus*

Though *S. conicus* is rare and sporadic in lower Miocene sediments from Leg 149, the LO of this species is recorded in the upper part of Zone NN2. The placement of this biohorizon is in concordance with the position of the LO of *S. conicus* documented below the FO of *S. belemnos* by Gartner (1992). Fornaciari et al. (1990) reported the LO of *S. conicus* at the level of *S. belemnos*.

Hole 898A: Sample 149-898A-23X-4, 51 cm.

FO of *Reticulofenestra pseudoumbilicus* (>7 µm)

Only specimens larger than 7 µm, with an open central area, are included in *R. pseudoumbilicus* (see Young et al., 1994). Smaller forms are either included in *Reticulofenestra minutula* or in *Reticulofenestra haqii* according to the outline and size of the central area (Backman, 1980; Flores, 1989). In the upper part of Zone NN2, *Reticulofenestra lockeri* becomes less common, and *R. minuta* increases in size to more than 7 µm. The abundance pattern of the ranges of *R. pseudoumbilicus* and *R. gelida* (form with a small opening) for Hole 900A are shown on Figure 17. Sharp first occurrence picks at slightly different levels are observed for both *R. pseudoumbilicus*

Table 7 (continued).

Age	Zone	Core, section, interval (cm)	Depth (mbsf)	Abundance	Preservation	*Isthmolithus recurvus*	*Lanternithus minutus*	*Micrantholithus aequalis*	*Orthozygus aureus*	*Pemma papillata*	*Pontosphaera anisotrema*	*Pontosphaera callosa*	*Pontosphaera enormis*	*Pontosphaera longiforaminis*	*Pontosphaera multipora*	*Pontosphaera segmenta*	*Pontosphaera* spp.	*Pyrocyclus hermosus*	*Pyrocyclus inversus*	*Pyrocyclus orangensis*	*Reticulofenestra bisecta bisecta*	*Reticulofenestra bisecta fileuiczii*	*Reticulofenestra circus*	*Reticulofenestra daviesi*	*Reticulofenestra hampdenensis*	*Reticulofenestra* cf. *R. haqii*	*Reticulofenestra haqii*	*Reticulofenestra hesslandii*	*Reticulofenestra lockeri*	*Reticulofenestra minuta*
early Miocene	NN2	1R-1, 138-139	231.88	C	M	.	.	.	.	.	.	.	.	.	P	.	.	.	.	P	.	.	.	.	.	.	F	.	P	P
		1R-2, 103-104	233.03	A	X	.	.	.	.	.	.	.	.	.	P	.	.	.	.	P	.	.	.	.	.	.	F	.	P	.
		1R-3, 32-33	233.82	A	X	.	.	.	.	.	.	.	.	.	P	.	.	.	.	P	.	.	.	.	.	.	F	.	P	P
		2R-1, 35-36	235.15	A	X	.	.	.	.	.	P	.	.	.	P	.	.	.	.	P	.	.	.	.	.	.	F	.	P	R
		2R-2, 88	237.18	A	X	.	.	.	.	.	.	.	.	.	P	.	.	P	.	P	.	.	.	.	.	.	F	.	P	P
		2R-3, 148-149	239.28	A	M	.	.	.	.	.	.	.	.	.	.	.	.	.	.	P	.	.	.	.	.	.	C	.	P	.
		23R-1, 16	244.56	A	X	.	.	.	.	.	P	.	.	.	P	.	.	P	.	P	.	.	.	.	.	.	F	.	P	R
		3R-1, 50-51	244.90	A	X	.	.	.	.	.	P	.	.	.	P	.	.	P	.	P	.	.	.	.	.	.	F	.	P	R
		3R-2, 103-104	246.93	A	X	.	.	.	.	.	.	.	.	P	P	.	.	P	.	.	.	.	.	.	.	.	F	.	P	F
		3R-4, 30	249.20	C	G	.	.	.	.	.	.	.	.	.	P	.	.	.	.	.	.	.	.	.	.	.	F	.	.	P
		3R-4, 124-125	250.14	A	X	.	.	.	.	.	.	.	.	.	R	.	.	.	.	.	.	.	.	.	.	.	C	P	P	F
		3R-5, 114-115	251.54	A	X	.	.	.	.	.	.	.	.	.	P	.	.	.	.	P	.	.	.	.	.	.	C	.	P	R
	NN1	3R-6, 59-60	252.49	A	X	.	.	.	.	.	.	.	.	.	P	.	.	P	.	P	.	.	.	.	.	.	C	P	P	.
		4R-2, 70-71	256.20	A	X	.	.	.	.	.	.	P	.	.	P	.	.	.	.	P	.	.	.	.	.	.	F	.	.	R
		4R-5, 54-55	260.54	A	X	.	.	.	.	.	.	P	.	.	P	.	.	.	.	P	.	.	.	.	.	.	C	.	.	F
		4R-6, 18	261.68	A	G	.	.	.	P	.	.	.	.	P	P	.	.	.	.	.	.	P	.	.	.	.	F	P	P	R
	NP25	5R-1, 16-17	263.86	A	G	.	.	P	P	.	.	P	.	P	P	.	.	.	.	.	P	P	.	.	.	.	F	P	P	.
		5R-1, 95-96	264.65	A	X	.	.	.	P	.	P	P	.	P	P	P	.	.	.	P	P	P	.	.	.	.	C	P	P	P
		5R-2, 62-63	265.82	A	X	.	.	.	P	.	.	.	.	.	P	.	.	.	R	.	P	P	.	.	.	.	A	.	R	.
		5R-3, 134-135	268.04	A	G	.	.	.	P	.	.	.	P	P	P	.	.	.	.	.	P	P	.	.	.	.	F	P	P	.
		5R-4, 128-129	269.48	A	G	.	.	.	P	.	.	.	P	P	P	.	.	.	P	.	.	P	.	.	.	.	C	R	P	.
		5R-5, 130-131	271.00	A	X	.	.	.	R	.	.	.	.	P	P	.	.	.	P	.	.	P	.	.	.	.	C	.	P	.
		5R-6, 15-16	271.35	A	E	.	.	.	.	.	.	.	.	P	.	P	.	.	P	P	P	P	.	P	.	.	C	P	P	.
		6R-1, 68-69	274.08	A	M	.	.	.	P	.	.	.	.	.	R	.	F	.	.	.	R	P	.	R	P	.	.	R	.	.
		6R-2, 75-76	275.65	V	P	.	.	.	.	.	.	.	.	.	.	.	R	.	.	.	.	R	.	F	.	.	.	.	.	.
		6R-3, 124-125	277.64	A	M	.	.	.	.	.	.	.	.	.	P	.	R	.	.	.	P	R	.	P	R	.	.	.	.	.
		6R-4, 145-146	279.35	V	M	.	.	.	P	.	.	.	.	.	.	.	F	.	.	.	.	P	.	R	.	.	.	.	.	.
		6R-5, 65-66	280.05	V	M	.	.	.	.	.	.	.	.	.	.	.	R	.	.	.	R	F	.	P	F	.	.	R	.	.
		7R-1, 34-35	283.34	A	M	.	.	.	P	.	.	.	.	.	.	.	F	.	.	.	.	R	.	F	R	.	.	.	.	.
		7R-2, 29-30	284.79	A	M	.	.	.	R	.	.	.	.	.	.	.	R	.	.	.	P	P	.	R	.	.	.	.	.	.
		7R-2, 122-123	285.72	V	M	.	.	.	P	.	.	.	.	.	.	.	F	.	.	.	.	P	.	F	.	.	.	.	.	.
		7R-3, 145-146	287.45	A	M	.	.	.	P	.	.	.	.	.	.	.	P	.	.	.	P	P	.	.	P	.	.	P	.	.
		7R-4, 72-73	288.22	V	M	.	.	.	.	.	.	.	.	.	.	.	P	.	.	.	.	R	.	.	P	.	.	.	.	.
		7R-5, 92-93	289.92	A	M	.	.	.	P	.	.	.	.	.	P	.	P	.	.	.	P	P	.	.	P	.	.	.	.	.
		7R-6, 126-127	291.76	A	M	.	.	.	P	.	.	.	.	.	.	.	F	.	.	.	.	P	.	P	.	.	.	.	.	.
		8R-1, 16-17	292.76	A	M	.	.	P	.	.	.	.	.	.	P	.	P	.	.	.	P	P	.	P	P	.	.	R	.	.
		8R-2, 23-24	294.33	V	M	.	.	.	P	.	.	.	.	.	.	.	R	.	.	.	P	P	.	R	.	.	.	.	.	.
		8R-2, 67-68	294.77	A	M	.	.	.	.	.	.	.	.	.	P	.	R	.	.	.	P	.	.	P	P	.	.	P	.	.
		8R-3, 44-45	296.04	A	V	.	.	.	P	.	.	.	.	.	.	.	R	.	.	.	.	P	.	P	P	.	.	.	.	.
		8R-4, 97-98	298.07	A	M	.	.	.	.	.	.	.	.	.	P	.	.	.	.	.	R	F	.	P	P	.	.	.	.	.
		8R-5, 21-22	298.81	A	V	.	.	.	.	.	.	.	.	.	.	.	P	.	.	.	.	P	.	R	.	.	.	.	.	.
		8R-6, 122-123	301.32	A	M	.	.	.	P	.	.	.	.	.	.	.	R	.	.	.	R	.	.	P	R	.	.	P	.	.
		9R-1, 19-20	302.49	A	P	.	.	.	.	.	.	.	.	.	.	.	.	.	.	P	.	.	.	P	.	R	.	.	.	.
		9R-2, 72-73	304.52	A	P	.	.	.	P	.	.	.	.	.	R	.	P	.	.	.	P	R	.	P	R	.	.	R	.	.
		9R-3, 83-84	306.13	A	P	.	.	.	.	.	.	.	.	.	.	.	.	.	.	.	.	P	.	P	P	.	.	.	.	.
		9R-4, 60-61	307.40	A	M	.	.	.	P	.	.	.	.	.	P	.	F	.	.	.	P	R	.	P	F	.	.	P	.	.
		9R-5, 21-22	308.51	A	P	.	.	.	P	.	.	.	.	.	.	.	F	.	.	.	R	R	.	R	R	.	.	.	.	.
		9R-6, 15-16	309.95	A	M	.	.	.	P	.	.	.	.	.	P	.	R	.	.	.	.	P	.	R	R	.	.	.	.	.
	NP24	10R-2, 147-148	314.97	V	P	.	.	.	.	.	.	.	.	.	.	.	P	.	.	.	.	P	P	F	R	.	.	.	.	.
		10R-5, 23-24	318.23	V	P	.	.	.	.	.	.	.	.	.	.	.	P	.	.	.	.	R	.	P	F	.	.	.	.	.
		11R-3, 90-91	325.50	V	M	.	.	.	.	.	.	.	.	.	.	.	P	.	.	.	.	R	.	P	F	.	.	.	.	.
early Oligocene	NP23	11R-5, 29-30	327.89	A	M	.	.	.	.	.	.	.	.	.	.	.	P	.	.	.	.	P	.	P	P	.	.	.	.	.
		12R-2, 139-140	334.09	A	M	.	.	.	P	P	.	.	.	.	.	.	P	.	.	.	.	P	.	R	R	.	.	.	.	.
		12R-5, 43-44	337.63	V	M	.	.	.	.	.	.	.	.	.	.	.	.	.	.	.	.	R	.	R	P	.	.	.	.	.
		13R-1, 141-142	342.31	A	M	.	.	.	.	.	.	.	.	.	.	.	.	.	.	.	.	R	.	.	F	.	.	.	.	.
	NP 22	14R-2, 15-16	352.25	A	M	P	.	.	P	.	.	.	.	.	.	.	.	.	.	.	.	.	.	F	F	.	.	.	.	.
		14R-4, 105-106	356.15	V	M	F	F	.	.	P	.	.	.	.	.	.	R	.	.	.	.	P	.	.	F	.	.	R	.	.

and *R. gelida* and both species show a sporadic occurrence to the upper part of Zone NN5.

Hole 898A: Sample 149-898A-22X-5, 86 cm.

FO of *Triquetrorhabdulus serratus*

Triquetrorhabdulus serratus occurs at two different levels: first from the upper part of Zone NN2 to the lower part of Zone NN4, and second from Zone NN5 to its LO in Zone NN6

Hole 900A: Sample 149-900A-25R-5, 37 cm.

FOs of *Helicosphaera ampliaperta* and *Sphenolithus belemnos,* and the LO of *Triquetrorhabdulus challengeri*

The FOs of *H. ampliaperta* and *S. belemnos* are observed at the same level in Holes 898A, 899A, and 900A. These events are recorded in the upper part of Zone NN2, just above the FO of *T. serratus.* The LO of *T. challengeri* and the FO of *H. ampliaperta* are recorded together in Hole 897C, and within a short interval in other sites.

Hole 900A: Sample 149-900A-24R-4, 19 cm.

Table 7 (continued).

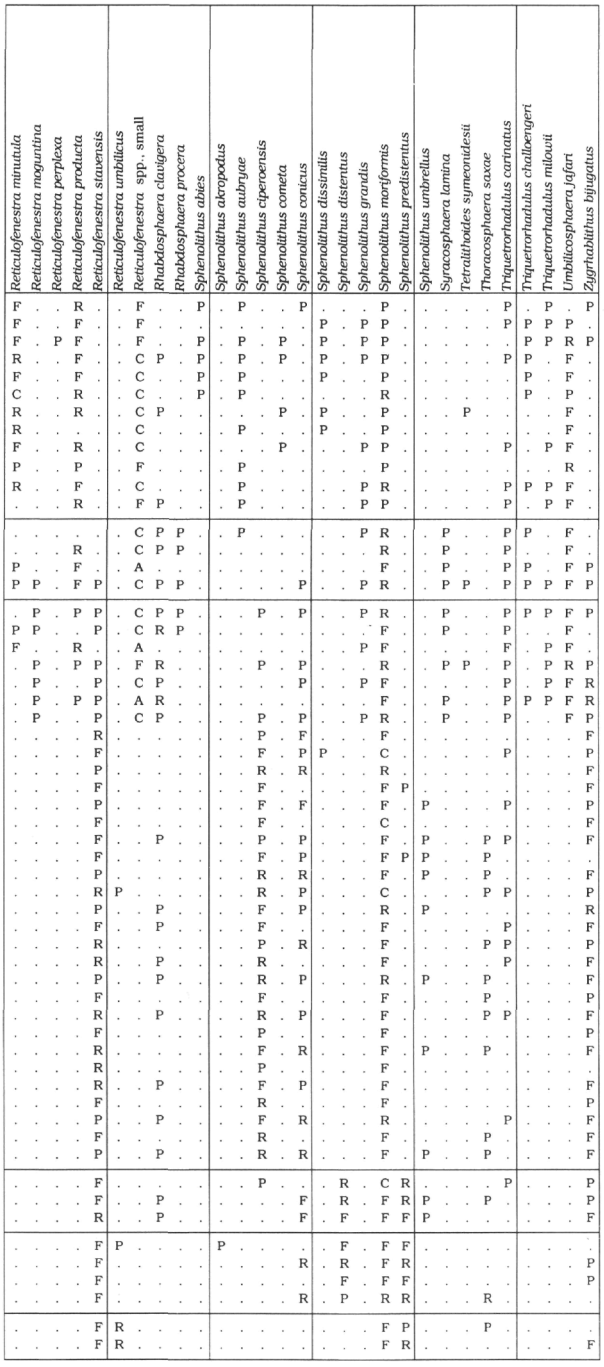

LO of *Sphenolithus aubryae*

The LO of *S. aubryae* is recorded within the lower part of the range of *S. belemnos.*

Hole 898A: Sample 149-898A-22X-4, 35 cm.

LO of *Hughesius tasmaniae*

The LO of *H. tasmaniae* near the top of Zone NN2 is consistent between the four sites, and is considered as a good biohorizon. The abundance pattern of the range of this species is shown on Figure 14.

Hole 898A: Sample 149-898A-22X-3, 100cm.

LO of *Triquetrorhabdulus carinatus*

The LO of *T. carinatus* occurs just below the LO of *S. belemnos* at Sites 898 and 900. At Site 897, the interval corresponding to this interval was not recovered. Core 149-897C-32R was lost. At Site 899, the LOs of *H. tasmaniae, T. carinatus,* and *S. belemnos* occur in the same sample, and they may indicate the presence of a condensed interval.

Hole 898A: Sample 149-898A-22X-2, 73 cm.

FO of *Helicosphaera scissura*

This bioevent is observed in the upper part of Zone NN3 at Sites 897, 898, and 900.

Hole 898A: Sample 149-898A-21-CC.

LO of *Sphenolithus belemnos*

The LO of *S. belemnos* is shown for Site 900 on Figure 13. The same abundance pattern is observed at the other sites. No overlap between the range of *S. heteromorphus* and *S. belemnos* are observed. These two bioevents are close, but always separated by a short interval.

Hole 900A: Sample 149-900A-24R-2, 128 cm.

FO of *Sphenolithus heteromorphus*

The abundance pattern of the range of *S. heteromorphus* for Hole 900A is shown on Figure 13 together with the range of *S. belemnos.*

Hole 900A: Sample 149-900A-24R-2, 61 cm.

LO of *Sphenolithus dissimilis*

The upper part of the range of *Sphenolithus dissimilis* has a very short overlap with the lower range of *S. heteromorphus.*

Hole 900A: Sample 149-900A-23R-6, 83 cm.

FO of *Cryptococcolithus mediaperforatus*

Small specimens of *C. mediaperforatus* (<5 µm) are present in Zone NN4. Larger forms occur after the LO of *H. ampliaperta* in Zone NN5.

Hole 900A: Sample 149-900A-23R-3, 101 cm.

FO *of Discoaster moorei*

This distinctive species *of Discoaster* first occurs in the lower part of Zone NN4.

Hole 900A: Sample 149-900A-23R-2, 137 cm.

FO of *Calcidiscus premacintyrei* (<9 µm)

The FO of *C. premacintyrei* (<9 µm) is detected in the upper part of Zone NN4. The abundance pattern and the range of *C. premacintyrei* (smaller and larger than 9 µm) are given on Figure 16 for Hole 900A. A sharp increase of *C. premacintyrei* is observed in both small and large forms at the end of Zone NN5.

Hole 899B: Sample 149-899B-14R-1, 110 cm.

FO *of Discoaster petaliformis* and *Discoaster exilis*

These two distinct forms of discoaster occur together at Sites 898 and 899.

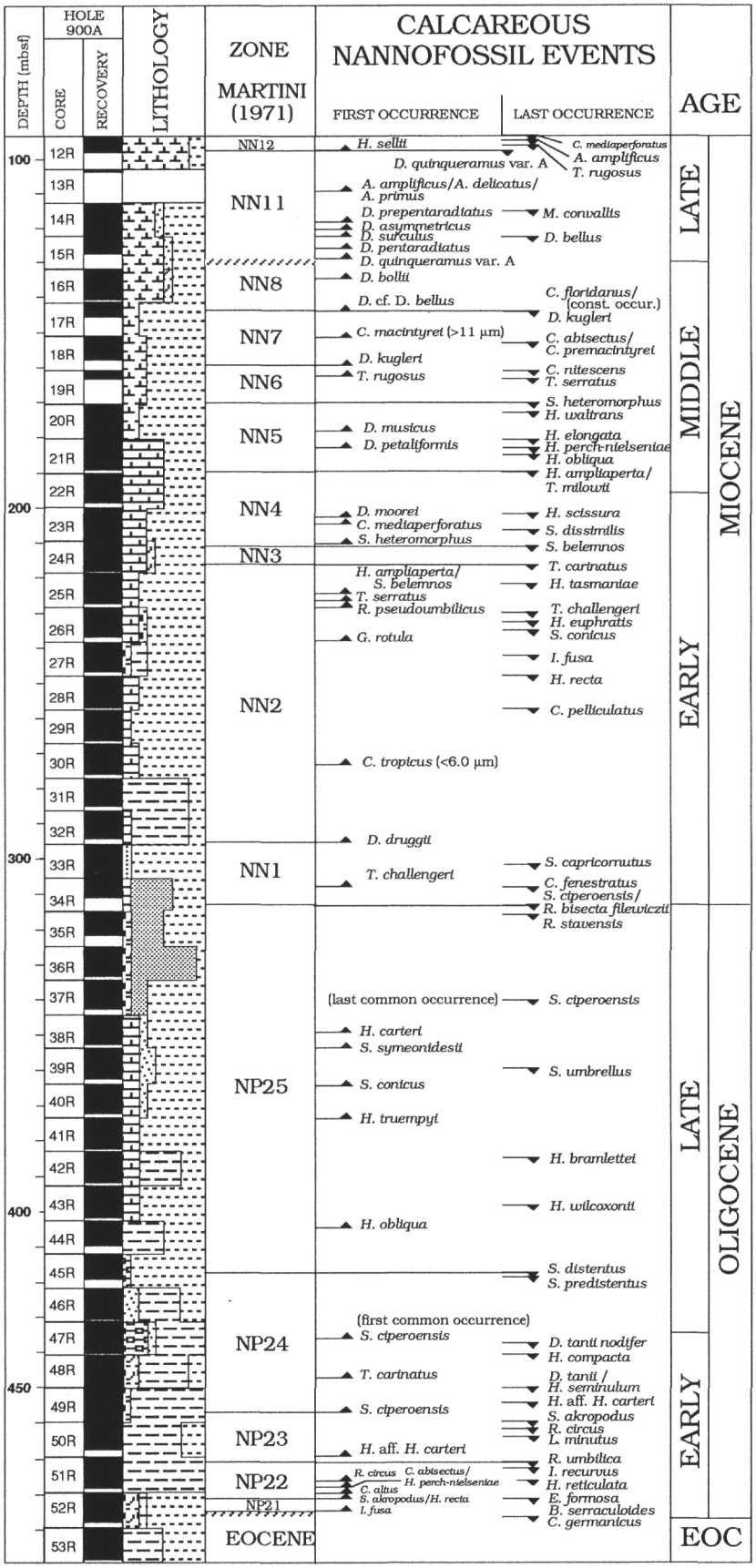

Figure 7. Calcareous nannofossil biostratigraphic summary of the Oligocene-Miocene interval of Hole 900A. See Figure 2 for symbol explanations.

Table 8. Summary of the key nannofossil biohorizons in Hole 900A.

Calcareous Nannofossil Event	Interval (cm)	Depth (mbsf)
Hole 900A		
C. mediaperforatus LO	11R-CC/12R-1, 48	93.59
C. miopelagicus (>13 µm) LO	11R-CC/12R-1, 48	93.59
A. amplificus LO	12R-1, 48/12R-1, 112	94.20
D. deflandrei LO	12R-1, 112/12R-2, 106	95.24
T. rugosus LO	12R-2, 106/12R-4, 10	96.98
H. sellii FO	12R-4, 10/12R-CC	98.15
D. quinqueramus var. A LO	12R-4, 10/12R-CC	98.15
A. amplificus FO	13R-CC/14-1, 50	103.07
A. delicatus FO	13R-CC/14-1, 50	103.07
A. primus FO	13R-CC/14-1, 50	103.07
M. convallis LO	14R-1, 50/14R-3, 63	114.76
D. prepentaradiatus FO	14R-5, 54/14R-5, 142	119.68
D. asymmetricus FO	14R-5, 142/14R-6, 66	120.49
D. surculus FO	14R-6, 66/14R-6, 112	121.09
D. bellus LO	14R-6, 112/14R-7, 44	121.73
D. pentaradiatus FO (consistent occ.)	15R-3, 30/15R-4, 3	126.31
D. quinqueramus var. A FO	15R-4, 43/15R-CC	127.46
Unconformity (TB 3.1)		
D. bollii FO	16R-2, 71/16R-3, 2	134.61
C. floridanus LO (consistent occ.)	17R-2, 89/17R-3, 7	144.33
D. kugleri LO	17R-2, 89/17R-3, 7	144.33
C. macintyrei FO	17R-3, 52/18R-1, 72	148.57
C. abisectus (>10 µm) LO	18R-1, 72/18R-2, 48	152.65
C. premacintyrei LO	18R-1, 72/18R-2, 48	152.65
D. kugleri FO	18R-5, 18/19R-1, 13	159.25
C. nitescens LO	19R-1, 13/19R-1, 99	161.46
T. rugosus FO	19R-1, 99/19R-2, 75	162.64
T. serratus LO	19R-2, 75/19R-CC	163.22
S. heteromorphus LO	19R-CC/20R-1, 26	167.08
H. elongata LO	20R-7, 38/21R-1, 97	180.62
H. perch-nielseniae LO	21R-1, 97/21R-1, 142	181.49
H. obliqua LO	21R-2, 41-21R-3, 139	183.45
T. milowii LO	21R-6, 38/22R-1, 122	189.65
H. ampliaperta LO	21R-6, 38/22R-1, 122	189.65
H. scissura LO	23R-1, 94/23R-2, 137	201.40
D. moorei FO	23R-2, 137/23R-3, 101	202.94
C. mediaperforatus FO	23R-3, 101/23R-4, 126	204.38
D. exilis FO	23R-3, 101/23R-4, 126	204.38
S. dissimilis LO	23R-5, 116/23R-6, 83	207.24
S. heteromorphus FO	24R-1, 107/24R-2, 61	210.79
S. belemnos LO	24R-2, 61/24R-2, 128	211.64
H. scissura FO	24R-3, 34/24R-3, 110	212.92
H. mediterranea LO	24R-4, 8/24R-5, 44	214.71
T. carinatus LO	24R-4, 8/24R-5, 44	214.71
H. tasmaniae LO	25R-2, 20/25R-2, 143	221.11
S. belemnos FO	25R-4, 19/25R-5, 37	224.33
H. ampliaperta FO	25R-4, 19/25R-5, 37	224.33
T. serratus FO	25R-5, 37/25R-6, 7	225.77
R. pseudoumbilicus FO	25R-5, 37/25R-6, 7	225.77
T. challengeri LO	26R-1, 43/26R-2, 136	230.04
Z. bijugatus LO	26R-2, 136/26R-4, 30	232.00
Unconformity (TB 3.1)		
H. euphratis LO	26R-2, 136/26R-4, 30	232.00
S. conicus LO	26R-4, 30/26R-5, 49	233.59
G. rotula FO	26R-6, 37/27R-1, 37	237.14
I. fusa LO	27R-3, 33/27R-4, 129	242.66
H. recta LO	27R-5, 110/28R-2, 56	247.53
C. pelliculatus LO	28R-5, 61/29R-1, 121	256.56
O. aureus LO	28R-5, 61/29R-1, 121	256.56
D. druggii FO	32R-6, 112/33R-1, 50	295.31
S. capricornutus LO	33R-4, 24/33R-5, 129	302.01
C. fenestratus LO	34R-1, 82/34R-2, 83	307.17
T. challengeri FO	34R-1, 82/34R-2, 83	307.17
R. bisecta filewiczii LO	34R-3, 121/35R-1, 125	313.18
S. ciperoensis LO	34R-3, 121/35R-1, 125	313.18
R. stavensis LO	35R-1, 125/35R-2, 121	317.28
S. ciperoensis LCO	37R-1, 90/37R-5, 53	338.26
H. carteri FO	38R-3, 136/38R-5, 47	349.61
T. symeonidesii FO	38R-5, 47/39R-1, 24	352.35
S. umbrellus LO	39R-3, 109/39R-4, 107	358.63
S. conicus FO	39R-6, 85/40R-2, 116	364.15
H. truempyi FO	40R-2, 116/41R-1, 40	369.88
H. bramlettei LO	42R-1, 57/42R-2, 76	384.31
Ericsonia sp. 1 LO	43R-1, 86/43R-2, 80	393.88
H. obliqua FO	44R-1, 131/44R-2, 18	403.80
S. distentus LO	45R-3, 123/45R-4, 112	416.90
S. predistentus LO	45R-4, 112/45R-5, 82	418.24
S. ciperoensis FCO	47R-3, 64/47R-4, 27	435.30
D. tanii nodifer LO	47R-6, 119/48R-2, 131	441.60
H. compacta LO	47R-6, 119/48R-2, 131	441.60
T. carinatus FO	48R-4, 142/48R-5, 103	447.07
D. tanii LO	48R-6, 16/49R-1, 52	449.49
H. seminulum LO	48R-6, 16/49R-1, 52	449.49
H. aff. H. carteri LO	49R-2, 44/49R-3, 113	453.23
H. compacta LCO	49R-3, 113/49R-4, 99	455.01
S. ciperoensis FO	49R-3, 113/49R-4, 99	455.01
S. akropodus LO	49R-7, 18/50R-2, 63	460.84
R. circus LO	50R-2, 63/50R-2, 120	462.31
L. minutus LO	50R-3, 15//50R-3, 129	463.62
E. detecta FO	50R-3, 129/50R-4, 16	464.37
H. aff. *H. carteri* FO	50R-5, 16/51R-1, 60	468.21
R. umbilicus LO	51R-1, 60/51R-2, 24	471.07
I. recurvus LO	51R-2, 24/51R-3, 50	472.52
R. circus FO	51R-3, 50/51R-4, 9	473.94
H. reticulata LO	51R-3, 50/51R-4, 9	473.94
H. perch-nielseniae FO	51R-4, 9/51R-5, 120	475.79
C. abisectus (>10 µm) FO	51R-4, 9/51R-5, 120	475.79
C. altus FO	51R-5, 120/51R-6, 47	477.48
B. ovatus FO	51R-5, 120/51R-6, 47	477.48
H. recta FO	51R-6, 47/52R-4, 143	481.50
S. akropodus FO	51R-6, 47/52R-4, 143	481.50
E. formosa LO	51R-6, 47/52R-4, 143	481.50
B. serraculoides LO	51R-6, 47/52R-4, 143	481.50
I. fusa FO	52R-3, 65/52R-4, 143	483.99
C. germanicus LO	52R-4, 143/52R-5, 86	485.59

Note: Table 2 for explanation.

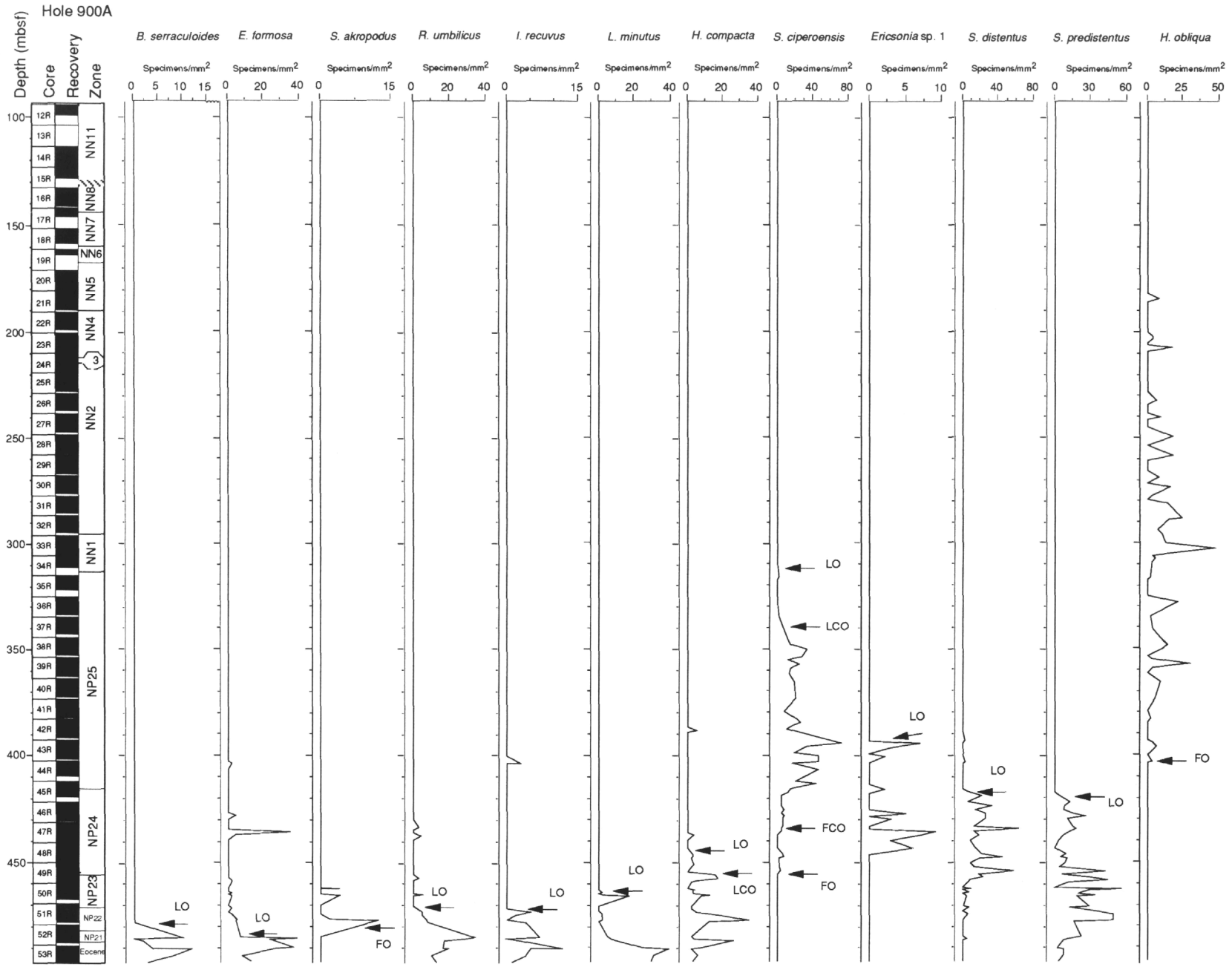

Figure 8. Abundance plot of the main Oligocene taxa in Hole 900A. The abundance scale is expressed as number of specimens per mm^2. LO = last occurrence, LCO = last common occurrence, FO = first occurrence, FCO = first common occurrence.

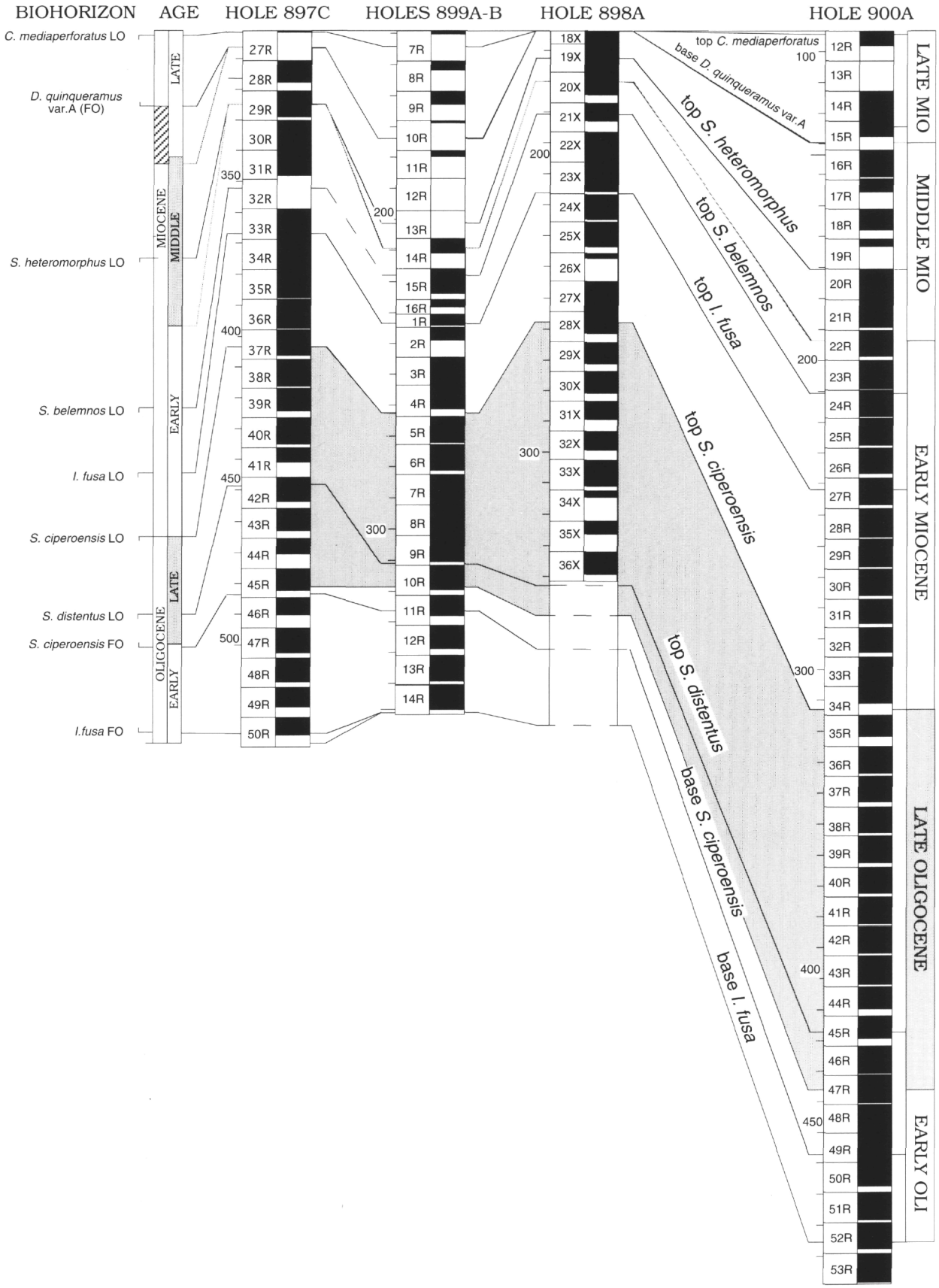

Figure 9. Oligocene-Miocene correlations among Leg 149 sites based on calcareous nannofossils. Major stratigraphic boundaries and some major biostratigraphic events are indicated.

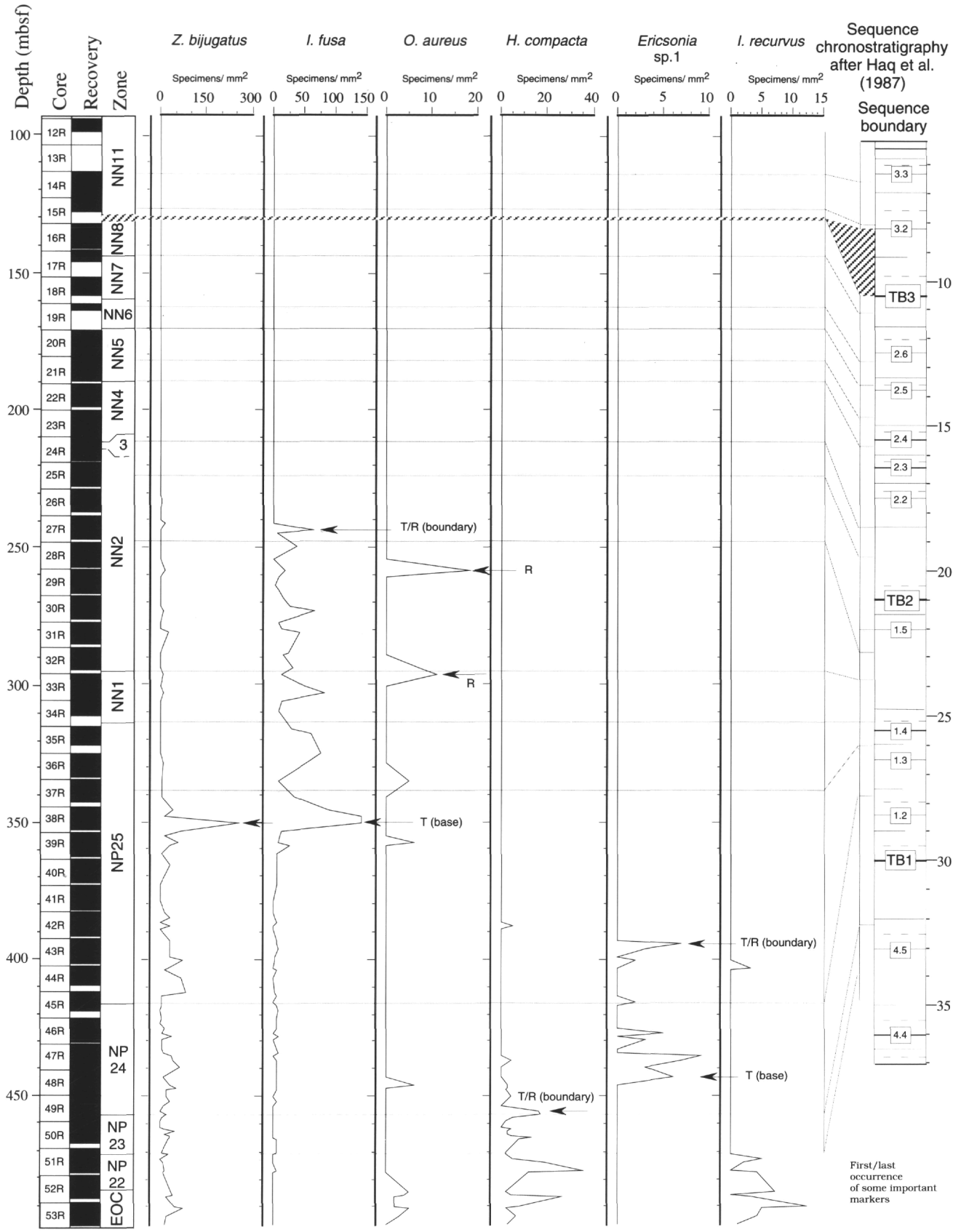

Figure 10. Correlations in Hole 900A of the abundance pattern for some holococcolith species and additional early Oligocene bioevents with the sequence chronostratigraphy of Haq et al. (1987). Horizontal lines represent the major bioevents. R = regressive; T = transgressive; T/R = maximum flooding surface.

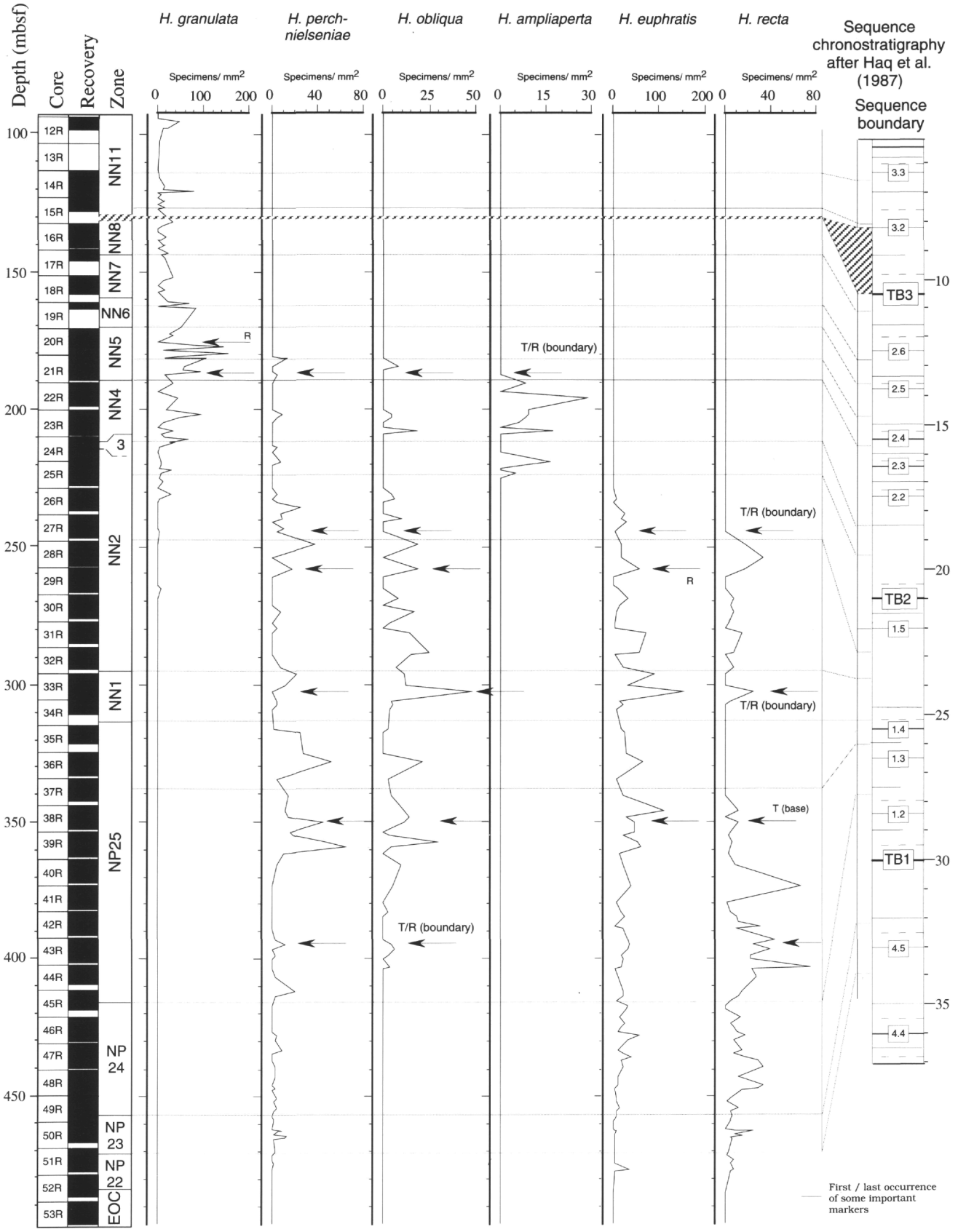

Figure 11. Correlations in Hole 900A of the abundance pattern of *Helicosphaera* species with the sequence chronostratigraphy of Haq et al. (1987). Horizontal lines represent the major bioevents. R = regressive; T = transgressive.

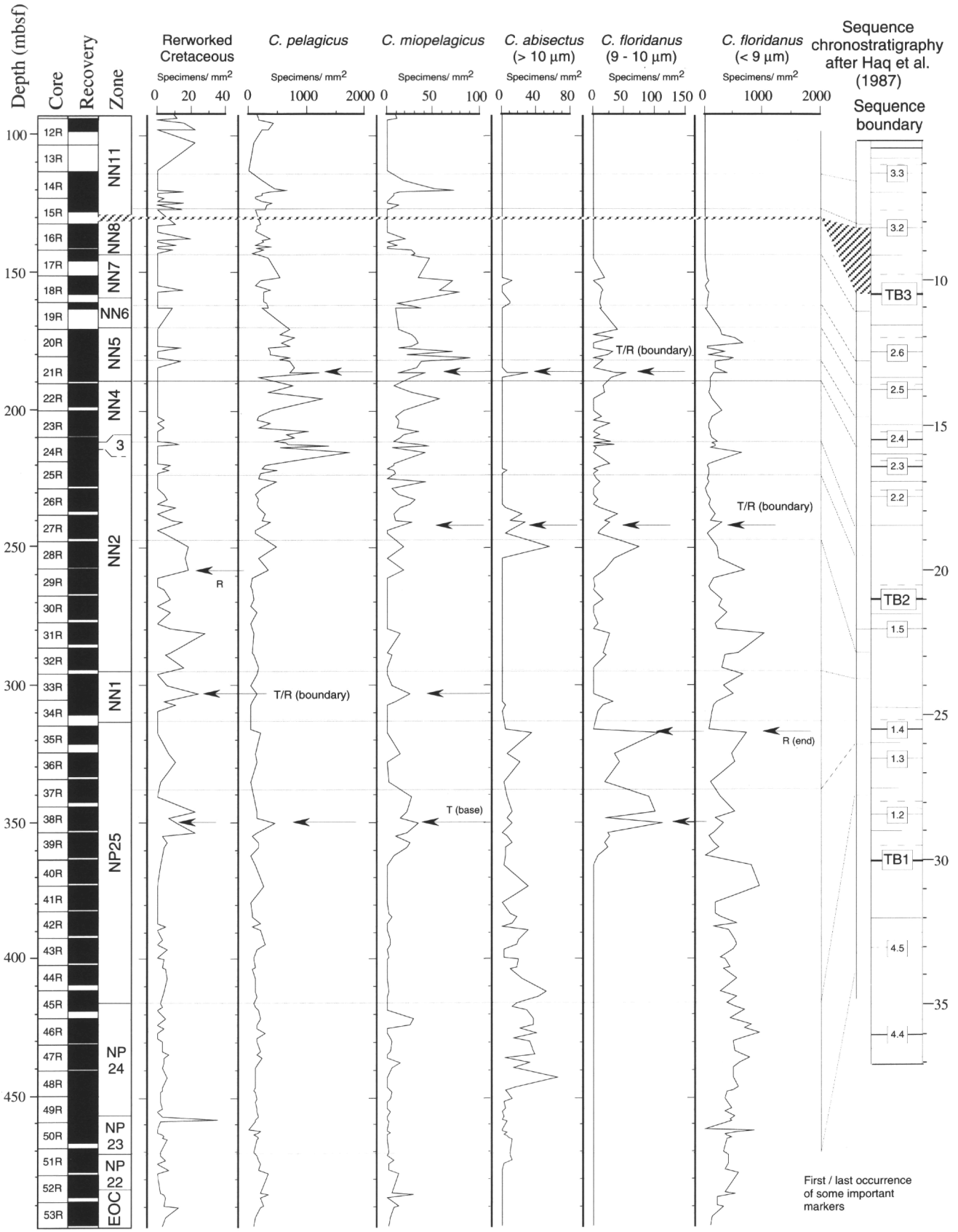

Figure 12. Correlations in Hole 900A of the abundance pattern of reworked Cretaceous, *Coccolithus,* and *Cyclicargolithus* species with the sequence chronostratigraphy of Haq et al. (1987). Horizontal lines represent the major bioevents (9 to 10 µm *C. floridanus* group is differentiated from Zone NP25). R = regressive; T = transgressive.

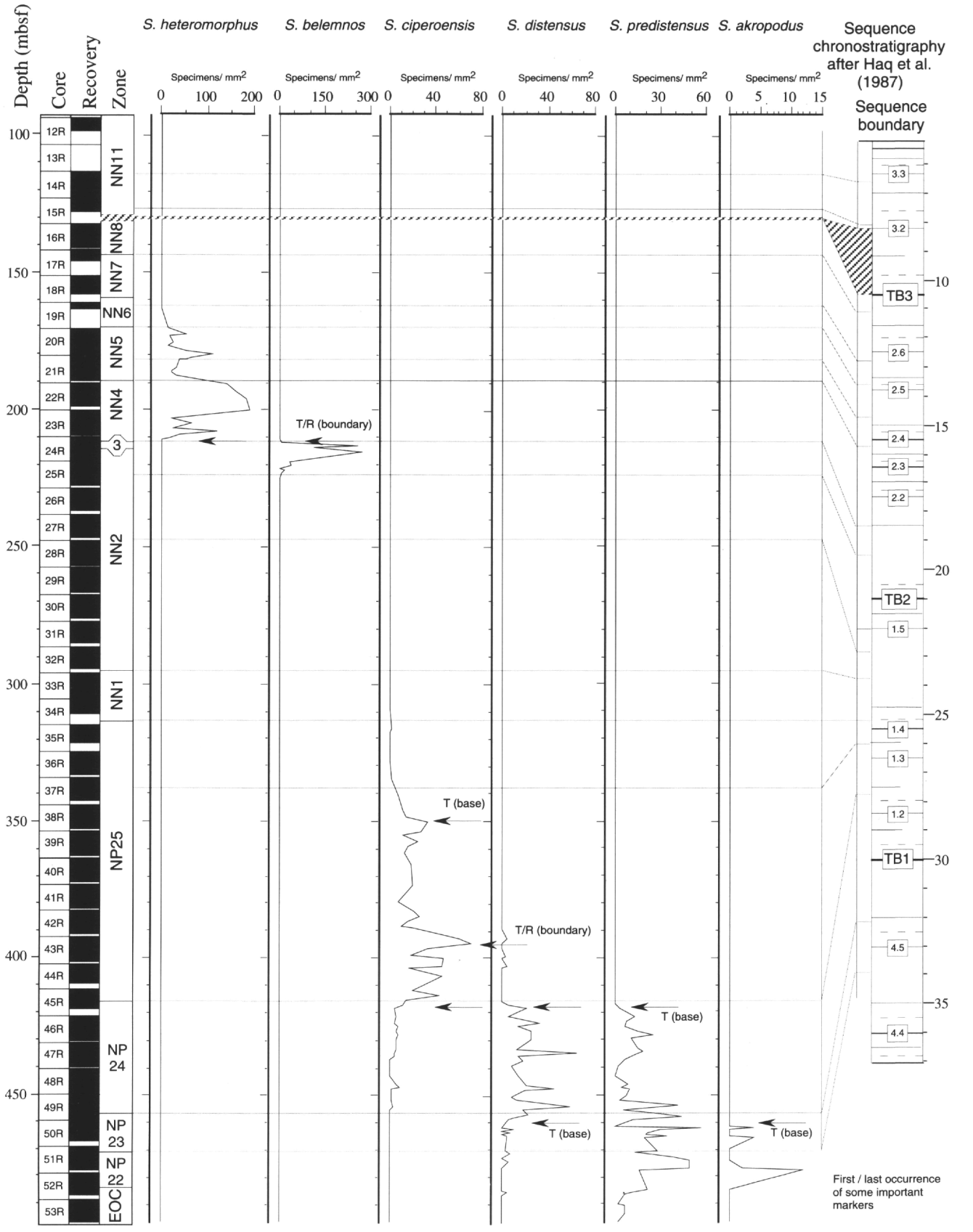

Figure 13. Correlations in Hole 900A of the abundance pattern of some Oligocene and Miocene *Sphenolithus* species with the sequence chronostratigraphy of Haq et al. (1987). Horizontal lines represent the major bioevents. R = regressive; T = transgressive.

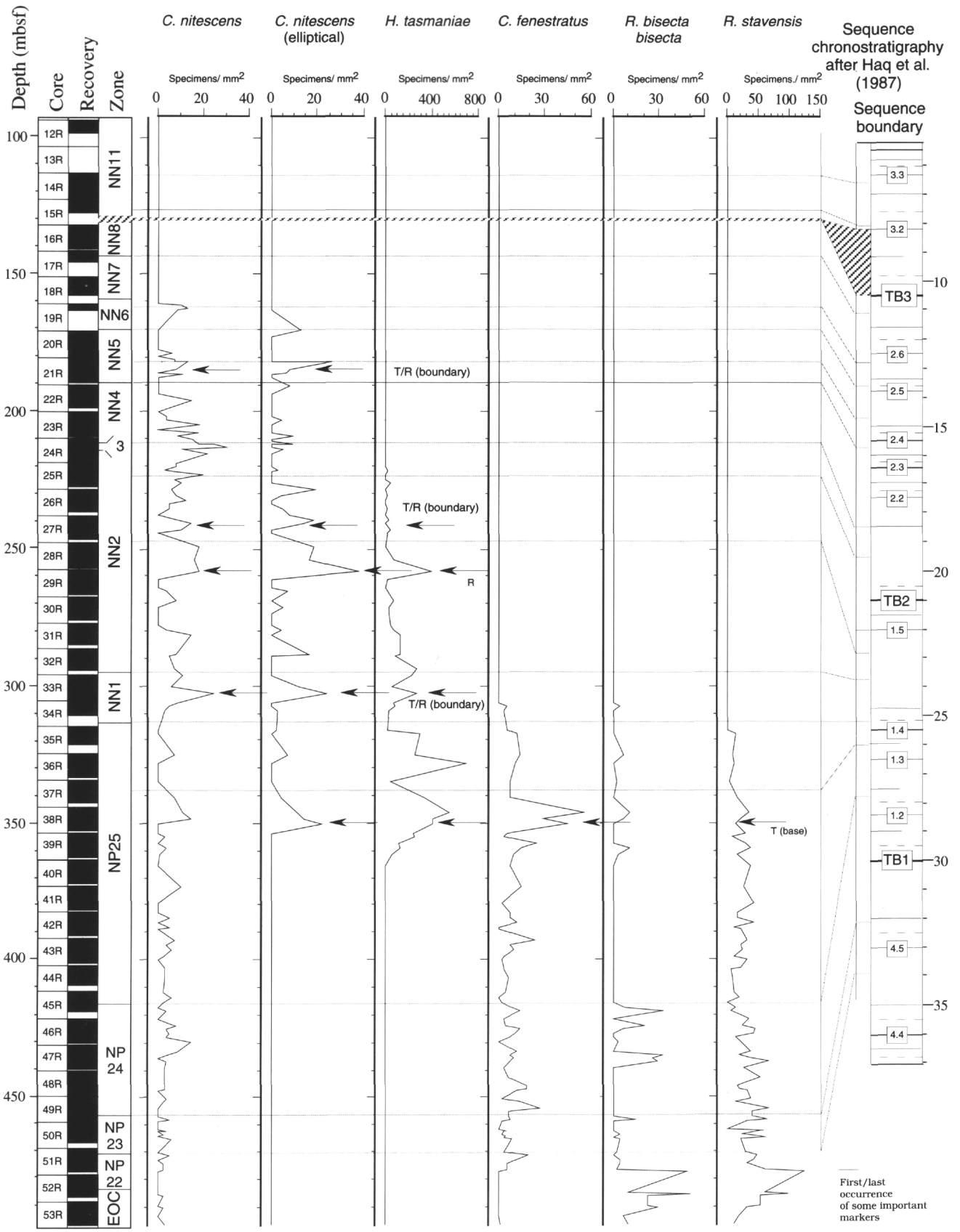

Figure 14. Correlations in Hole 900A of the abundance pattern of some important secondary markers across the Oligocene/Miocene boundary with the sequence chronostratigraphy of Haq et al. (1987). Horizontal lines represent the major bioevents. R = regressive; T = transgressive.

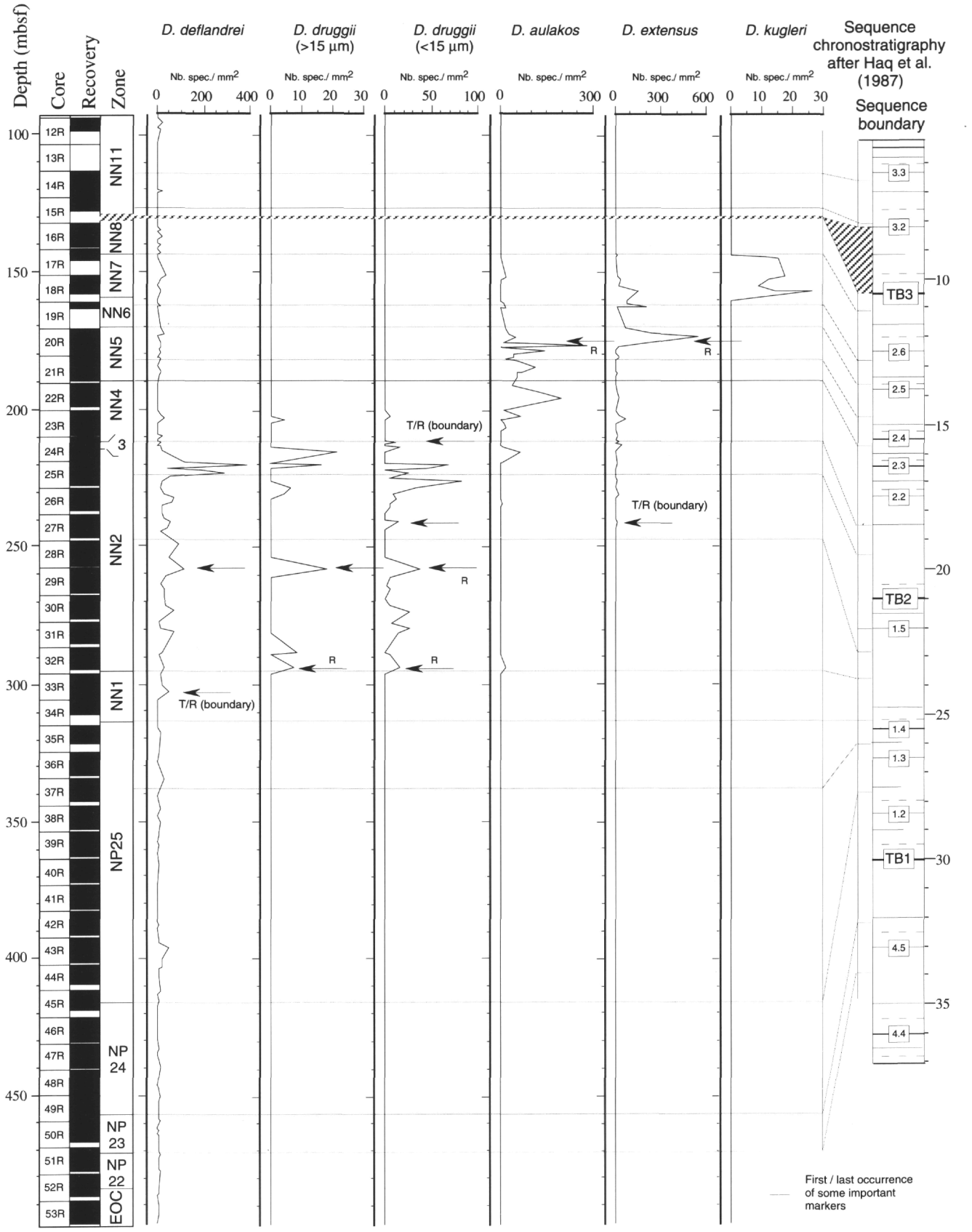

Figure 15. Correlations in Hole 900A of the abundance pattern of discoaster taxa (species with large central area) with the sequence chronostratigraphy of Haq et al. (1987). Horizontal lines represent the major bioevents. R = regressive; T = transgressive.

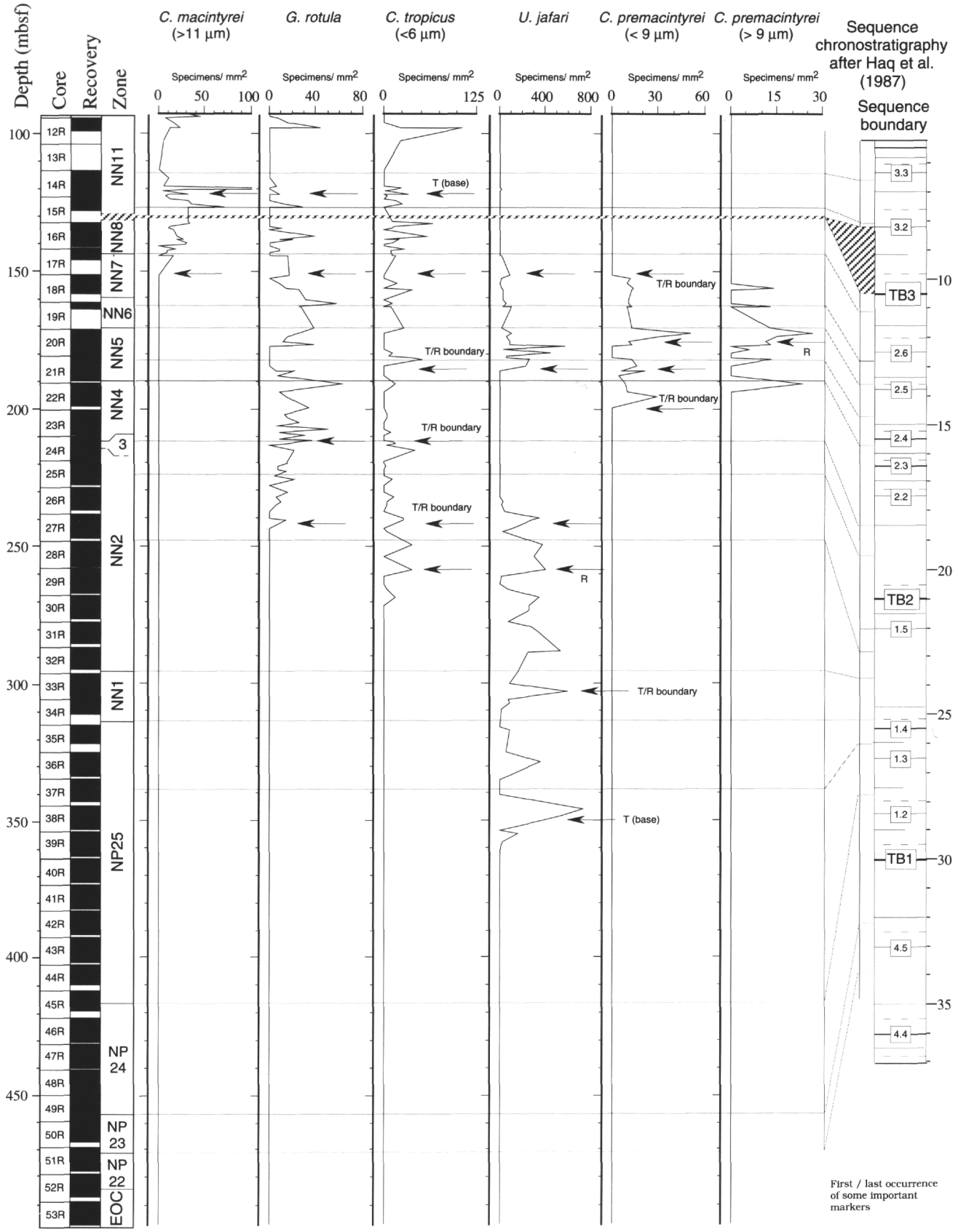

Figure 16. Correlations in Hole 900A of the abundance pattern of *Calcidiscus* and *Geminilithella* species with the sequence chronostratigraphy of Haq et al. (1987). Horizontal lines represent the major bioevents. R = regressive; T = transgressive.

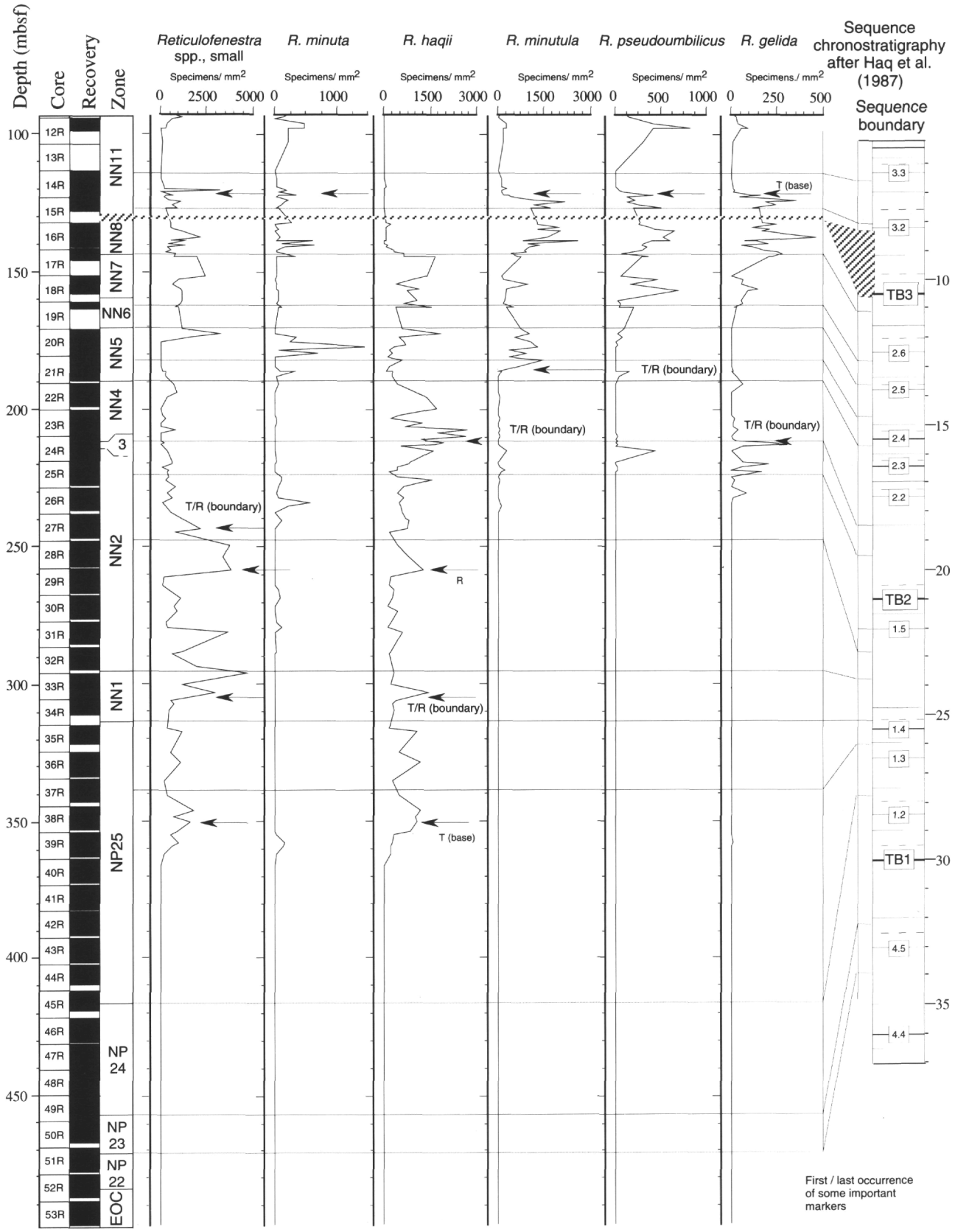

Figure 17. Correlations in Hole 900A of the abundance pattern of very small, small, and medium-sized *Reticulofenestra* species with the sequence chronostratigraphy of Haq et al. (1987). Horizontal lines represent the major bioevents. R = regressive; T = transgressive.

Hole 899B: Sample 149-899B-14R-1, 40 cm.

LOs of *Helicosphaera ampliaperta* and *Triquetrorhabdulus milowii*

The LO of these two markers is recorded together in the four sites from Leg 149. The abundance pattern of the range of *H. ampliaperta* for Site 900 is shown on Figure 11.

Hole 900A: Sample 149-900A-22R-1, 122 cm.

LO of *Helicosphaera obliqua*

The lower part of Zone NN5 is marked by a short succession of LOs among the genus *Helicosphaera.* The LO of *H. obliqua* occurs near the LO of *H. ampliaperta* at the bottom of Zone NN5 (Fig. 11).

Hole 900A: Sample 149-900A-21R-3, 139cm.

FO of *Discoaster musicus*

The FO of this distinct *Discoaster* occurs in the lower part of Zone NN5.

Hole 898A: Sample 149-898A-19X-6, 80 cm.

LO of *Helicosphaera perch-nielseniae*

This characteristic form *of Helicosphaera* has its LO in the lower part of Zone NN5 (Fig. 11).

Hole 900A: Sample 149-900A-21R-1, 142cm.

LO of *Helicosphaera elongata*

This narrow-shaped species is the last Oligocene species of *Helicosphaera.* Its LO is observed in the middle part of Zone NN5.

Hole 900A: Sample 149-900A-21R-1, 97 cm.

LO of *Helicosphaera waltrans*

H. waltrans has a short range from Zones NN4 to NN5, and its LO is a very distinct event in the upper part of Zone NN5 in Site 900.

Hole 900A: Sample 149-900A-20R-2, 91 cm.

LO of *Sphenolithus heteromorphus*

The LO of *Sphenolithus heteromorphus* is a useful middle Miocene biohorizon. The abundance pattern of *S. heteromorphus* for Site 900 (Fig. 13) shows a consistent and frequent occurrence to the top of its range.

Hole 900A: Sample 149-900A-20R-1, 26 cm.

LO of *Triquetrorhabdulus serratus*

This distinct event is very close to the LO of *S. heteromorphus.* In Site 900 this event is observed just above it, and in Site 898, a few cm below it.

Hole 900A: Sample 149-900A-19-CC

FO of *Triquetrorhabdulus rioi*

This species occurs near the base of Zone NN6, and below the FO of *Triquetrorhabdulus rugosus.*

Hole 898A: Sample 149-898A-19X-1, 106 cm.

FO of *Triquetrorhabdulus rugosus*

This species is rare at the base of its range. A sharp increase in its abundance is observed few cm above its FO, and defines a distinct biohorizon. The LO of *T. rioi* is recorded within the lower part of the range of *T. rugosus.* No overlap occurs between the stratigraphic ranges of *T. rugosus* and *S. heteromorphus.*

Hole 897C: Sample 149-897C-29R-1, 126 cm.

LO of *Coronocyclus nitescens*

Several morphotypes of *C. nitescens* have been differentiated. The abundance pattern of the ranges of two of these forms, *C. nitescens* with a thin rim and *Coronocyclus* with a thin elliptical rim are shown on Figure 14. The elliptical morphotype of *C. nitescens* has its LO in the lower part of Zone NN6, whereas circular *C. nitescens* occurs almost to the upper part of Zone NN6. The two plots of the abundance are almost similar from Zones NP25 to NN6.

Hole 897C: Sample 149-897C-28-CC.

FOs of *Discoaster* cf. *D. bollii*

The FO of these long-rayed *Discoaster bollii* (see "Appendix A") is observed in Site 900 with the FO of *D. kugleri,* and few meters below in Site 898.

Hole 898A: Sample 149-898A-18X-7, 42 cm.

FOs of *Discoaster kugleri* and *Calcidiscus macintyrei* (>11 µm)

The abundance pattern of the range of these two markers is shown on Figures 15 and 16. Only large (>11 µm) specimens of *Calcidiscus* with a close central area are included in *C. macintyrei* (see "Appendix A").

Hole 898A: Sample 149-898A-18X-5, 53 cm.

LOs of *Calcidiscus premacintyrei* and *Cyclicargolithus abisectus* (>10 µm)

The abundance pattern of these two markers is shown respectively on Figures 16 and 12. These events may be correlated with a general decrease in the size of the total assemblage of coccoliths.

Hole 900A: Sample 149-900A-18R-2, 48 cm.

LO of *Discoaster kugleri* and *Cyclicargolithus floridanus* (last consistent occurrence)

Both events are recorded together at Site 900. The plots of the abundance pattern of these two species are shown on Figures 12 and 15. Rare, and sporadic *C. floridanus* are present to the middle Zone NN8.

Hole 900A: Sample 149-900A-17R-2, 89 cm.

FO of *Discoaster bollii*

The FO of *D. bollii* is observed in Zone NN8 few meters below the upper Miocene hiatus, and is only recorded at Site 900. At Sites 897, 898, and 899, the lower part of Zone NN8 is missing.

Hole 900A: Sample 149-900A-16R-2, 71 cm.

After a hiatus involving uppermost middle/lower upper Miocene sediments, the following bioevents are observed:

FO of *Discoaster quinqueramus* var. A

This variety of D. *quinqueramus* (with a small knob, see "Appendix A") occurs just above the upper Miocene unconformity. The abundance pattern of the range of this species shows a consistent occurrence throughout Zone NN11. According to the abundance pattern of other *Discoaster* taxa (e.g., *D. bellus)* observed in Site 900, this event is believed to be close to the base of Zone NN11.

Hole 900A: Sample 149-900A-15R-4, 43 cm.

FO of *Discoaster tamalis*

Rare to few *D. tamalis* occurs sporadically from the lower part of Zone NN11 in Site 900. The FO of four-rayed *Discoaster brouweri (D. tamalis)* is found 40 cm above the FO of *Discoaster brouweri* with 3 rays. This latter species shows a consistent abundance pattern range through the upper Miocene. A 5-rayed *Discoaster brouweri,* is also present from the lower part of Zone NN11.

Hole 900A: Sample 149-900A-15R-4, 3 cm.

FCO of *Discoaster pentaradiatus*

Its FO is reported in the upper part of Zone NN10 (e.g., Gartner, 1992) and has a rare and discontinuous distribution along its lower range. Therefore, the occurrence of few *D. pentaradiatus* at the beginning of its range in Hole 900A is interpreted as a FCO. Because of the hiatus, the lower part of its range is not recorded.

Hole 900A: Sample 149-900A-15R-3, 30 cm.

FO of *Gephyrocapsa* sp. (<3.5 µm)

The FO of small *Gephyrocapsa* sp. has been observed in the lower part of Zone NN11. Though this species has a sporadic occurrence in the upper Miocene, common *Gephyrocapsa* sp. are recorded in the middle of the lower part of Zone NN11. Gartner (1992) reported the occurrence of small *Gephyrocapsa* sp. from Site 608 in the North Atlantic near the middle part of Zone NN11.

Hole 900A: Sample 149-900A-14R-7, 44 cm.

LO of *Discoaster bellus*

The LO of *D. bellus* is a reliable event in the lower part of Zone NN11. This event occurs slightly above the FCO of D. *pentaradiatus.*

Hole 900A: Sample 149-900A-14R-7, 44 cm.

FO *of Discoaster surculus*

The FO of this distinct species is observed in the lower part of Zone NN11. At the beginning of its range in Site 900, few specimens are observed, and the abundance pattern of the range of *D. surculus* shows a discontinuous occurrence.

Hole 900A: Sample 149-900A-14R-6, 66 cm.

FO of *Discoaster asymmetricus*

The FO of D. *asymmetricus* is a late Miocene biohorizon. Though rare at the beginning of its range in Zone NN11, *D. asymmetricus* is more abundant and shows a consistent occurrence in the uppermost Miocene. This form has been carefully distinguished from other asymmetric 5-rayed *Discoaster* species (e.g., *D. variabilis 5* ray asymmetric).

Hole 900A: Sample 149-900A-14R-5, 142 cm.

LO of *Minylitha convallis*

The LO of *M. convallis* is a distinct event in Site 900, and is used to separate Zone NN11 into a lower and upper part.

Hole 900A: Sample 149-900A-14R-3, 63 cm.

FO of *Amaurolithus amplificus*

The FOs *of Amaurolithus primus, Amaurolithus ninae, Amaurolithus delicatus,* and *Amaurolithus amplificus* are observed in the same sample in Site 900. This is due to the poor recovery of this interval. Only sediments from the core-catcher were recovered.

Hole 900A: Sample 149-900A-13-CC.

LO of *Discoaster quinqueramus* var. A

The LO of D. *quinqueramus* var. A. is used in this study to place the Zone NN11/NN12 boundary.

Hole 900A: Sample 149-900A-12-CC.

FO of *Helicosphaera sellii*

The FO of *H. sellii* is recorded in the lowermost part of Zone NN12. In Site 900, this bioevent occurs 30 cm above the LO of D. *quinqueramus* var. A.

Hole 900A: Sample 149-900A-12R-4, 10 cm.

LO of *Triquetrorhabdulus rugosus*

At Sites 897, 899, and 900, the LO of *T. rugosus* is observed in the lower part of Zone NN12 (= Zone CN10a of Okada and Bukry's zonal scheme, 1980), above the LO of *D. quinqueramus* var. A. Though rare, in the upper part of its range, this event is consistent and reliable between Site 897, 899, and 900.

Hole 900A: Sample 149-900A-12R-4, 10 cm.

LO of *Discoaster deflandrei*

The last consistent occurrence of *Discoaster deflandrei* is recorded in Hole 900A in Sample 149-900A-18R-1, 78 cm within Zone NN7. Rare specimens of D. *deflandrei* are observed above Core 149-900A-18R in Zones NN8 and NN11 (Fig. 15, Table 9, back pocket). Theodoridis (1984) reported this species ranging up to the late Miocene Zone NN11 (= *C. pelagicus* Zone of Theodoridis, 1984) in land sections from Sicily. The presence of D. *deflandrei* in upper Miocene sediments is considered as a real event, and its LO is placed in the uppermost Miocene, at the base of Zone NN12.

Hole 900A: Sample 149-900A-12R-2, 106 cm.

LO of *Amaurolithus amplificus*

The LO of A. *amplificus* is observed near the bottom of Zone NN12 in Site 900 in the uppermost Miocene within a short interval between the LO of *D. quinqueramus* var. A, and the FO of *Ceratolithus* spp. (Sample 149-900A-11R-5, 45 cm). This latter interval corresponds to the *Triquetrorhabdulus rugosus* Subzone (CN10a) in the zonal scheme of Bukry (1973, 1975).

Hole 900A: Sample 149-900A-12R-1, 112 cm.

LOs of *Cryptococcolithus mediaperforatus* and *Coccolithus miopelagicus* (>13 µm)

The LO of *C. mediaperforatus* (specimens between 6 and 7 µm), observed in Holes 899A and 900A, is recorded in the lower part of Zone NN12. This species is rare near the end of its range, and its LO may be situated in the lowermost part of the Pliocene. More detailed biostratigraphic data and correlation to magnetostratigraphy records of the upper range of C. *mediaperforatus* are necessary to determine if its LO position is above the Miocene/Pliocene boundary. The abundance pattern range of *Coccolithus miopelagicus* in Hole 900A is shown on Figure 12, together with the plot of the abundance of *C. pelagicus.* The presence of rare *C. miopelagicus* (coccolith length between 13 and 15 µm) is recorded up to the upper part of Zone NN11. At Sites 897, 899, and 900, a decrease in the abundance of *C. miopelagicus* is observed in the lower part of Zone NN8, and also a marked increase in abundance occurs in the early part of Zone NN11. The presence of *C. miopelagicus* in Zones NN11 and NN12 is not considered to be due to reworking. The distribution pattern of *C. miopelagicus* corresponds to the variation of the distribution of *Coccolithus pelagicus,* and to that of Reworked Cretaceous (Table 9, back pocket).

It has been reported in other studies (e.g., in NN11 by Gartner, 1992), but never considered as a reliable bioevent. Only the abrupt decrease in abundance observed in NN8 is reported by different studies (e.g., Raffi et al., 1995).

Hole 900A: Sample 149-900A-12R-1, 48 cm.

DISCUSSION

Calcareous Nannofossil Assemblage Variability

Oceanic regions such as those along the western edges of continents are characterized by upwelling of nutrient-enriched intermediate waters (500-1500 m). The high surface productivity in the oceans is dependent on the rate of supply of nutrients to the surface water where they can be utilized by phytoplankton. Upwelling of nutrient-enriched intermediate waters represents one of the two major sources of nutrients for phytoplankton. The second source of nutrients for the Iberia Abyssal Plain is provided by the nutrient store in the sediment deposited on the Galicia and Lusitanian margins (shelves) during sea-level highstand. As the sea-level falls during glacial intervals, these nutrients return to the sea. With increased supplies of nutrients and increased mixing rates (upwelling), increased productivity in calcareous nannoplankton may be expected. Quantitative studies on calcareous nannofossil abundance correlated to the sea-level curve of Haq et al. (1987) indicate that nannofossil assemblage variations could be mainly related to the sea-level variations (Gaboardi et al., 1994).

On the basis of a detailed quantitative analysis we draw abundance curves of nannofossil species and observe several trends in the nannofossil association that have been related to the sea-level variation.

Changes in species diversity are correlated to the sequence chronostratigraphy in Figure 18. We plotted the total abundance and the nannofossil species diversity to the sea-level curve of Haq et al. (1987, 1988) using both direct and indirect correlations with the transgressive-regressive cycles of the third-order sequence. The first kind of correlation was made possible by drawing bioevents previously correlated to the magnetostratigraphy (e.g., Backman 1987, Rio et al., 1990, and Gartner 1992). The second kind of correlation, indirect, was obtained by positioning other bioevents (Fig. 19) proportionally between two directly correlated bioevents. A general trend (Fig. 18) shows that important decreases in species diversity (e.g., in NP25, NN2, NN4, NN5) occur during short periods of time and in the regressive phase of highstand system tract.

In Figure 19, three classes of environmentally controlled forms were distinguished. Most of the helicolith events occur during a regressive period, most of the sphenolith events are recorded during a transgressive period, and some other species events coincide with the maximum flooding surface (T/R boundary in Figures 10 to 17) or with the lowstand system tract.

Several trends are observed in the calcareous nannofossil distribution patterns (Figs. 10 to 17). A general signal, corresponding to the maximum flooding surface of the third-order cycle, is determined by a maximum increase in the number of calcareous nannofossil families and genera (e.g., *Calcidiscus, Discoaster, Helicosphaera,* and *Sphenolithus).* The correlations with the sea-level curve indicate that *Discoaster* species with thin rays and small central area have their FO in the lowstand phase of the third-order cycle. Conversely, *Discoaster* taxa with thick rays and a large central area have their FO in the highstand phase of the third-order cycle (Fig. 15). In the middle Miocene, the first marked increase in *Discoaster* with a central knob occurs during the regressive phase. The late Miocene hiatus at Holes 897C and 900A does not allow us to conclude the presence or absence of a central knob with sea level variation.

The presence of common helicoliths in the association was often referred to shallow-water, near-shore conditions (Bukry et al., 1971). In the Iberian Abyssal Plain the sea-floor depth of the four studied Sites is nearly 5000 m. Although the water depth at the time of the sedimentation was probably shallower than at present day, occurring above the CCD, as proved by the nannofossil preservation and abundance, it is presumable that the basin conditions were not shallow water. On the correlation of peaks of abundance of helicoliths (Fig. 11) with regressive phases of the third-order cycle, we interpret the common abundance of helicoliths related to nutrient supply from sediments from the margins during the sea level falls.

Another group of calcareous nannofossils often related to shallow-water conditions is represented by holococcoliths (Kleijne, 1991). The correlation with the sea-level curve (Fig. 10) shows that peaks in abundance of holococcoliths coincide with regressive sequence, and the same explanation as the one above suggested for helicoliths could be true also for holococcoliths.

Abundance patterns of selected sphenoliths correlated with the sea level curve (Fig. 13) evidence peaks in abundance in coincidence of the maximum flooding surface or within the transgressive system tract of the third-order cycle, suggesting a preference for more open ocean conditions for this group.

Moreover, reworked Cretaceous specimens (Fig. 12) are plotted against the sea level curve and their abundance increases in the regressive phase of a third-order cycle. Gaboardi et al. (1994) in the south central Pyrenees show that reworked Cretaceous taxa increase and reach a maximum during the highstand system tract of fourth-order units, influenced by the prograding sediments that induce a relative sea-level fall.

At the scale of third-order sequences, several preferences in the nannofossil association were recognized in relation to different physical phases. A statistical approach would be necessary to recognize more univocal significance of calcareous nannofossil abundance patterns. Such an approach could be the subject of further work.

ACKNOWLEDGMENTS

The study was financially supported by the Swiss National Science Foundation (Grant 8220-033188). G. V. was supported by 60% MURST grant (to G. Zanzucchi). The authors give many thanks to James J. Pospichal for reviewing part of an early version of this manuscript, and J. Mitchener Covington for providing us with BugWare. We thank Kim Riddle for her time and assistance during the work on the scanning electron microscope. We thank Mario Cachao and José-Abel Flores for thorough reviews that resulted in an improved paper.

REFERENCES

Backman, J., 1980. Miocene-Pliocene nannofossils and sedimentation rates in the Hatton-Rockall Basin, NE Atlantic Ocean. *Stockholm Contrib. Geol.,* 36:1-91.

----------, 1987. Quantitative calcareous nannofossil biochronology of middle Eocene through early Oligocene sediment from DSDP Sites 522 and 523. *Abh. Geol. Bundesanst. (Austria),* 39:21-31.

Backman, J., and Shackleton, N.J., 1983. Quantitative biochronology of Pliocene and early Pleistocene calcareous nannofossils from the Atlantic, Indian and Pacific oceans. *Mar. Micropaleontol.,* 8:141-170.

Best, G., and Müller, C., 1972. Nannoplankton-Lagen im Unter-Miozän von Frankfurt am Main. *Senckenbergiana Lethaea,* 53:103-107.

Bramlette, M.N., and Wilcoxon, J.A., 1967. Middle Tertiary calcareous nannoplankton of the Cipero Section, Trinidad, W.I. *Tulane Stud. Geol,* 5:93-132.

Bukry, D., 1971. Cenozoic calcareous nannofossils from the Pacific Ocean. *Trans. San Diego Soc. Nat. Hist.,* 16:303-327.

-------- , 1973. Low-latitude coccolith biostratigraphic zonation. *In* Edgar, N.T., Saunders, J.B., et al., *Init. Repts. DSDP,* 15: Washington (U.S. Govt. Printing Office), 685-703.

-------- , 1975. Coccolith and silicoflagellate stratigraphy, northwestern Pacific Ocean, Deep Sea Drilling Project Leg 32. *In* Larson, R.L., Moberly, R., et al., *Init. Repts. DSDP,* 32: Washington (U.S. Govt. Printing Office), 677-701.

Bukry, D., Douglas, R.G., Kling, S.A., and Krasheninnikov, V.A., 1971. Planktonic microfossil biostratigraphy of the northwestern Pacific Ocean. *In* Fischer, A.G., Heezen, B.C., et al., *Init. Repts. DSDP,* 6: Washington (U.S. Govt. Printing Office), 1253-1300.

Deflandre, G., 1952. Classe des Coccolithophoridés (Coccolithophoridae Lohmann, 1902). *In* Grassé, P.P. (Ed.), *Traité de Zoologie. Anatomie, Systématique, Biologie* (Vol. 1, Pt. 1): *Phylogénie. Protozoaires: Généralités. Flagelles:* Paris (Masson), 439-470.

Edwards, A.R., and Perch-Nielsen, K., 1975. Calcareous nannofossils from the southern Southwest Pacific, DSDP Leg 29. *In* Kennett, J.P., Houtz, R.E., et al., *Init. Repts. DSDP,* 29: Washington (U.S. Govt. Printing Office), 469-539.

Flores, J.A., 1989. Calcareous nannoflora and planktonic foraminifera in the Tortonian-Messinian boundary interval of the East Atlantic DSDP sites and their relation to Spanish and Moroccan sections. *In* Crux, J.A., and van Heck, S.E. (Eds.), *Nannofossils and their Application.* Proc. INA Conf. London 1987, 249-266.

Fornaciari, E., Backman, J., and Rio, D., 1993. Quantitative distribution patterns of selected lower to middle Miocene calcareous nannofossils from the Ontong Java Plateau. *In* Berger, W.H., Kroenke, L.W., Mayer, L.A., et al., *Proc. ODP, Sci. Results,* 130: College Station, TX (Ocean Drilling Program), 245-256.

Fornaciari, E., Raffi, I., Rio, D., Villa, G., Backman, J., and Olafsson, G., 1990. Quantitative distribution patterns of Oligocene and Miocene calcareous nannofossils from the western equatorial Indian Ocean. *In* Duncan, R.A., Backman, J., Peterson, L.C., et al., *Proc. ODP, Sci. Results,* 115: College Station, TX (Ocean Drilling Program), 237-254.

Gaboardi, S., Reale, V., Iaccarino, S., Monechi, S., and Villa, G., 1994. Paleontological response to sea-level change in depositional sequences of the Figols Allogroup between the Isabena and Esera Valleys. *In* Mutti, E., Davoli, G., Mora, S., and Sgavetti, M. (Eds.), *The Eastern Sector of the South-Central Folded Pyrenean Foreland: Criteria for Stratigraphic Analysis and Excursion Notes.* 2nd High-resolution Sequence Stratigr. Conf.: TREMP, Catalunya, Spain, 66-76.

Gartner, S., 1992. Miocene nannofossil chronology in the North Atlantic, DSDP Site 608. *Mar. Micropaleontol,* 18:307-331.

Haq, B.U., Hardenbol, J., and Vail, P.R., 1987. Chronology of fluctuating sea levels since the Triassic. *Science,* 235:1156-1167.

---------, 1988. Mesozoic and Cenozoic chronostratigraphy and cycles of sea-level change. *In* Wilgus, C.K., Hastings, B.S., Kendall, C.G.St.C, Posamentier, H.W., Ross, C.A., and Van Wagoner, J.C. (Eds.), *Sea-Level Changes—An Integrated Approach.* Spec. Publ.—Soc. Econ. Paleontol. Mineral., 42:72-108.

Hay, W.W., 1977. Calcareous nannofossils. *In* Ramsay, A.T.S. (Ed.), *Oceanic Micropaleontology:* London (Academic), 1055-1200

Jiang, M.J., and Gartner, S., 1984. Neogene and Quaternary calcareous nannofossil biostratigraphy of the Walvis Ridge. *In* Moore, T.C., Rabinowitz, P.O., et al., *Init. Repts. DSDP,* 74: Washington (U.S. Govt. Printing Office), 561-595.

Kleijne, A., 1990. Distribution and malformation of extant calcareous nannoplankton in the Indonesian Sea. *Mar. Micropaleontol,* 16:293-316.

---------, 1991. Holococcolithophorids from the Indian Ocean, Red Sea, Mediterranean Sea and North Atlantic Ocean. *Mar. Micropaleontol,* 17:1-76.

Knüttel, S., 1986. Calcareous nannofossil biostratigraphy of the central East Pacific Rise, Deep Sea Drilling Project Leg 92: evidence for downslope transport of sediments. *In* Leine, M., Rea, D.K., et al., *Init. Repts. DSDP,* 92: Washington (U.S. Govt. Printing Office), 255-290.

Martini, E., 1971. Standard Tertiary and Quaternary calcareous nannoplankton zonation. *In* Farinacci, A. (Ed.), *Proc. 2nd Int. Conf. Planktonic Microfossils Roma:* Rome (Ed. Tecnosci.), 2:739-785.

---------, 1988. Nannoplankton-Massenvorkommen in den *Corbicula- (=* Schichten mit *Hydrobia inflata)* und Hydrobienschichten des Oberrheingrabens, des Mainzer und des Hanauer Beckens (Miozän). *Geol. Jahrb,* Al 10:205-227.

Martini, E., and Müller, C., 1975. Calcareous nannoplankton from the type Chattian (Upper Oligocene). *6th Congr. Reg. Comm. Mediterr. Neogene Stratigr. Proc. (Bratislava),* 1:37-41.

---------, 1986. Current Tertiary and Quaternary calcareous nannoplankton stratigraphy and correlations. *Newsl. Stratigr.,* 16:99-112.

Martini, E., and Worsley, T., 1971. Tertiary calcareous nannoplankton from the western equatorial Pacific. *In* Winterer, E.L., Riedel, W.R., et al., *Init. Repts. DSDP, 1* (Pt. 2): Washington (U.S. Govt. Printing Office), 1471-1507.

Muza, J.P., Wise, S.W., Jr., and Mitchener Covington, J., 1987. Neogene calcareous nannofossils from Deep Sea Drilling Project Site 603, Lower Continental Rise, western North Atlantic: biostratigraphy and correlations with magnetic and seismic stratigraphy. *In* van Hinte, J.E., Wise, S.W., Jr., et al., *Init. Repts. DSDP,* 93 (Pt. 2): Washington (U.S. Govt. Printing Office), 593-616.

Okada, H., 1990. Quaternary and Paleogene calcareous nannofossils, Leg 115. *In* Duncan, R.A., Backman, J., Peterson, L.C., et al., *Proc. ODP, Sci. Results,* 115: College Station, TX (Ocean Drilling Program), 129-174.

Okada, H., and Bukry, D., 1980. Supplementary modification and introduction of code numbers to the low-latitude coccolith biostratigraphic zonation (Bukry, 1973; 1975). *Mar. Micropaleontol,* 5:321-325.

Olafsson, G., 1989. Quantitative calcareous nannofossil biostratigraphy of upper Oligocene to middle Miocene sediment from ODP Hole 667A and middle Miocene sediment from DSDP Site 574. *In* Ruddiman, W., Sarnthein, M., et al., *Proc. ODP, Sci. Results,* 108: College Station, TX (Ocean Drilling Program), 9-22

---------, 1992. Oligocene/Miocene morphometric variability of the *Cyclicargolithus* group from the equatorial Atlantic and Indian Oceans. *Mem. Sci. Geo.,* 43:283-295.

Olafsson, G., and Villa, G., 1992. Reliability of sphenoliths as zonal markers in Oligocene sediments from the Atlantic and Indian Oceans. *Mem. Sci. Geol,* 43:261-275.

Parker, M.E., Clark, M., and Wise, S.W., Jr., 1985. Calcareous nannofossils of Deep Sea Drilling Project Sites 558 and 563, North Atlantic Ocean: biostratigraphy and the distribution of Oligocene braarudosphaerids. *In* Bougault, H., Cande, S.C., et al., *Init. Repts. DSDP,* 82: Washington (U.S. Govt. Printing Office), 559-589.

Perch-Nielsen, K., 1977. Albian to Pleistocene calcareous nannofossils from the western South Atlantic, DSDP Leg 39. *In* Supko, P.R., Perch-Nielsen, K., et al., *Init. Repts. DSDP,* 39: Washington (U.S. Govt. Printing Office), 699-823.

---------, 1985. Cenozoic calcareous nannofossils. *In* Bolli, H.M., Saunders, J.B., and Perch-Nielsen, K. (Eds.), *Plankton Stratigraphy:* Cambridge (Cambridge Univ. Press), 427-554.

Premoli Silva, I., Orlando, M., Monechi, S., Madile, M., Napoleone, G., and Ripepe, M., 1988. Calcareous plankton biostratigraphy and magnetostratigraphy at the Eocene-Oligocene transition in the Gubbio area. *In* Premoli Silva, I., Coccioni, R., and Montanari, A., *Int. Subcomm. Paleog. Strat., Eocene/Oligocene Meeting, Ancona, Oct. 1987 Spec. Publ.,* II, 6:137-161.

Prins, B., 1979. Notes on nannology—1. *Clausicoccus,* a new genus of fossil coccolithophorids. *INA Newsl,* 1:N2-N4.

Raffi, I., Rio, D., d'Atri, A., Fornaciari, E., and Rocchetti, S., 1995. Quantitative distribution patterns and biomagnetostratigraphy of middle and late Miocene calcareous nannofossils from equatorial Indian and Pacific oceans (Legs 115, 130, and 138). *In* Pisias, N.G., Mayer, L.A., Janecek, T.R., Palmer-Julson, A., and van Andel, T.H. (Eds.), *Proc. ODP, Sci. Results,* 138: College Station, TX (Ocean Drilling Program) 479-502.

Rio, D., Fornaciari, E., and Raffi, I., 1990. Late Oligocene through early Pleistocene calcareous nannofossils from western equatorial Indian Ocean (Leg 115). *In* Duncan, R.A., Backman, J., Peterson, L.C., et al., *Proc. ODP, Sci. Results,* 115: College Station, TX (Ocean Drilling Program), 175-235.

Roth, P.H., and Thierstein, H., 1972. Calcareous nannoplankton: Leg 14 of the Deep Sea Drilling Project. *In* Hayes, D.E., Pimm, A.C., et al., *Init. Repts. DSDP,* 14: Washington (U.S. Govt. Printing Office), 421-485.

Sawyer, D.S., Whitmarsh, R.B., Klaus, A., et al., 1994. *Proc. ODP, Init. Repts.,* 149: College Station, TX (Ocean Drilling Program).

Shipboard Scientific Party, 1994. Site 898. *In* Sawyer, D.S., Whitmarsh, R.B., Klaus, A., et al., *Proc. ODP, Init. Repts.,* 149: College Station, TX (Ocean Drilling Program), 115-146.

Steininger, F.F., 1994. A proposal for the global boundary stratotype section and point (GSSP) of the Neogene and the Paleogene/Neogene, resp. the Oligocene/Miocene Boundary. *Neogene Newsl,* Spec. Publ. Inst. Paleontol., Univ. of Vienna, 1:17-21.

Theodoridis, S.A., 1984. Calcareous nannofossil biozonation of the Miocene and revision of the helicoliths and discoasters. *Utrecht Micropaleontol. Bull,* 32:1-271.

Varol, O., 1989a. Eocene calcareous nannofossils from Sile (Northwest Turkey). *Rev. Esp. Micropaleontol,* 21:273-320.

--------- , 1989b. Calcareous nannofossil study of the central and western Solomon Islands. *In* Vedder, J.G., and Bruns, T.R. (Eds.), *Geology and*

offshore resources of Pacific island arcs—Solomon Islands and Bougainville, Papua and New Guinea Regions: Houston, Texas, Circum-Pac. Council for Energy and Min. Res., Earth Sciences Ser., 12:239-268.

Varol, O., 1991. New Cretaceous and Tertiary calcareous nannofossils. *N. Jb. Geol. Palaeont. Abh.,* 182:211-237.

Wei, W., and Wise, S.W., Jr., 1989. Paleogene calcareous nannofossil magnetobiochronology: results from South Atlantic DSDP Site 516. *Mar. Micropaleontol,* 14:119-152.

--------, 1990. Biogeographic gradients of middle Eocene-Oligocene calcareous nannoplankton in the South Atlantic Ocean. *Palaeogeogr., Palaeoclimatol, Palaeoecol,* 79:29-61.

Young, J.R., Flores, J.-A., and Wei, W., 1994. A summary chart of Neogene nannofossil magnetobiostratigraphy. *J. Nannoplankton Res.,* 16:21-27.

Date of initial receipt: 5 December 1994
Date of acceptance: 25 **August 1995**
Ms 149SR-208

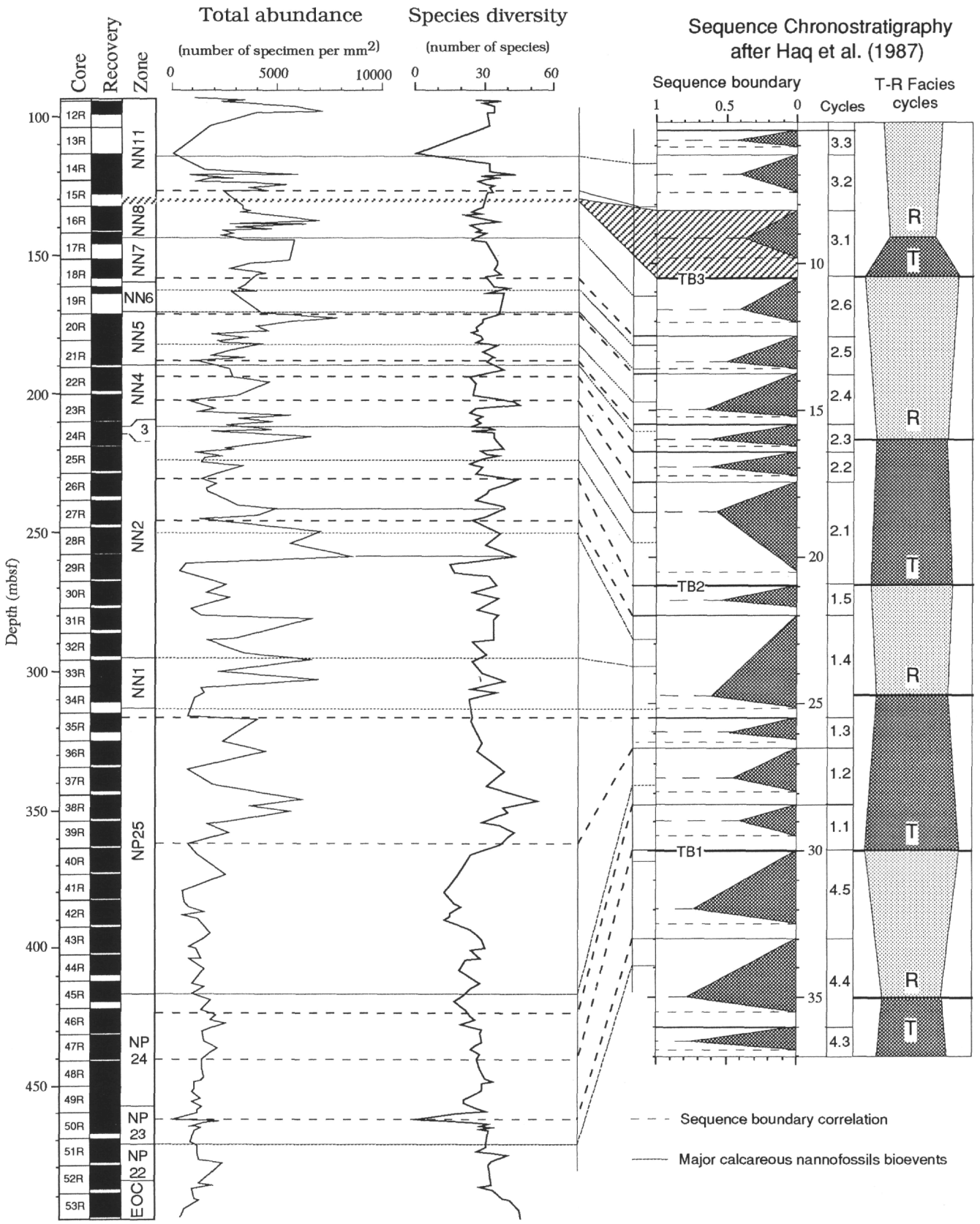

Figure 18. Correlation in Hole 900A of the sequence chronostratigraphy of Haq et al. (1987) with the total abundance and species diversity of calcareous nannofossils for the Oligocene-Miocene interval in Hole 900A. R = regressive; T = transgressive.

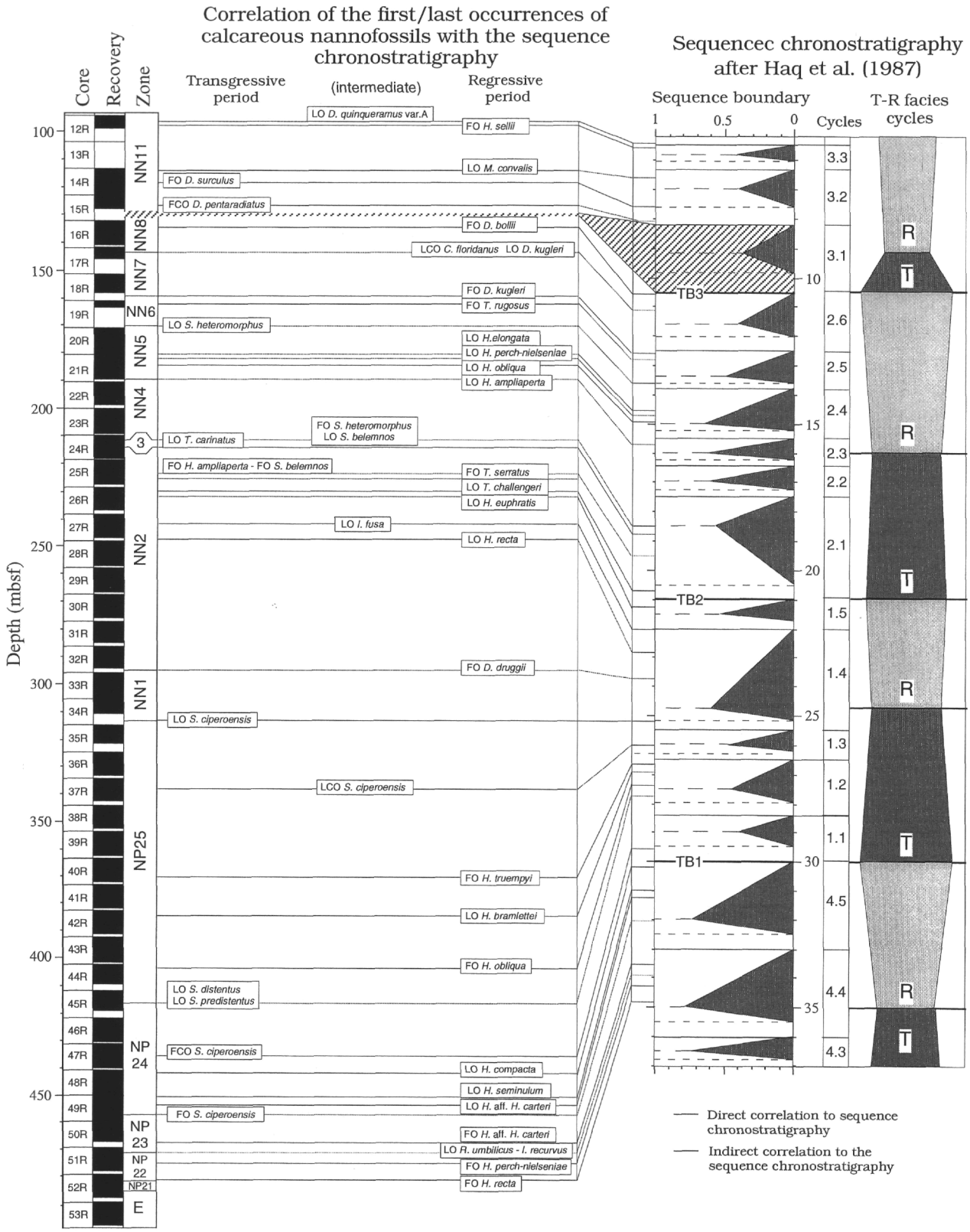

Figure 19. Correlations in Hole 900A occurrences of zonal markers, sphenoliths, and helicoliths with the sequence chronostratigraphy of Haq et al. (1987). Calcareous nannofossil first and last occurrences are grouped according to their position within the third-order sequences.

APPENDIX A

Paleontological Systematic Description

FSU and UP abbreviations for the holotypes of the new species refer to film and frame numbers that are stored, respectively, at the Department of Geology of the Florida State University (U.S.A.) and at the Istituto di Geologia at the Università degli Studi di Parma (Italy). Holotype measurements are indicated in parentheses.

Genus *AMAUROLITHUS* Gartner and Bukry, 1975

Amaurolithus delicatus Gartner and Bukry, 1975
(Pl. 13, Figs. 25 and 26)

Amaurolithus primus (Bukry and Percival, 1971) Gartner and Bukry, 1975
(Pl. 13, Figs. 23 and 24)

Genus *BICOLUMNUS* Wei and Wise, 1990

Bicolumnus ovatus Wei and Wise, 1990
(Pl. 7, Figs. 15 and 16)

Genus *BLACKITES* Hay and Towe, 1962

Blackites tenuis (Bramlette and Sullivan, 1961) Bybell, 1975
(Pl. 10, Figs. 7-9)

Genus *BRAARUDOSPHAERA* Deflandre, 1947

Braarudosphaera bigelowii (Gran and Braarud, 1935) Deflandre, 1947
(Pl. 14, Fig. 12)

Genus *BRAMLETTEIUS* Gartner, 1969

Bramletteius serraculoides Gartner, 1969
(Pl. 14, Figs. 17-20)

Genus *CALCIDISCUS* Kamptner, 1950

Remarks. Variations in size, shape, and central area features are used to differentiate the *Calcidiscus* species. Circular to elliptical placoliths have been observed. Most of the specimens have a sub-elliptical outline which make shape a difficult criteria for differentiating the diverse species. This is particularly evident in the late Oligocene to early Miocene, where most of the forms are smaller than 6 (am. The various species used for this study have been differentiated in the light microscope by overall size, the presence of a distinct central pore, and by the variable degree of imbrication of the elements of the shields (straight or kinked sutures).

Calcidiscus carlae (Lehotayova and Priewalder, 1978) Janin, 1992
(Pl. 1, Figs. 19 and 20)

Calcidiscus fuscus (Backman, 1980) Janin, 1987
(Pl. 1, Figs. 7-10)

Calcidiscus leptoporus (Murray and Blackman, 1898)
Loeblich and Tappan, 1978
(Pl. l, Figs. 1-6)

Calcidiscus macintyrei (Bukry and Bramlette, 1966)
Loeblich and Tappan, 1978
(Pl. 1, Figs. 29 and 30)

Remarks. The FO of large (>11 μm), circular *Calcidiscus* with a closed central area occurs in the middle Miocene Zone NN7. Similar sized forms with a large central opening are grouped into *Calcidiscus tropicus* (Pl. 1, Figs. 21-28), which occurs earlier in the middle Miocene Zone NN6.

Calcidiscus pataecus (Gartner, 1967) n. comb.
(Pl. 1,Figs. 11 and 12)

Coccolithus pataecus Gartner, 1967, p. 4, pl. 5, figs. 6, 7a, b, 8a, 8b.

Remarks. *Calcidiscus pataecus* include small, subelliptical *Calcidiscus* specimens (<6 μm) with a closed center and few elements. *Calcidiscus leptoporus* is a larger form with more elements, strongly imbricated and non-radial sutures.

Calcidiscus radiatus (Kamptner, 1954) Martin Perez and Aguodo, 1990
(Pl. 1, Figs. Band 14)

Genus *CAMURALITHUS* n. gen.

Type species. *Camuralithus pelliculathus,* n. gen., n. sp.

Diagnosis. An elliptical placolith composed of three shields. The proximal and intermediate shields are strongly curved, closely adpressed and are equal in diameter. The third shield, in the distal position, is smaller and has steeply inclined elements. The central area is large and may be spanned by diverse structure.

Derivation of name. From Latin *camur,* bent, and Greek, *lithos,* rock.

Camuralithus pelliculathus n. sp.

(Pl. 2, Figs. 1-12)

Diagnosis. A species of *Camuralithus* composed of three shields and a central area spanned by an X-shaped cross. A central plate may be present on the proximal side that supports the central cross.

Description. A small to medium elliptical form with 40 to 45 elements in the two lower shields. In cross-polarized light, the rim exhibits a unicyclic, white extinction pattern and the central cross is faintly birefringent. In phase contrast light, the central cross appears dark.

Size. 4 to 6 μm (holotype: 4.0 μm).

Differentiation. *Camuralithus pelliculathus* is differentiated from species of the genus *Chiasmolithus* by its three superimposed shield structure and by the absence of a large, bicyclic distal shield with a well developed outer cycle.

Derivation of name. From Latin *pellicula,* skin.

Holotype. FSU-F138 (Pl. 2, Fig. 1); FSU-F145 (PL 2, Fig. 2); FSU-F147 (Pl. 2, Fig. 3); FSU-FO53-D19 (Pl. 2, Fig. 4); FSU-FO53-D20 (Pl. 2, Fig. 5).

Type locality. ODP Site 900, Iberia Abyssal Plain.

Type level. ODP Sample 149-900-33R-5, 129 cm; early Miocene, Zone NN1.

Occurrence. Rare to common in late Oligocene to early Miocene from ODP Holes 897C, 898A, 899B, and 900A.

Range. Zones NP25 to NN2. The LO observed in Zone NN2 is a good event that can be used to subdivide Zone NN2. The LO of *C. pelliculathus* occurs between the LO of *H. recta* and the LO of *I. fusa.*

Genus *CHIASMOLITHUS* Hay, Mohler, and Wade, 1966

Chiasmolithus altus Bukry and Percival, 1971
(Pl. 2, Figs. 19 and 20)

Chiasmolithus medius Perch-Nielsen, 1971
(Pl. 2, Figs. 17 and 18)

Chiasmolithus oamaruensis (Deflandre, 1954) Hay, Mohler, and Wade, 1966
(Pl. 2, Figs. 21 and 22)

Genus *CLAUSICOCCUS* Prins, 1979

Clausicoccus fenestratus (Deflandre and Fert, 1954) Prins, 1979
(Pl. 3, Figs. 1-7)

Clausicoccus obrutus (Perch-Nielsen, 1971) Prins, 1979
(Pl. 3, Figs. 10, 11 and 13-16)

Clausicoccus vanheckae (Perch-Nielsen, 1986) n. comb.

Cruciplacolithus vanheckae Perch-Nielsen, 1986, p. 835, pl. 1, figs. 1-8.

Remarks. This medium-sized species has a wide, porous central plate. In cross-polarized light, the extinction pattern gives the false impression of the presence of a cross-bars. *C. vanheckae* is distinguished from *C. fenestratus* by

its greater number of perforations in the central area and by its extinction pattern. *C. cribellus* has a central porous plate supporting a very thin, slightly offset axial cross. Other Oligocene *Clausicoccus* have fewer central perforations.

Genus *COCCOLITHUS* Schwarz, 1894

Coccolithus pelagicus (Wallich, 1977) Schiller, 1930
(Pl. 4, Figs. 7, 8, and 21)

Coccolithus sp. 1
(Pl. 4, Figs. 10-13)

Remarks. This elliptical to subelliptical placolith consists of two incompletely developed shields connected by a thick, high inner wall surrounding a very large, open central area. In cross-polarized light, the rim exhibits a faint striated extinction pattern. The collar is bright. In phase contrast light, the collar appears thick and high. The placolith size measures from 6 to 13 µm.

These forms may represent a proto-coccolith ring tube of *Coccolithus pelagicus.* According to Kleijne (1990), their occurrence in high abundance may result from the very rapid successive production of coccoliths. The presence of malformed specimens may be related to changes in the environment (temperature, salinity, or nutrient availability).

They are rare in the early Miocene and rare to few in the middle to late Miocene.

Genus *CORONOCYCLUS* Hay, Mohler, and Wade, 1966

Coronocyclus aff. C. *prionion*
(PL 5, Figs. 24-27)

Coronocyclus nitescens (Kamptner, 1963)
(Pl. 5, Figs. 18-23)

Genus *CRENALITHUS* Roth, 1973

Crenalithus doronocoides (Black and Burns, 1961) Roth, 1973
(Pl. 7, Fig. 32)

Genus *CRYPTOCOCCOLITHUS Gartner,* 1992

Cryptococcolithus mediaperforatus (Varol, 1991) n. comb.
(Pl. 2, Figs. 13-16)

Birkelundia mediaperforata Varol 1991, p. 221, fig. 7 (17-20).
Cryptococcolithus takayamae Gartner 1992, p. 330, pl. 2, figs. 3a, b.

Remarks. *Cryptococcolithus mediaperforatus* has a nonbirefringent proximal and distal shield. The inner collar typically has a narrow elliptical outline and exhibits faint birefringence. Only rare specimens in upper Miocene Zone NN11 have the diagnostic central perforation. *C. mediaperforatus* is differentiated from similar size *C. premacintyrei* by its two non-birefringent shields and by the unique shape of its collar.

Most forms lack the central plate. The same feature is observed among the *Calcidiscus* species with a large central opening. *Calcidiscus carlae* (PL 1, Figs. 19 and 20) is a form of *C. tropicus* where the central plate is preserved.

Genus *CYCLICARGOLITHUS* Bukry 1971

Cyclicargolithus abisectus (Muller, 1970) Wise, 1983
(PL 7, Figs. 5 and 6)

Remarks. Circular to subcircular placoliths with a small central opening, which lacks a grid, are included in this genus. *Cyclicargolithus abisectus* is restricted to forms larger than 10 µm. In cross-polarized light, *C. abisectus* exhibits a typical disjunct extinction line between the tube and the outer cycle of the shield. Forms smaller than 10 µm are included in *C. floridanus.* For this study, two groups of *C. floridanus* have been recognized based on the placolith size: forms smaller than 9 µm and forms between 9 to 10 µm. The typical disjunct extinction line of the large *C. abisectus* may be identifiable among the large *C. floridanus.*

Cyclicargolithus floridanus (Roth and Hay in Hay et al., 1967) Bukry, 1971
(PL 7, Figs. 7 and 8)

Genus *DISCOASTER* Tan, 1927

Discoaster aulakos Gartner, 1967
(PL 6, Fig. 3)

Discoaster asymmetricus Gartner, 1969
(PL 6, Fig. 27)

Discoaster bellus Bukry and Percival, 1971
(PL 6, Figs. 29 and 30)

Discoaster cf. *D. bellus*
(PL 6, Fig. 28)

Remarks. This *Discoaster* has pointed, slightly bent rays similar to *Discoaster bellus.* The tips of the rays appear bright in phase contrast light. The central area differs from *D. bellus* by being slightly larger and with a small proximal knob. *Discoaster* cf. *D. bellus* differs from *Discoaster quinqueramus* var. A by lacking the small stellate knob on the distal side.

Discoaster bollii Martini and Bramlette, 1963
(Pl. 6, Fig. 13)

Discoaster cf. *D. bollii*

Eu-discoaster cf. *E. bollii* Theodoridis, 1984, p. 166, pl. 33, figs. 6, 7.

Remarks. The forms included in this group are differentiated from *D. bollii* by having longer rays and a relatively smaller central area. A knob is present on both proximal and distal sides. *Discoaster* cf. *D. bollii* is restricted to the middle Miocene and occurs from the middle Miocene Zones NN6 to NN8. Its FO is placed just above the FO of *T. rugosus.* The top of its range overlaps the range of *D. bollii.*

Discoaster braarudii Bukry, 1971
(Pl. 6, Fig. 23)

Discoaster broweri Tan, 1927 emend. Bramlette and Riedel, 1954
(PL 6, Figs. 24 and 32)

Discoaster deflandrei (Bramlette and Riedel, 1954) var. *nodosus* n. var.
(PL 6, Figs. 5 and 6)

Remarks. This large *Discoaster* is distinguished from *Discoaster deflandrei deflandrei* by the position of a pair of lateral nodes on the arms. The pair of nodes are completely separated from the terminal bifurcation, as are the nodes in *Discoaster tanii nodifer.* Intermediate forms (PL 6, Fig. 6), with the pair of nodes still at the level of the bifurcation, are also observed. This group of large *discoasters* with a large central area have a very short range restricted to the highstand of the third-order sequence TB1.4 (upper Zone NN1 to lower Zone NN2). They also co-occur with the first occurrence peak of *D. druggii* (PL 6, Fig. 7) in the early Miocene. The diameter measures between 14 to 18 µm.

Discoaster druggii Bramlette and Wilcoxon, 1967
(PL 6, Fig. 7)

Discoaster extensus Hay, 1967
(PL 6, Fig. 4)

Discoaster kugleri Martini and Bramlette, 1963
(PL 6, Fig. 12)

Discoaster micros Theodoridis, 1984 n. comb.
(PL 6, Figs. 9 and 10)

Eu-discoaster micros Theodoridis 1984, p. 170—171, pl. 36, figs. 1—3.

Remarks. The morphologic differences introduced by Theodoridis (1984) between *Helio-discoaster* (straight sutures) and *Eu*-discoaster (curved sutures) is not followed here. *Discoaster micros* has a relatively large central area, short bifurcated arms, and a low proximal knob. According to Theodoridis (1984) *Discoaster micros* is restricted to the *E. kugleri* Subzone (= Martini's Zone NN7). The forms observed at Site 900A are very similar to the

holotype but have been recorded in the middle of Zone NN11. This *Discoaster* has a diameter between 5 and 6 µm.

Discoaster musicus Stradner, 1959
(Pl. 6, Fig. 11)

Discoaster obtusus Gartner, 1967
(Pl. 6, Fig. 1)

Discoaster prepentaradiatus Bukry and Percival, 1971
(PL 6, Fig. 20)

Discoaster quinqueramus (Gartner, 1969) var. A n. var.
(Pl. 6, Fig. 31)

Remarks. *Discoaster quinqueramus* var. A is differentiated from *Discoaster quinqueramus* by lacking a well-developed polygonal knob on the distal side. The FO and LO of *D. quinqueramus* var. A is used in this study to define the Zone NN11. Forms of *Discoaster quinqueramus* with a prominent stellate distal knob have not been observed at Holes 897C and 900A. Their absence may be due to some ecological exclusion, but there is no clear evidence to explain the absence of central knob.

Discoaster surculus Martini and Bramlette, 1963
(PL 6, Fig. 22)

Discoaster tamalis Kamptner, 1967
(PL 6, Figs. 25 and 26)

Discoaster variabilis Martini and Bramlette, 1963 (5 ray asymmetric)
(PL 6, Fig. 19)

Remarks. Most of the five rays *of Discoaster variabilis* are slightly asymmetrical and do not have well-developed depressions around the center. Only rare forms (PL 6, Fig. 18) with five symmetrical rays exhibit a distal side with well-developed depressions. Therefore the FO of *Discoaster prepentaradiatus* (PL 6, Fig. 20) (forms without a developed central area), is not easily identifiable because many intergrading forms exist.

Genus *ERICSONIA* Black, 1964

Ericsonia formosa (Kamptner, 1963) Haq, 1971
(Pl. 4, Figs. 14-17)

Ericsonia detecta n. sp.
(PL 4, Figs. 1-6)

Diagnosis. An elliptical species *of Ericsonia* with a thin margin composed of two unequal shields; the proximal shield being much smaller or undeveloped. The central opening is large and open.

Description. The distal shield is composed of 30 to 34 slightly imbricated elements. The proximal shield has one fourth to one fifth the dimension of the distal shield and is composed of about the same number of elements. A very thin tube connects the two shields. In cross-polarized light, the distal shield is slightly birefringent and striated. The proximal shield and the inner cycle (tube) are bright. In phase contrast light, both shield appear dark.

Size. 5 to 7 µm (holotype: 5.3).

Differentiation. The rim margin is very similar to other species of the genus *Ericsonia,* but *E. detecta* lacks the typical plate elements filling the central area. *E. detecta* is differentiated from species of the genus *Coccolithus* by its very narrow proximal shield and by its large central opening. Its consistent occurrence throughout the Oligocene-Miocene interval and its presence in samples which an excellent preservation clearly indicate that *E. detecta* represents a separate species among the genus *Ericsonia. E. detecta* is differentiated from *Ericsonia* sp. 1 by its elliptical outline.

Derivation of name. From Latin *detectus,* unroof.

Holotype. FSU-F140 (PL 4, Fig. 1); FSU-FO53-D24 (PL 4, Fig. 2); FSU-FO53-D25 (PL 4, Fig. 3).

Type locality. ODP Site 900, Iberia Abyssal Plain.

Type level. ODP Sample 149-900-33R-5, 129 cm; early Miocene, Zone NN1.

Occurrence. Rare to common in Oligocene to Miocene sediments from ODP Holes 897C, 898A, 899B, and 900A. The FO is observed at Hole 897C in the upper part of Zone NP22 and at Holes 899B, 900A, in the lower part of Zone NP23. *E. detecta* occurs throughout the whole Miocene.

Ericsonia sp. 1
(PL 4, Fig. 20)

Remarks. This is a form similar to *E. detecta,* but having a distinct circular outline. *Ericsonia* sp. 1 has a large, open central area with a bright inner wall and a dark distal shield. It occurs from the Oligocene Zone NP22 to the lower part of Zone NP25. The diameter of this form is between 6 to 8 µm

Genus *GEMINILITHELLA* Backman, 1980

Geminilithella bramlettei (Hay and Towe, 1962) Varol, 1989a
(Pl. 4, Figs. 18 and 19)

Cyclolithus bramlettei Hay and Towe, 1962, p. 500, pl. 5, fig. 6; pl. 7, fig. 2.
Cydococcolithina protoannula Gartner, 1971, p., pl. 5, figs 1a-c, 2.
Geminilithella bramlettei (Hay and Towe, 1962) Varol, 1989a, p. 296, pl. 1, figs. 22-24; pl. 3, figs. 41-42.

Remarks. *C. protoannula* is placed in synonymy with *G. bramlettei.* The holotype of *C. protoannula* (distal view) has two nearly equal-sized shields and a large central opening. This latter form is similar to the holotype of *C. protoannula* (proximal view).

Geminilithella rotula (Kamptner, 1956) Backman, 1980
(PL 5, Figs. 3 and 8-11)

Genus *HAYELLA* Gartner, 1969

Hayella aperta Theodoridis, 1984 (elliptical)

Remarks. In cross-polarized light, this elliptical form has a large, striated shield surrounding a large central opening. The central tube exhibits a bright, diffused extinction pattern. Elliptical forms observed at Hole 900A are similar to the elliptical specimens illustrated by Theodoridis (1984, pl. 3, figs. 5, 6). The holotype of *H. aperta* has a distinct circular outline (Theodoridis, 1984, pl. 3, fig. 3). Elliptical forms of *H. aperta* are observed in early Miocene Zones NN1 to NN2 in Hole 900A.

Genus *HELICOSPHAERA* Kamptner, 1954 emend Theodoridis, 1984

Helicosphaera ampliaperta Bramlette and Wilcoxon, 1967
(PL 10, Figs. 1-3)

Helicosphaera bramlettei Muller, 1970
(PL 9, Figs. 16)

Helicosphaera aff. *H. carteri* (Wallich, 1877) Kamptner, 1954
(PL 8, Figs. 21-24; PL 10, Figs. 14 and 15)

Remarks. This medium-sized *Helicosphaera* has two distinct openings aligned with the longer axis of the shield. The flange is rounded and terminates by a small inner crescent-shaped expansion along the side of the shield. The bar is in optical continuity with the rim and separates two openings. This helicolith measures between 8 to 10 µm and has a short range restricted to Oligocene Zone NP23 to the early part of Zone NP24. In cross-polarized light, *Helicosphaera* aff. *H. carteri* exhibits the same intense birefringence as *H. carteri* and is distinguished from the latter by its smaller size, the larger openings and the abrupt termination of the flange.

Helicosphaera compacta Bramlette and Wilcoxon, 1967
(Pl. 9, Figs. 8-11)

Helicosphaera elongata Theodoridis, 1984
(Pl. 9, Figs. 15, and 24-27)

Helicosphaera euphratis Haq, 1966 (<8.0 µm)

Remarks. This form *of Helicosphaera* has a small central opening almost filled by the bar. Because of the small size of the bar, it is difficult to differentiate the small form *of H. intermedia,* a species *of Helicosphaera* with a less inclined, sigmoidal-shaped bar. Both *H euphratis* and *H. intermedia* have a

rounded flange that terminates gradually along the side of the shields. The LO of *H. euphratis* (<8.0µm) has been observed with the LO of large form of *H. euphratis* (Pl. 9, Figs. 3, 12-14) in the upper part of the early Miocene Zone NN2. This event occurs just below the last occurrence of *Triquetrorhabdulus challengeri.*

Helicosphaera gartneri Theodoridis, 1984
(Pl. 9, Fig. 19)

Helicosphaera intermedia Martini, 1965
(Pl. 9, Figs. 20-23)

Helicosphaera limasera n. sp.
(Pl. 10, Figs. 12 and 13)

Helicosphaera aff. *H. seminulum* Bramlette and Wilcoxon, 1967, p. 106, pl. 5, figs. 11, 12.

Diagnosis. A medium-sized species *of Helicosphaera* with a small rounded flange and an open central area spanned by a normal oblique bar that is in optical discontinuity with the shield. The flange does not extend outside the shield and terminates gradually along the side of the shield.

Description. In cross-polarized light, this medium-sized *Helicosphaera* has an open central opening spanned by a thick oblique bar which is birefringent and in discontinuity with the shield. The bar forms a distinct angle with the shield which is between 30° and 40° to the short axis. The flange is smoothly rounded and has a faint to dark extinction pattern.

Size. 8 to 12 µm; specimen from Bramlette and Wilcoxon (1967): 10.3 µm.

Differentiation. *H. limasera* differs from *H. seminulum* by having an oblique bar without a longitudinal suture. *H. limasera* is differentiated from *H. bramlettei* by its rounded flange and its more inclined bar.

Derivation of name. From Latin *limus,* oblique, and *sera,* bar.

Holotype. UP-FO-D (Pl. 10, Fig. 12); UP-FO-D (Pl. 10, Fig. 13).

Type locality. ODP Site 897, Iberia Abyssal Plain.

Type level. ODP Sample 149-897C-47R-6, 6 cm; early Oligocene, Zone NP23.

Occurrence. *H. limasera* is found Oligocene sediments from Sites 897 and 898.

Range. Zone NP23 to lower part of Zone NP25.

Helicosphaera obliqua Bramlette and Wilcoxon, 1967
(Pl. 8, Figs. 16-20)

Helicosphaera paleocarteri Theodoridis, 1984
(Pl. 10, Figs. 4-6)

Helicosphaera perch-nielseniae Haq, 1971
(Pl. 8, Figs. 3, 12, and 15)

Helicosphaera recta Haq, 1966
(Pl. 8, Figs. 1, 2, and 4-11)

Helicosphaera reticulata Bramlette and Wilcoxon, 1967
(Pl. 9, Fig. 17)

Helicosphaera truempyi Biolzi and Perch-Nielsen, 1982
(Pl. 9, Fig. 18)

Helicosphaera wilcoxonii Gartner, 1971
(Pl. 9, Figs. 4-7)

Genus *HOMOZYGOSPHAERA* Deflandre, 1952

Homozygosphaera macropora (Deflandre in Deflandre and Fert, 1954) n. comb.
Discolithus macroporus Deflandre in Deflandre and Fert, 1954, p. 138, pl. 11, fig. 5.
Holodiscus macroporus (Deflandre in Deflandre and Fert, 1954) Roth, 1970, p. 866, pl. 11, fig. 6.

Remarks. Deflandre (1952) defined *Homozygosphaera* for monomorphic coccosphere composed of zygoliths. According to Kleijne (1991), the distal side of *Homozygosphaera* may be spanned by a bridge or by several arches The type species, *Conusphaera spinosa,* is a coccolith tube with a distal side spanned by a high bridge. *Homozygosphaera macropora* (new combination) is a tube coccolith spanned by arches or septae surrounding 9 to 14 holes.

Genus *HUGHESIUS* Varol, 1989b

Hughesius gizoensis Varol, 1989b
(Pl. 3, Figs. 12, 17 and 18)

Hughesius gizoensis Varol, 1989b, p. 261, pl. 4, figs 9-13.

Remarks. *H. gizoensis* (form with two unicyclic shields and two central plates) has been grouped together with *H. tasmaniae* (form with central perforations) in the beginning of this study and therefore is not represented on the range charts. *H. gizoensis* has a consistent occurrence through the early middle Miocene. The holotype has been described from the upper Miocene and Varol (1989b) indicated an occurrence from Zones NN6 to NN11. *H. gizoensis* is present from Zone NN1 in the Iberia Abyssal Plain and overlaps the range of *H. tasmaniae.*

Hughesius tasmaniae (Edwards and Perch-Nielsen, 1975) n. comb.
(Pl. 3, Figs. 8 and 9)

Ericsonia tasmaniae Edwards and Perch-Nielsen, 1975, p.481-482, pl. 20, figs. 5-12.

Remarks. As mentioned in the diagnosis by Edwards and Perch-Nielsen (1975), this small placolith lacks an inner distal cycle. Varol (1989b) described a new genus, *Hughesius,* for placoliths with two equal-sized unicyclic shields and a central area occupied by a variable number of plates. In cross-polarized light, the shields and central plate of *Hughesius* are non-birefringent. Species of *Clausicoccus* have a bright inner cycle in cross-polarized light. In phase contrast light, the shields and plates are dark and the central perforations are clearly identifiable. Forms with six or more perforations are included into *H. tasnamiae.* Forms with a central area occupied by two plates are identified as *H. gizoensis.* In the present study, forms with four perforations *(Hughesius* sp. from Varol, 1989b) have not been separated from *H. tasmaniae,* but are present at Sites 897, 898, 899 and 900. *H. tasmaniae* is present from the upper Oligocene Zone NP25 to the upper part of the early Miocene Zone NN2. Forms *of Hughesius* with four perforations have the same range. The LO of *H. tasmaniae* has been observed just earlier than the LO of *Triquetrorhabdulus carinatus* and is a reliable event that can be used alternatively to define the top of Zone NN2 when *T. carinatus* is missing.

Genus *ILSELITHINA* Stradner in Stradner and Adamiker, 1966

Ilselithina fusa Roth, 1970
(Pl. 12, Figs. 18-27)

Genus *ISTHMOLITHUS* Deflandre, 1954

Isthmolithus recurvus Martini, 1973
(Pl. 14, Figs. 1 and 2)

Genus *LANTERN ITUS* Stradner, 1962

Lianternithus minutus Stradner, 1962
(Pl. 14, Fig. 6 and 7)

Genus *LITHOSTROMANION* Deflandre, 1942

Lithostromanion operosum (Deflandre, 1954) Bybell, 1975
(Pl. 14, Fig. 5)

Genus *MICRANTHOLITHUS* Deflandre in Deflandre and Fert, 1954

Micrantholithus aequalis Sullivan, 1964
(Pl. 14, Fig. 13)

Genus *MINYLITHA* Bukry, 1973

Minylitha convallis Bukry, 1973
(Pl. 13, Figs. 27 and 28)

Genus *ORTHOZYGUS* Bramlette and Wilcoxon, 1967

Orthozygus aureus (Stradner, 1962) Bramlette and Wilcoxon, 1967
(Pl. 14, Figs. 8 and 9)

Genus *PEDINOCYCLUS* Bukry and Bramlette, 1971

Pedinocyclus larvalis (Bukry and Bramlette, 1969) Loeblich and Tappan, 1973
(Pl. 14, Figs. 14 and 15)

Genus *PEMMA* Klump, 1953

Pemma papillata Martini, 1959
(Pl. 14, Figs. 10 and 11)

Genus *PERITRACHELINA* Deflandre, 1952

Peritrachelina joidesa Bukry and Bramlette, 1968
(Pl. 14, Fig. 3)

Genus *PONTOSPHAERA* Lohmann, 1902

Pontosphaera anisotrema (Kamptner, 1956) Backman, 1980
(PL 12, Figs. 12 and 13)

Pontosphaera callosa (Martini, 1969) Varol, 1982
(Pl. 12, Figs. 10 and 11)

Pontosphaera longiforaminis (Báldi-Becke, 1964) n. comb.
(Pl. 12, Figs. 1-4)

Discolithus longiforaminis Báldi-Becke, 1964, p. 164, pl. 1, figs. 3, 3a, 3b.

Remarks. This species has a central plate composed of 15 to 18 radial elements. Only one complete cycle of perforations is present on the outer part of the plate. The other central perforations are slit-shaped pores between the radial elements and do not form an additional cycle of perforations. *P. longiforaminis* is distinguished from *P. multipora* by the shape and arrangement of its central perforations. *P. multipora* has rounded perforations (Pl. 12, Fig. 5) arrange in a complete cycle.

Pontosphaera multipora (Kamptner, 1948) Roth, 1970
(Pl. 12, Figs. 5-9)

Genus *PYROCYCLUS* Hay and Towe, 1962

Pyrocyclus orangensis (Bukry, 1971) Backman, 1980
(Pl. 7, Figs. 25-29)

Genus *RETICULOFENESTRA* Hay et al. 1966, emend Gallagher, 1989

Reticulofenestra bisecta (Hay, Mohler, and Wade, 1966) Roth, 1970 *bisecta*
(Pl. 7, Figs. 11 and 12)

Reticulofenestra bisecta (Hay, Mohler, and Wade) Roth, 1970, p. 847, pl. 3, fig. 6.

Remarks. Forms of *Reticulofenestra bisecta* have been separated according to the size and the presence in the central area of a small plate or large plug. Two subspecies and one species are distinguished among this group: *R. bisecta bisecta, R. bisecta filewiczii,* and *R. stavensis.* The recognition of three forms presents some advantages for defining the Oligocene/Miocene boundary. *R. bisecta bisecta* (forms smaller than 10 µm) has its LO at the level of the LO of *Sphenolithus ciperoensis.* and can be use to define the Oligocene/Miocene boundary. *R. stavensis* (=*R. bisecta bisecta* larger than 10 µm) has its LCO slightly above the LO of *Sphenolithus ciperoensis,* in the lower part of Zone NN1. *R. bisecta filewiczii* (forms with a small central plate) are usually observed up to the lower part of Zone NN2, but its last consistent occurrence level occurs in the lower part of Zone NN1.

Reticulofenestra bisecta (Hay, Mohler, and Wade, 1966) Roth, 1970*filewiczii* Wise and Wiegand, 1983
(Pl. 7, Figs. Band 14)

Reticulofenestra bisecta (Hay, Mohler, and Wade) Roth, 1970 filewiczii Wise and Wiegand in Wise 1983, p. 505, pl. 5, fig. 3, pl. 6, figs. 1-2.

Remarks. As for the other subspecies of *Reticulofenestra bisecta,* different last occurrence levels are recorded in Holes 897C, 898A, 899B, and 900A. On the base of the biostratigraphic data from Hole 899B, the last consistent occurrence of *R. bisecta filewiczii* is placed in the lower part of Zone NN1, but sporadic specimens are observed in Hole 897C and 898A up to the lower part of Zone NN2.

Reticulofenestra circus n. sp.
(Pl. 7, Figs. 3 and 4)

Diagnosis. A medium-sized, subcircular species of *Reticulofenestra* with a thin collar and a medium-sized central opening having a quadrate outline. The central area is either vacant or closed by a grid.

Description. A medium-sized placolith with a subcircular outline having an axial ratio of about 1.05. The proximal shield is slightly smaller than the distal shield and has a thin collar (or tube cycle). The central opening appears quadrate and represents 25% to 30% of the total length of the coccolith.

Size. Diameter: 8-9 (8.2) µm.

Differentiation. *R. circus* is distinguished from other medium-sized *Reticulofenestra* by its subcircular outline, the presence of a thin collar, and by the typical quadrated-shape of its central opening. *R. circus* is differentiated from *R. hillae* by its smaller size and its subcircular outline, and from *C. floridanus* by its larger, quadrated central opening.

Derivation of name. From Latin *circus,* round.

Holotype. UP-FOA-D32 (Pl. 7, Fig. 3).

Type locality. ODP Site 900, Iberia Abyssal Plain.

Type level. ODP Sample 149-900A-50R-5, 6 cm.

Occurrences. Present to few in lower Oligocene sediments from ODP Holes 897C, 899B and 900A.

Range. Restricted to the early Oligocene: Zones NP22 to NP23. The LO *of R. circus* is a good event and is usually found with the LO of *L. minutus* or just above it.

Reticulofenestra daviesi (Haq, 1968) Haq, 1971
(Pl. 7, Fig. 23)

Reticulofenestra hampdensis Edwards, 1973
(Pl. 7, Fig. 24)

Reticulofenestra lockeri Muller, 1970
(Pl. 7, Figs. 19 and 20)

Reticulofenestra haqii Backman, 1978
(Pl. 7, Figs. 17 and 18)

Reticulofenestra moguntina Martini, 1988
(Pl. 7, Figs. 21 and 22)

Reticulofenestra francofurtana Best and Müller, 1972, p. 107, pl. 1, fig. 2, pl. 2, fig. 17 (non pl. 1, fig. 1).
Reticulofenestra moguntina Martini, 1988, p.217, pl. 1, figs. 3-4.

Reticulofenestra producta (Kamptner, 1963) Wei and Thierstein, 1991
(Pl. 7, Fig. 33)

Reticulofenestra stavensis (Levin and Joerger, 1967) Varol, 1989b
(Pl. 7, Figs. 9 and 10)

Coccolithus stavensis Levin and Joerger, 1967, p. 165, pl. 1, figs. 7a-d.
Reticulofenestra stavensis (Levin and Joerger, 1967) Varol 1989b, p. 261.

Remarks. Species of *Reticulofenestra* with a large central plug closing the central area are distinguished in this study according to the placolith length. Forms larger than 10 µm are included in *Reticulofenestra stavensis* and forms smaller than 10 µm are included in *Reticulofenestra bisecta bisecta.* On the basis of the biostratigraphic results of Hole 899B, the last consistent occurrence of *R. stavensis* is placed in the lower part of Zone NN1, at the same level as the last consistent occurrence of *R. bisecta filewiczii.*

Reticulofenestra umbilicus (Levin, 1965) Martini and Ritzkowski, 1968
(Pl. 7, Figs. 1 and 2)

Genus RHABDOSPHAERA Haeckel, 1894

Rhabdosphaera procera Martini, 1969
(Pl. 10, Figs. 10 and 11)

Genus *SPHENOLITHUS* Deflandre, 1952

Sphenolithus akropodus n. sp.
(Pl. 11, Figs. 1, 2, and 4-11)

Sphenolithus sp. aff. *S. distentus* Okada 1990, p. 154, pl. 2, figs. 7, 8.
Sphenolithus sp. 1 Fornaciari et al., 1990, pl. 2, figs. 1-3.

Diagnosis. A large species of *Sphenolithus* with a long tapering apical spine, sometimes bifurcated, and a short proximal elements extending laterally to form a small basal part.

Description. This sphenolith has a short proximal shield and a long apical spine. About 8 to 10 thick, elongated elements form the apical spine, which may be curved or bifurcated at the top. In cross-polarized light and at 45° to the crossed nicols, the apical spine is completely bright. The extinction suture line of the base curves downward, separating the proximal basal elements which extend laterally as two pointed feet. At 0° to the crossed nicols, the apical spine is weakly birefringent.

Size. Length: 7 to 9 (8.5) µm; basal part: 2.5 to 3.5 (3.0) µm.

Differentiation. *S. akropodus* differs from *S. distentus* by its larger size, the presence of more developed basal elements, and by a more massive apical spine. In crossed-polarized light and at 45° to the nicols, the extinction pattern of the basal shield elements of *S. akropodus* form two bright, pointed feet. In *S. distentus* the proximal elements are almost parallel to the long axis of the sphenolith and form two bright, less developed, and more blocky feet. *S. akropodus* differs from *S. predistentus* by its curved extinction suture line and from *S. ciperoensis* by its relatively shorter proximal shield and its extinction suture line, which does not extend proximally.

Derivation of name. From Greek *akros,* highest point, and *pous,* foot.

Holotype. FSU-F165 (Pl. 11, Fig. 1); FSU-FO54-D26 (Pl. 11, Fig. 4); FSU-FO54-D25 (Pl. 11, Fig. 5); FSU-FO54-D27 (Pl. 11, Fig. 6).

Type locality. ODP Site 900, Iberia Abyssal Plain.

Type level. ODP Sample 149-900A-51R-6, 47 cm.

Occurrence. Present to rare in early Oligocene sediments from Sites 897, 899, and 900. The LO of *S. akropodus* is a reliable event and is observed at Site 900 just below the FO of *S. ciperoensis.*

Range. Early Oligocene Zones NP22 to NP23.

Sphenolithus aubryae n. sp.
(Pl. 11, Figs. 16-18)

Sphenolithus dissimilis Sphenolithus belemnos intergrade Rio, Fornaciari, and Raffi, 1990, pl. 12, figs. 2.

Diagnosis. A short, compressed species of *Sphenolithus* with a proximal shield, about 2/3 the total length. The proximal elements are parallel to the long axis of the sphenolith. The apical, multispinate spine is very short and composed of few elements which are radially arranged and bell-shaped.

Description. In cross-polarized light, and at 0° to the nicols, the narrow basal shield is birefringent. The extinction line forms an asymmetric cross with a basal shield nearly twice the height of the apical spine. At 45° to the crossed nicols, the short, multipartite apical spine is birefringent and the extinction suture line between the proximal shield and the apical spine is V-shaped. In phase contrast light, a large dark cavity is present at the center of the apical spine.

Size. Length: 3.5 to 4.5 µm (holotype: 4.1); basal part: 2.0 to 2.5 µm (2.4).

Differentiation. *S. aubryae* differs from *S. belemnos* by the structure and length of its apical spine and by the nearly parallel sides of its proximal shield. At 45°, *S. belemnos* has a longer and slender apical spine. *S. aubryae* is differentiated from *S. dissimilis* by its shorter apical spine formed by short, non parallel elements. *S. dissimilis* has a large, extended base.

Derivation of name. In honor of Professor Marie-Pierre Aubry, Laboratoire de Géologie du Quaternaire, CNRS Luminy, Marseille (France).

Holotype. FSU-FO43-D33 (Pl. 11, Fig. 16); FSU-FO43-D34 (Pl. 11, Fig. 17); FSU-FO43-D35 (Pl. 11, Fig. 18).

Type locality. ODP Site 900, Iberia Abyssal Plain.

Type level. ODP Sample 149-900A-29R-6, 23 cm.

Occurrence. Present to few in early Miocene sediments from Sites 897, 898, 899, and 900.

Range. Early Miocene Zones NN2 to NN3.

Sphenolithus belemnos Bramlette and Wilcoxon, 1967
(Pl. 11, Figs. 25, 27)

Sphenolithus calyculus Bukry, 1985
(Pl. 10, Figs. 24, 26, and 27)

Sphenolithus capricornutus Bukry and Percival, 1971
(Pl. 11, Fig. 19)

Sphenolithus ciperoensis Bramlette and Wilcoxon, 1967
(PL 10, Figs. 22, 23, 25)

Sphenolithus cometa n. sp.
(Pl. 11, Figs. 22-24)

?*Sphenolithus multispinatus* Fornaciari et al., 1990, p. 254, pl. 3, figs. 1-3 (nomen nudum).

Diagnosis. A species of *Sphenolithus* with a short narrow base and a long diverging apical spine in which the elements are longitudinally divided to form three to four separated elongated spines that flare upwards.

Description. In cross-polarized light and at 0° to the nicols, the bright basal elements are slightly laterally extended, the apical spine is bipartite and diverging; at 45° to the nicols, the proximal shield and the lateral elements are faintly birefringent and the apical spine exhibits a decreasing birefringence from its base towards the three delicate spines (giving an aspect similar to a comet).

Size. Length: 5 to 7 µm (holotype: 5.3); basal part: 1.5 to 2.5 µm (2.0).

Differentiation. *S. cometa* differs from all other sphenoliths by its typical apical spine. *S. dissimilis* also possesses a spine formed by three elements, but they are not separated longitudinally as the apical elements of *S. cometa.* At 0° to the nicols, *S. capricornutus* differs from *S. cometa* by has a more diverging and thicker spine; at 45° to the nicols, the apical spine of *S. cometa* is birefringent.

Derivation of name. From Latin *cometa,* comet.

Holotype. FSU-FO50-D6 (Pl. 11, Fig. 22); FSU-FO50-D5 (Pl. 11, Fig. 23); FSU-FO50-D7 (Pl. 11, Fig. 24).

Type locality. ODP Site 898, Iberia Abyssal Plain.

Type level. ODP Sample 149-898A-24R-5, 24 cm.

Occurrence. Rare to few in early Miocene sediments from Sites 897, 898, 899, and 900. *S. cometa* has its FO in the lower part of Zone NN2 and its LO in the upper part of Zone NN2 at the FO of *S. belemnos.*

Range. Early Miocene Zone NN2.

Sphenolithus delphix Bukry, 1973
(Pl. 11, Figs. 20 and 21)

Sphenolithus distentus (Martini, 1965) Bramlette and Wilcoxon, 1967
(Pl. 10, Figs. 18-21)

Sphenolithus orphanknollensis Perch Nielsen, 1971
(Pl. 10, Figs. 16 and 17)

Sphenolithus predistentus Bramlette and Wilcoxon, 1967
(Pl. 11, Figs. 3, and 12-15)

Genus *SYRACOSPHAERA* Lohmann, 1902

Syracosphaera lamina n. sp.
(PL 14, Figs. 21-22)

Diagnosis. A medium-sized species of *Syracosphaera* with a narrow, strongly convex rim and a very thin central plate formed by elongated radial laths supporting a small, hollow central stem.

Description. In cross-polarized light, the narrow rim exhibits a bicyclic, sigmoidal extinction pattern. The narrow inner rim cycle has a faint birefringence and the outer cycle is brightly birefringent. The central plate is non-birefringent and the central stem appears slightly bright. In phase contrast light, the outer rim cycle is dark and the inner one is bright. The stem appears dark and hollow.

Size. Length: 5 to 6 µm (holotype: length: 5.9; width: 4.7).

Differentiation. *S. lamina* differs from *S. clathrata* (Roth 1970) by its rim construction, its large central area, and by its central plate. *S. lamina* is differentiated from *S. histrica* and *S. pulchra* by its non-birefringent central plate, and by the presence of a stem. *Syracosphaera? fragilis* (Theodoridis, 1984) has a unicyclic rim extinction pattern and a birefringent central plate.

Derivation of name. From Latin *lamina,* thin plate.

Holotype. FSU-FO48-D25 (Pl. 14, Fig. 21); FSU-FO48-D27 (Pl. 14, Fig. 22).

Type locality. ODP Site 900, Iberia Abyssal Plain.

Type level. ODP Sample 149-900A-27R-2, 72 cm.

Occurrence. Rare to few in late Oligocene to early Miocene sediments from Sites 897, 898 and 899. At Site 900, *S. lamina* has an extended range to the upper Miocene Zone NN11.

Genus *TETRALITHOIDES* Theodoridis, 1984

Tetralithoides symeonidesii Theodoridis, 1984
(Pl. 12, Figs. 14-17)

Genus *TRANSVERSOPONTIS* Hay, Mohler, and Wade, 1966

Transversopontis obliquipons (Deflandre in Deflandre and Fert, 1954) Hay, Mohler, and Wade, 1966
(Pl. 14, Fig. 16)

Genus *TRIQUETRORHABDULUS Martini,* 1965

Triquetrorhabdulus carinatus Martini, 1965
(Pl. 13, Figs. 17-21)

Triquetrorhabdulus challengeri Perch-Nielsen, 1977
(Pl. 13, Figs. 4-6)

Triquetrorhabdulus milowiii Bukry, 1971
(Pl. 13, Figs. 2 and 3)

Triquetrorhabdulus rioi Olafsson, 1989
(Pl. 13, Figs. Band 14)

Triquetrorhabdulus rugosus Bramlette and Wilcoxon, 1967
(Pl. 13, Figs. 15, 16, and 22)

Triquetrorhabdulus serratus (Bramlette and Wilcoxon, 1967) Olafsson, 1989
(Pl. 13, Figs. 11 and 12)

Genus *UMBILICOSPHAERA* Lohmann, 1902

Umbilicosphaera cricota (Gartner, 1967) Cohen and Reonhardt, 1968
(Pl. 5, Figs. 14 and 15)

Umbilicosphaera sibogae foliosa (Kamptner, 1963) Okada and McIntyre, 1977
(Pl. 5, Figs. 12 and 13)

Umbilicosphaera sp. (elliptical)
(PL 5, Figs. 16 and 17)

Remarks. This large, subelliptical to elliptical species of *Umbilicosphaera* has a narrow rim and a very large central opening. No other elliptical *Umbilicosphaera* have been described in the literature for the Miocene interval. *Umbilicosphaera huburtiana* (Gaarder, 1970) also has an elliptical rim but is a living taxa which first occurs in the Pleistocene. Rare to few elliptical, thin rim *Umbilicosphaera* occur from late Miocene Zone NN11 to the early Pliocene Zone NN15.

Genus *ZYGRHABLITHUS* Deflandre, 1959

Zygrhablithus bijugatus (Deflandre in Deflandre and Fert, 1954) Deflandre, 1959
(Pl. 13, Figs. 1 and 7)

Zygrhablithus sp. 1
(Pl. 13, Figs. 8-10)

Remarks. This form of *Zygrhablithus* has a distinct thin base and a long distal process consisting of four elongated blade-shaped elements. An opening (canal) is present from the base to the upper part of the distal process. In cross-polarized light, the thin base and the upper part of the distal process are bright. The four elongated arches of the distal process are not- or faintly birefringent. *Zygrhablithus* sp. 1 is differentiated from *Z. bijugatus* (Pl. 13, Fig. 1, 7) by its faint birefringence, and from *Z. kerabyi,* and *Z. sileensis* by its thinner basal base and its longer, narrow distal process. *Zygrhablithus* sp. 1 is a form similar to the Eocene Z. *sagittus* but differs by having a longer distal process. *Zygrhablithus* sp. 1 has been observed from the base of the late Oligocene Zone NP24 to the early Miocene Zone NN2.

APPENDIX B

Calcareous nannofossils considered in this report are listed by alphabetical order of generic epithets. Entries not found in the References for the following taxa are given in Perch-Nielsen (1985). Some species distinctions are based on the nannofossil size. Measurements are in micrometers and are indicated in parenthesis.

Amaurolithus amplificus (Bukry and Percival, 1971) Gartner and Bukry, 1975
Amaurolithus delicatus Gartner and Bukry, 1975
Amaurolithus ninae Perch-Nielsen, 1977
Amaurolithus primus (Bukry and Percival, 1971) Gartner and Bukry, 1975
Bicolumnus ovatus Wei and Wise, 1990
Blackites spinosus (Deflandre and Fert, 1954) Hay and Towe, 1962
Blackites tenuis (Bramlette and Sullivan, 1961) Bybell, 1975
Braarudsphaera bigelowii (Gran and Braarud, 1935) Deflandre, 1947
Braarudosphaera discula Bramlette and Riedel, 1954
Bramletteius serraculoides Gartner, 1969a
Calcidiscus carlae (Lehotayova and Priewalder, 1978) Janin, 1992
Calcidiscus fuscus (Backman, 1980) Janin, 1987
Calcidiscus leptoporus (Murray and Blackman, 1898) Loeblich and Tappan, 1978
Calcidiscus macintyrei (Bukry and Bramlette, 1969b) Loeblich and Tappan, 1978
Calcidiscus pataecus (Gartner, 1967) n. comb.
Calcidiscus premacintyrei Theodoridis, 1984
Calcidiscus premacintyrei (<9.0 µm)
Calcidiscus radiatus (Kamptner, 1954) Martin Perez and Aguado, 1990
Calcidiscus tropicus (Kamptner, 1954) Varol, 1989b
Calcidiscus tropicus (<6.0 µm)
Camuralithus pelliculatus n. gen,, n. spec.
Chiasmolithus altus Bukry and Percival, 1971
Chiasmolithus grandis (Bramlette and Riedel, 1954) Radomski, 1968
Chiasmolithus medius Perch-Nielsen, 1971
Chiasmolithus oamaruensis (Deflandre, 1954) Hay, Mohler, and Wade, 1966
Chiasmolithus sp.
Clausicoccus fenestratus (Deflandre and Fert, 1954) Prins, 1979
Clausicoccus obrutus (Perch-Nielsen, 1971) Prins, 1979
Clausicoccus subdistichus (Roth and Hay, in Hay et al., 1967) Prins, 1979
Clausicoccus vanheckae (Perch-Nielsen, 1986) n. comb.
Coccolithus miopelagicus Bukry, 1971
Coccolithus pelagicus (Wallich, 1877) Schiller, 1930
Coccolithus sp. 1
Coccolithus streckeri Takayama and Sato, 1986
Corannulus germanicus Stradner, 1962
Coronocyclus aff. *C. prionion* (Deflandre and Fert, 1954) Stradner in Stradner and Edward, 1968
Coronocyclus nitescens (Kamptner, 1963) Bramlette and Wilcoxon, 1967
Coronocyclus nitescens (ell.)
Coronocyclus nitescens (thick)
Crenalithus doronicoides (Black and Burns, 1961) Roth, 1973
Cryptococcolithus mediaperforatus (Varol, 1991) n. comb.
Cyclicarglithus abisectus (Muller, 1970) Wise, 1973
Cyclicargo. floridanus (Roth and Hay in Hay et al., 1967) Bukry, 1971
Cyclicargo. floridanus (9— 10 µm)
Discoaster adamanteus Bramlette and Wilcoxon, 1967
Discoaster asymmetricus Gartner, 1969
Discoaster aulakos Gartner, 1967
Discoaster barbadiensis Tan, 1927
Discoaster bellus Bukry and Percival, 1971
Discoaster cf. *D. bellus*
Discoaster binodosus Martini, 1958
Discoaster bollii Martini and Bramlette, 1963
Discoaster cf. *D. bollii*
Discoaster braarudii Bukry, 1971
Discoaster brouweri (Tan, 1927) emend. Bramlette and Riedel, 1954
Discoaster brouweri (3 ray)
Discoaster calculosus Bukry, 1971
Discoaster challengeri Bramlette and Riedel, 1954

Discoaster deflandrei Bramlette and Riedel, 1954
Discoaster deflandrei var. *nodosus* new variation
Discoaster deflandrei (5 ray)
Discoaster druggii Bramlette and Wilcoxon, 1967
Discoaster druggii (<15.0 µm)
Discoaster exilis Martini and Bramlette, 1963
Discoaster extensus Hay, 1967
Discoaster formosus Martini and Worsley, 1971
Discoaster intercalcaris Bukry, 1971
Discoaster kugleri Martini and Bramlette, 1963
Discoaster lautus Hay, 1967
Discoaster micros (Theodoridis, 1984) n. comb.
Discoaster moorei Bukry, 1971
Discoaster musicus Stradner, 1959
Discoaster neorectus Bukry, 1971
Discoaster nephados Hay in Hay, Mohler, Roth, Smidt, and Boudreaux, 1967
Discoaster obtusus Gartner, 1967
Discoaster pansus (Bukry and Percival, 1971) Bukry, 1973
Discoaster pentaradiatus (Tan, 1927) emend. Bramlette and Riedel, 1954
Discoaster petaliformis Moshkovitz and Ehrlich, 1980
Discoaster prepentaradiatus Bukry and Percival, 1971
Discoaster quinqueramus var. A
Discoaster saipanensis Bramlette and Riedel, 1954
Discoaster spp. (5 ray)
Discoaster spp. (6 ray)
Discoaster subsurculus Gartner, 1967
Discoaster surculus Martini and Bramlette, 1963
Discoaster tamalis Kamptner, 1967
Discoaster tanii Bramlette and Riedel, 1954
Discoaster tani nodifer Bramlette and Riedel, 1954
Discoaster tanii Bramlette and Riedel, 1954 *ornatus* Bramlette and Wilcoxon, 1967
Discoaster trinidadensis Hay, 1967
Discoaster variabilis Martini and Bramlette, 1963
Discoaster variabilis (3 ray)
Discoaster variabilis (5 ray asymmetric)
Discoaster variabilis (5 ray)
Discoaster woodringii Bramlette and Riedel, 1954
Ericsonia detecta n. sp.
Ericsonia formosa (Kamptner, 1963) Haq, 1971
Ericsonia sp. 1
Geminilithella bramlettei (Hay and Towe, 1962) Varol, 1989a
Geminilithella rotula (Kamptner, 1956) Backman, 1980
Gephyrocapsa sp., (<3.5 µm)
Hayaster perplexus (Bramlette and Riedel, 1954) Bukry, 1973
Hayella aperta Theodoridis, 1984
Hayella aperta (ell.)
Helicosphaera ampliaperta Bramlette and Wilcoxon, 1967
Helicosphaera bramlettei Muller, 1970
Helicosphaera burkei Black, 1971a
Helicosphaera carteri (Wallich, 1877) Kamptner, 1954
Helicosphaera aff. *H. carteri*
Helicosphaera compacta Bramlette and Wilcoxon, 1967
Helicosphaera elongata Theodoridis, 1984
Helicosphaera euphratis Haq, 1966
Helicosphaera euphratis (<8.0 µm)
Helicosphaera gartneri Theodoridis, 1984
Helicosphaera gertae Bukry, 1981
Helicosphaera granulata Burky and Percival, 1971
Helicosphaera intermedia Martini, 1965
Helicosphaera limasera n. sp.
Helicosphaera lophota Bramlette and Sullivan, 1961
Helicosphaera mediterranea Muller, 1981
Helicosphaera obliqua Bramlette and Wilcoxon, 1967
Helicosphaera paleocarteri Theodoridis, 1984
Helicosphaera perch-nielseniae Haq, 1971
Helicosphaera recta Haq, 1966
Helicosphaera reticulata Bramlette and Wilcoxon, 1967
Helicosphaera rhomba Bukry, 1971
Helicosphaera scissura Miller, 1981
Helicosphaera sellii Bukry and Bramlette, 1969
Helicosphaera seminulum Bramlette and Sullivan, 1961
Helicosphaera spp.
Helicosphaera truempyi Biolzi and Perch-Nielsen, 1982
Helicosphaera vedderi Bukry, 1981
Helicosphaera waltrans Theodoridis, 1984
Helicosphaera wilcoxonii Gartner, 1971
Homozygosphaera macropora (Deflandre in Deflandre and Fert 1954) n. comb.
Hughesius gizoensis Varol, 1989b
Hughesius tasmaniae (Edward and Perch-Nielsen, 1975) n. comb.
Ilselithina fusa Roth, 1970
Isthmolithus recurvus Martini, 1973
Lanternithus minutus Stradner, 1962
Lithostromation operosum (Deflandre, 1954) Bybell, 1975
Lithostromation simplex (Klumpp, 1953) Bybell, 1975
Micrantholithus aequalis Sullivan, 1964
Minylitha convallis Bukry, 1973
Neocrepidolithus spp. Romein, 1979
Orthozygus aureus (Stradner, 1962) Bramlette and Wilcoxon, 1967
Pedinocyclus larvalis (Burky and Bramlette, 1969b) Loeblich and Tappan, 1973
Pemma papillata Martini, 1959
Peritrachelina joidesa Bukry and Bramlette, 1968
Pontosphaera anisotrema (Kamptner, 1956) Backman, 1980
Pontosphaera callosa (Martini, 1969) Varol, 1982
Pontosphaera desueta (Muller, 1970) Perch-Nielsen, 1984
Pontosphaera enormis (Locker, 1967) Perch-Nielsen, 1984
Pontosphaera latoculata (Burky and Percival, 1971) Perch-Nielsen, 1984
Pontosphaera longiforaminis (Baldi-Beke, 1964) n. comb.
Pontosphaera multipora (Kamptner, 1948) Roth, 1970
Pontosphaera pygmaea (Locker, 1972) Bystricka and Lehotayava, 1974
Pontosphaera segmenta (Bukry and Percival, 1971) Knüttel, 1986
Pontosphaera spp.
Pyrocyclus hermosus Roth and Hay in Hay et al., 1967
Pyrocyclus inversus Hay and Towe, 1962
Pyrocyclus orangensis (Bukry, 1971) Backman, 1980
R. pseudoumbilicus var. *amplius* (Gartner, 1967) Gartner, 1969 var. *amplius* Gartner, 1992
Reticulofenestra ampliumbilicus Theodoridis, 1984
Reticulofenestra bisecta bisecta (Hay, Mohler, and Wade, 1966) Roth, 1970
Reticulofenestra bisecta (Hay, Mohler, and Wade, 1966) Roth, 1970 *filewiczii* Wise and Wiegand in Wise, 1983
Reticulofenestra circus n. sp.
Reticulofenestra daviesi (Haq, 1968) Haq, 1971
Reticulofenestra dictyoda (Deflandre in Deflandre and Fert, 1954) Stradner in Stradner and Edwards, 1968
Reticulofenestra gartneri Theodoridis, 1984
Reticulofenestra gelida (Geitzenauer, 1972) Backman, 1978
Reticulofenestra hampdenensis Edwards, 1973
Reticulofenestra haqii Backman, 1978
Reticulofenestra cf. *H. haqii*
Reticulofenestra hesslandii (Haq, 1966) Roth, 1970
Reticulofenestra hillae Bukry and Percival, 1971
Reticulofenestra lockerii Muller, 1970
Reticulofenestra minuta Roth, 1970
Reticulofenestra minutula (Gartner, 1967) Haq and Berggren, 1978
Reticulofenestra moguntina Martini, 1988
Reticulofenestra perplexa (Burns, 1975) Wise 1983
Reticulofenestra producta (Kamptner, 1963) Wei and Thierstein, 1991
Reticulofenestra pseudoumbilicus Gartner, 1969
Reticulofenestra reticulata (Gartner and Smith, 1967) Roth and Thierstein, 1972
Reticulofenestra stavensis (Levin and Joerger, 1967) Varol 1989b
Reticulofenestra spp., small
Reticulofenestra umbilicus (Levin, 1965) Martini and Ritzkowski, 1968
Rhabdosphaera clavigera Murray and Blackman, 1898
Rhabdosphaera procera Martini, 1969
Scapholithus fossilis Deflandre in Deflandre and Fert, 1954
Scyphosphaera spp.
Sphenolithus abies Deflandre in Deflandre and Fert, 1954
Sphenolithus akropodus n. sp.
Sphenolithus aubryae n. sp.
Sphenolithus belemnos Bramlette and Wilcoxon, 1967
Sphenolithus calyculus Bukry, 1985
Sphenolithus capricornutus Bukry and Percival, 1971
Sphenolithus ciperoensis Bramlette and Wilcoxon, 1967
Sphenolithus cometa n. sp.

Sphenolithus compactus Backman, 1980
Sphenolithus conicus Bukry, 1971
Sphenolithus delphix Bukry, 1973
Sphenolithus dissimilis Bukry and Percival, 1971
Sphenolithus distentus (Martini, 1965) Bramlette and Wilcoxon, 1967
Sphenolithus grandis Haq and Berggren, 1978
Sphenolithus heteromorphus Deflandre, 1953
Sphenolithus moriformis (Bronnimann and Stradner, 1960) Bramlette and Wilcoxon, 1967
Sphenolithus neoabies Bukry and Bramlette, 1969
Sphenolithus orphanknollensis Perch-Nielsen, 1971
Sphenolithus predistentus Bramlette and Wilcoxon, 1967
Sphenolithus pseudoradians Bramlette and Wilcoxon, 1967
Sphenolithus spiniger Bukry, 1971
Sphenolithus umbrellus (Bukry, 1971) Aubry and Knüttel, 1986
Syracosphaera lamina n. sp.
Syracosphaera spp.
Tetralithoides symeonidesii Theodoridis, 1984
Thoracosphaera operculata Bramlette and Martini, 1964
Thoracosphaera saxea Stradner, 1961
Thoracosphaera spp.
Transversopontis obliquipons (Deflandre in Deflandre and Fert, 1954) Hay, Mohler, and Wade, 1966
Transversopontis pulcher (Deflandre in Deflandre and Fert, 1954) Perch-Nielsen, 1967
Triquetrorhabdulus carinatus Martini, 1965
Triquetrorhabdulus challengeri Perch-Nielsen, 1977
Triquetrorhabdulus extensus Theodoridis, 1984
Triquetrorhabdulus milowii Bukry, 1971
Triquetrorhabdulus rioi Olafsson, 1989
Triquetrorhabdulus rugosus Bramlette and Wilcoxon, 1967
Triquetrorhabdulus serratus (Bramlette and Wilcoxon, 1967) Olafsson, 1989
Triquetrorhabdulus sp.
Umbilicosphaera cricota (Gartner, 1967) Cohen and Reinhardt, 1968
Umbilicosphaera jafari Müller, 1974
Umbilicosphaera sibogae foliosa (Kamptner, 1963) Okada and McIntyre, 1977
Umbilicosphaera sibogae (Weber-Van Bosse, 1901) Gardner, 1970 var. *sibogae*
Umbilicosphaera sp. (elliptical)
Zygrhablithus bijugatus (Deflandre in Deflandre and Fert, 1954) Deflandre, 1959
Zygrhablithus sp. 1

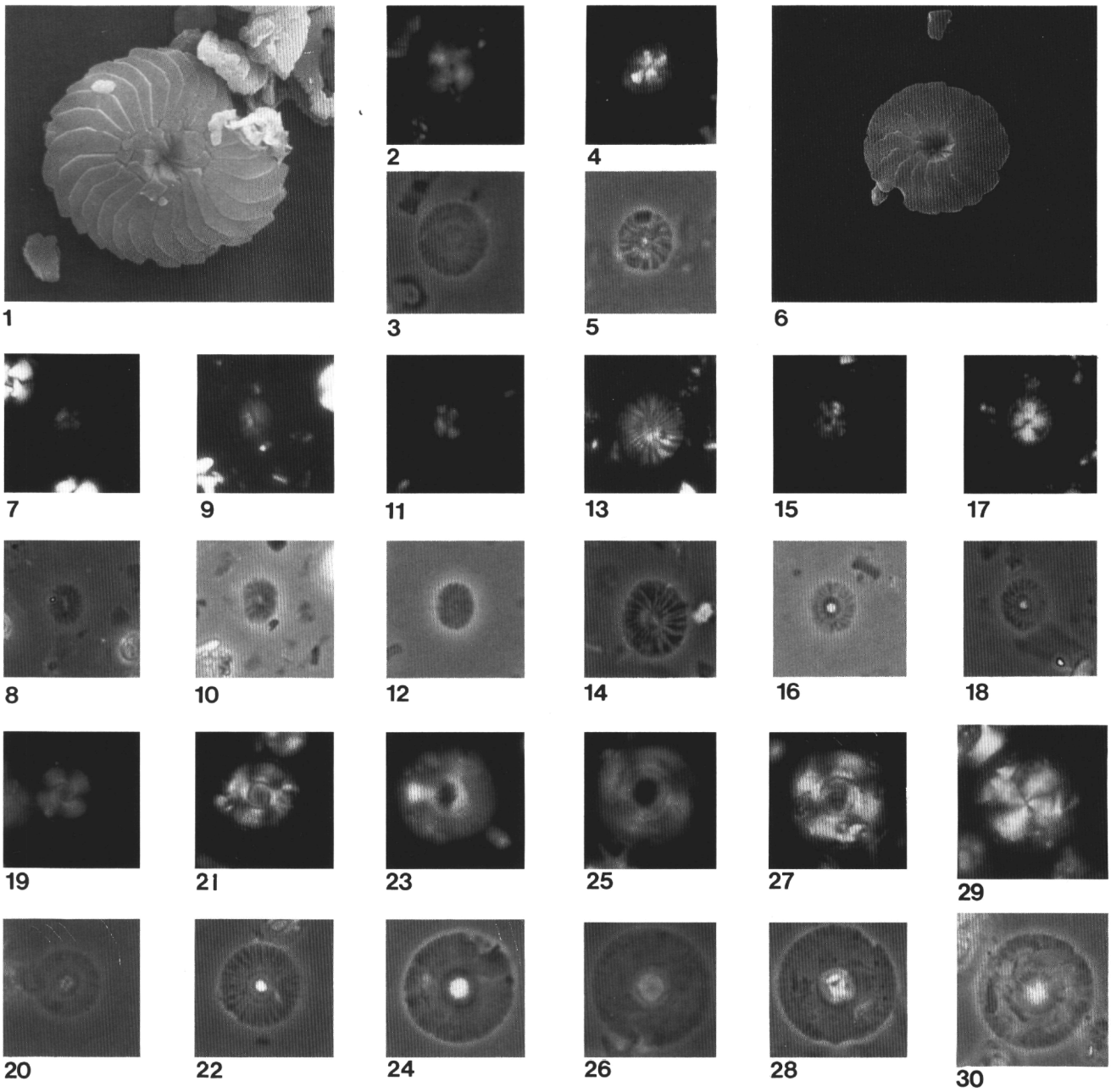

Plate 1. The illustrations of Plates 1-14 are scanning electron microscope (SEM) and light microscope (LM) micrographs. XP = cross-polarized light; Ph = phase contrast; PL = parallel light. Transferred specimens from the LM to the SEM are denoted on the plate captions by ^{TR}. Magnification for all LM micrographs is ×1700, except where otherwise indicated, and magnification for SEM micrographs is indicated (×3000, ×4000, ×5000, ×6000, or ×8000). Each plate represents one major group of forms, which may include one or several genera. **1-6.** *Calcidiscus leptoporus* (Murray and Blackman) Loeblich and Tappan. (1, 6) Distal view, ×6000, Sample 149-900A-22R-1, 122 cm. (2, 3) Sample 149-900A-25R-1, 79 cm, XP (2) and Ph (3). (4, 5) Sample 149-900A-34R-2, 83 cm, XP (4) and Ph (5). **7-10.** *Calcidiscus fuscus* (Backman) Janin. (7, 8) Sample 149-900A-32R-3, 7 cm, XP (7) and Ph (8). (9, 10) Sample 149-900A-38R-2, 57 cm, XP (9) and Ph (10). **11, 12.** *Calcidiscus pataecus* (Gartner) n. comb., Sample 149-900A-29R-1, 122 cm, XP (11) and Ph (12). **13, 14.** *Calcidiscus radiatus* (Kamptner) Martin Perez and Aguado, Sample 149-900A-32R-2, 100 cm, XP (13) and Ph (14). **15-18.** *Calcidiscus tropicus* (<6.0 µm) (Kamptner) Varol. (15, 16) Sample 149-900A-30R-4, 16 cm, XP (15) and Ph (16). (17, 18) Sample 149-900A-30R-2, 41 cm, XP (17) and Ph (18). **19, 20.** *Calcidiscus carlae* (Lehotayova and Priewalder) Janin, Sample 149-900A-12R-4, 10 cm, XP (19) and Ph (20). **21-28.** *Calcidiscus tropicus* (>6.0 µm) (Kamptner) Varol. (21, 22) Sample 149-900A-24R-5, 44 cm, XP (21) and Ph (22). (23, 24) Sample 149-900A-16R-1, 133 cm, XP (23) and Ph (24). (25, 26) Sample 149-900A-14R-5, 142 cm, XP (25) and Ph (26). (27, 28) XP, Sample 149-900A-15R-1, 16 cm, XP (27) and Ph (28). **29, 30.** *Calcidiscus macintyrei* (Bukry and Bramlette) Loeblich and Tappan, Sample 149-900A-12R-1, 48 cm, XP (29) and Ph (30).

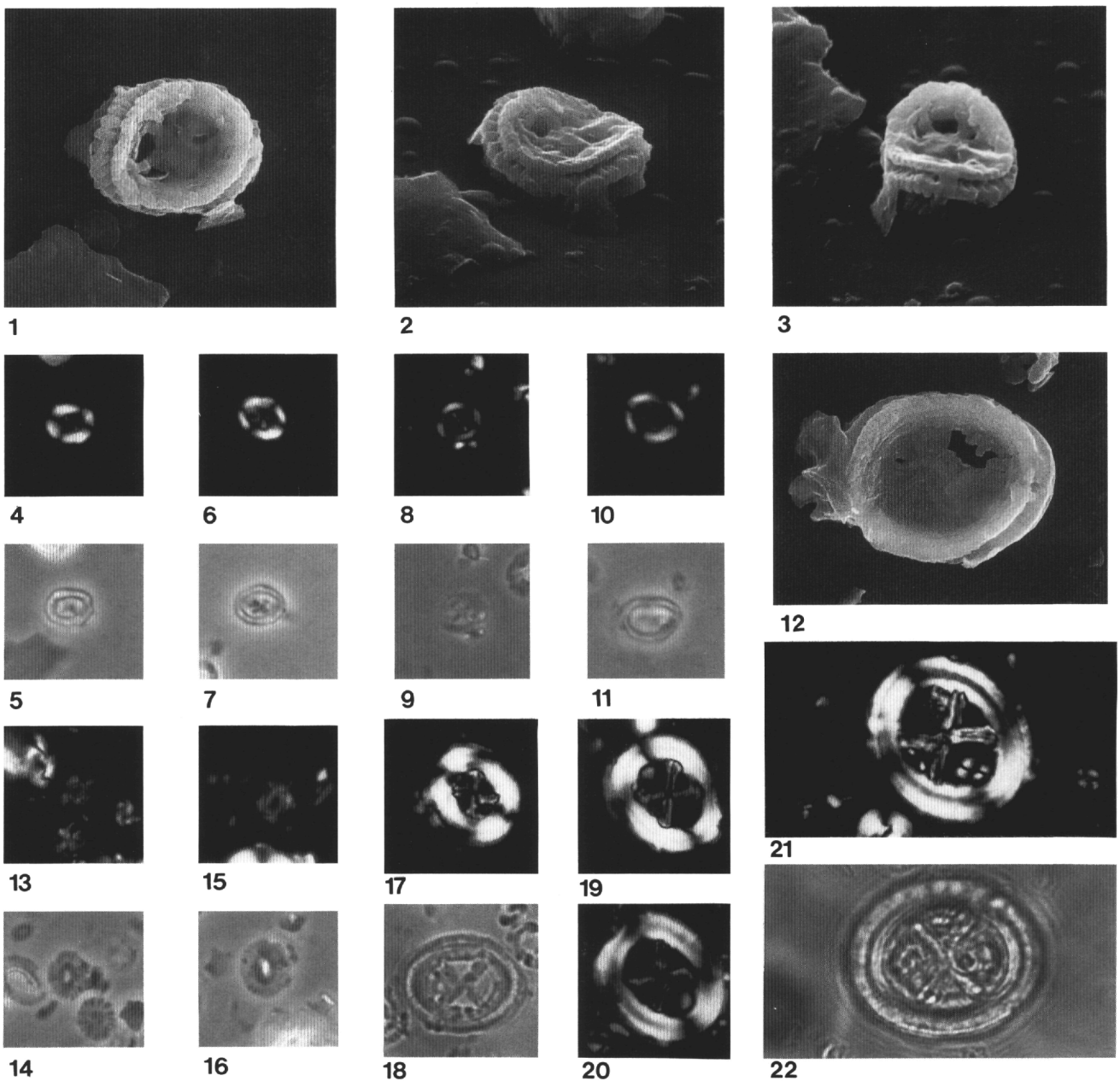

Plate 2. **1-12.** *Camuralithus pelliculatus* n. gen., n. spec. (1-5)[TR], holotype. (1) Proximal view, ×6000, Sample 149-900A-33R-5, 129 cm. (2, 3) Oblique proximal view, ×6000. (4, 5) XP and Ph. (6, 7) Sample 149-900A-33R-5, 129 cm, XP (6) and Ph (7). (8, 9) Sample 149-900A-38R-2, 57 cm, XP (8) and Ph (9). (10-12)[TR], Sample 149-900A-29R-1, 122 cm. (12) Proximal view, ×6000. (10, 11) XP and Ph. **13-16.** *Cryptococcolithus mediaperforatus* (Varol) n. comb. (13, 14) Sample 149-900A-29R-1, 121 cm, XP (13) and Ph (14). (15, 16) Sample 149-898A-2R-1, 72 cm, XP (15) and Ph (16). **17, 18.** *Chiasmolithus medius* Perch-Nielsen. (17) XP, Sample 149-900A-48R-4, 112 cm. (18) Ph, Sample 149-900A-50R-4, 16 cm. **19, 20.** *Chiasmolithus altus* Bukry and Percival. (19) XP, Sample 149-900A-51R-5, 120 cm. (20) XP, Sample 149-900A-51R-6, 47 cm. **21, 22.** *Chiasmolithus oamaruensis* (Deflandre) Hay, Mohler, and Wade, Sample 149-900A-53R-7, 45 cm, XP (21) and Ph (22).

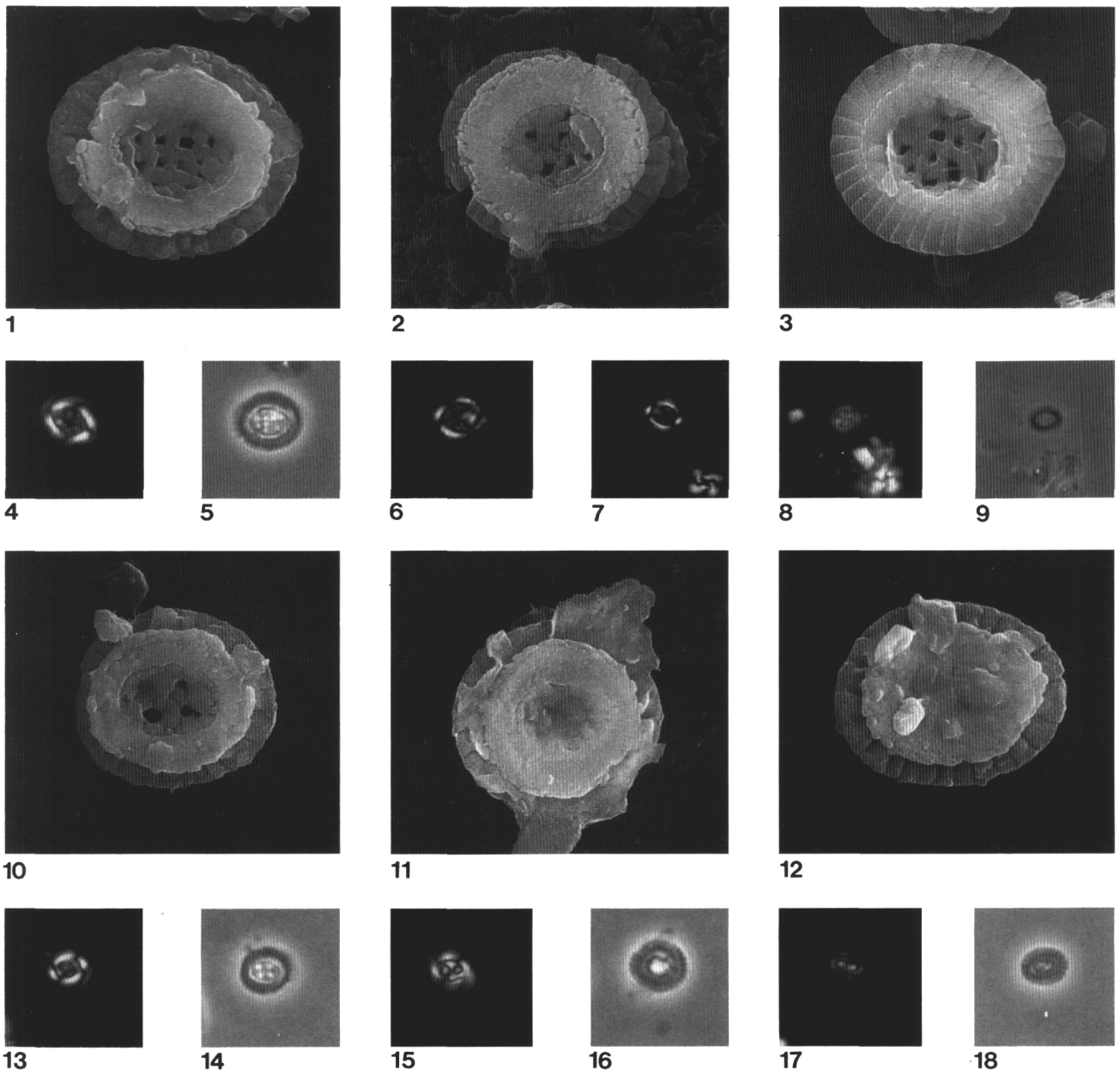

Plate 3. **1-7.** *Clausicoccus fenestratus* (Deflandre and Fert) Prins. (1, 4, 5)[TR], Sample 149-900A-39R-3, 109 cm. (1) Proximal view, ×6000, (4, 5) XP and Ph. (2) Proximal view, ×6000, Sample 149-900A-39R-3, 109 cm. (3) Distal view, ×6000, Sample 149-900A-39R-3, 109 cm. (6) XP, Sample 149-900A-51R-5, 120 cm. (7) XP, Sample 149-900A-49R-2, 44 cm. **8, 9.** *Hughesius tasmaniae* (Edward and Perch-Nielsen) n. comb., Sample 149-900A-27R-2, 72 cm, XP (8) and Ph (9). **10, 11, 13-16.** *Clausicoccus obrutus* (Perch-Nielsen) Prins, Sample 149-900A-39R-3, 109 cm. (10, 13, 14)[TR]. (10) Proximal view, ×6000, (13, 14) XP and Ph. (11, 15, 16)[TR]. (11) Proximal view, ×6000, (15, 16) XP and Ph. **12, 17, 18**[TR]. *Hughesius gizoensis* Varol and Girgis, Sample 149-900A-39R-3, 109 cm. (12) Proximal view, ×8000, (17, 18)XP and Ph.

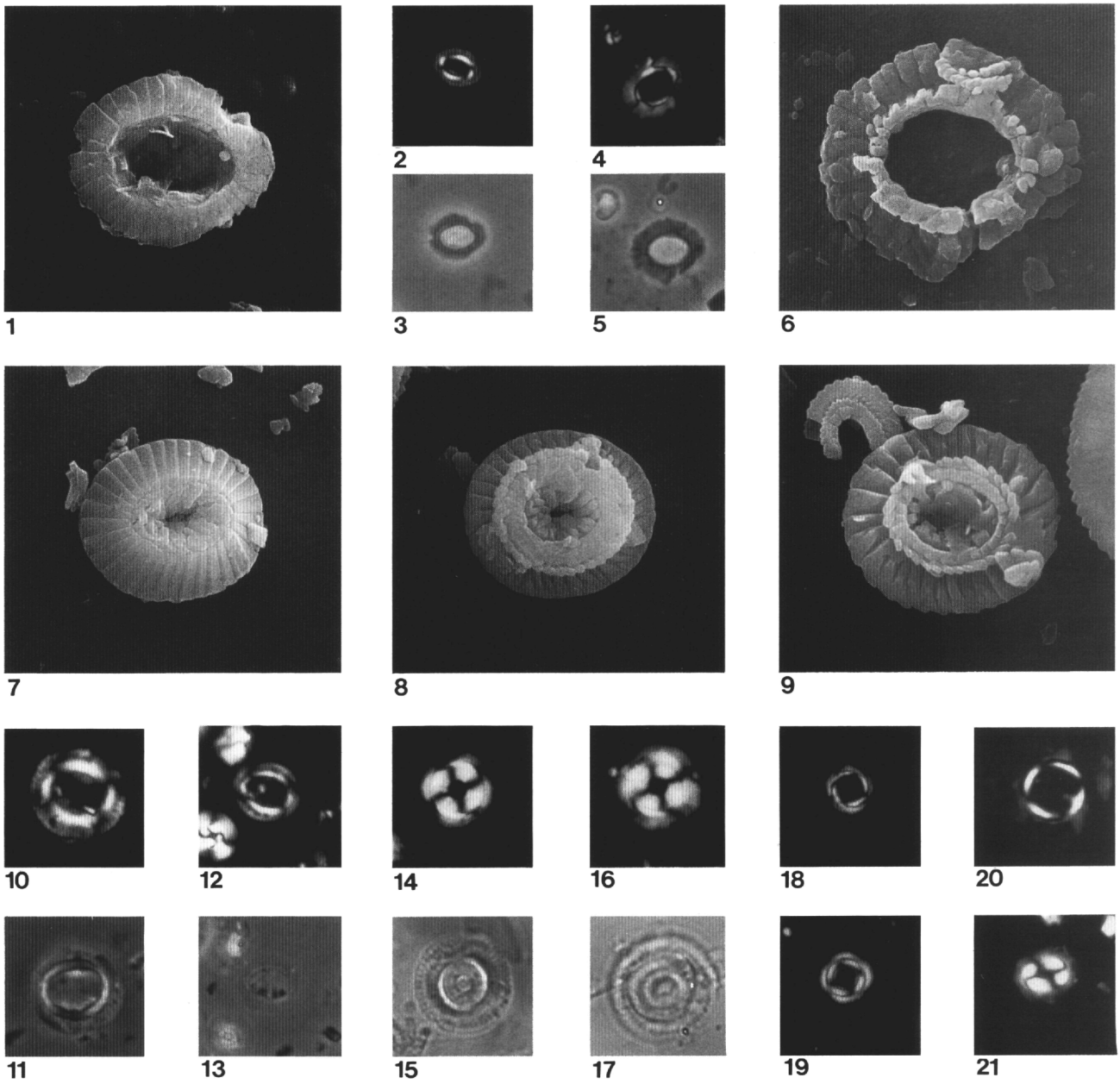

Plate 4. **1-6.** *Ericsonia detecta* n. sp. (1-3)[TR], holotype, Sample 149-900A-33R-5, 129 cm. (1) Distal view, ×6000. (2, 3) XP and Ph. (4-6)[TR], Sample 149-900A-51R-6, 47 cm. (6) Proximal view, ×6000, (4, 5) XP and Ph. **7, 8, 21.** *Coccolithus pelagicus* (Wallich) Schiller. (7) Distal view, ×4000, Sample 149-900A-29R-21, 122 cm. (8) Proximal view, ×4000, Sample 149-900A-29R-21, 122 cm. (21) XP. **9.** *Ericsonia* sp., Proximal view, ×6000, Sample 149-900A-29R-1, 122 cm. **10-13.** *Coccolithus* sp. 1. (10, 11) Sample 149-900A-25R-1, 79 cm, XP (10) and Ph (11). (12, 13) Sample 149-900A-27R-2, 72 cm, XP (12) and Ph (13). **14-17.** *Ericsonia formosa* (Kamptner) Haq. (14, 15) Sample 149-900A-52R-6, 14 cm, XP (14) and Ph (15). (16, 17) Sample 149-900A-53R-6, 86 cm, XP (16) and Ph (17). **18, 19.** *Geminilithella bramlettei* (Hay and Towe) Varol. (18) XP, Sample 149-900A-53R-6, 86 cm. (19) XP, Sample 149-900A-53R-4, 91 cm. **20.** *Ericsonia* sp. 1, ×2500, XP, Sample 149-900A-48R-4, 142 cm.

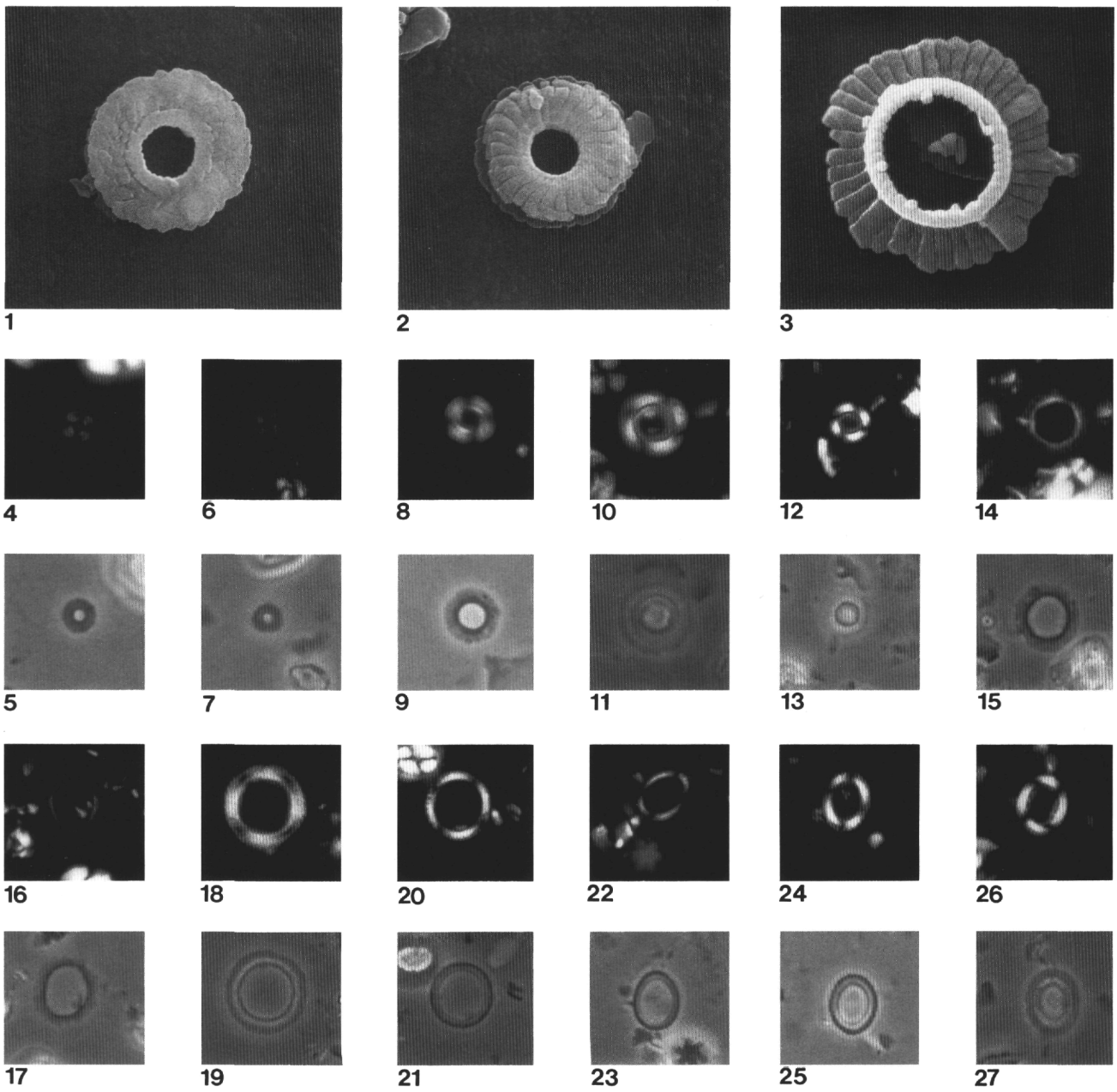

Plate 5. **1, 2, 4-7.** *Umbilicosphaera jafari* Muller. (1, 4, 5)[TR]. (1) Distal view, ×8000, Sample 149-900A-22R-1, 122 cm. (4, 5) XP and Ph. (2, 6, 7)[TR], Sample 149-900A-22R-1, 122 cm. (2) Proximal view, ×8000. (6, 7) XP and Ph. **3, 8-11.** *Geminilithella rotula* (Kamptner) Backman. (3) Proximal view of distal shield, ×8000, Sample 149-900A-22R-1, 122 cm. (8, 9) (small) Sample 149-898A-23R-5, 70 cm, XP (8) and Ph (9). (10, 11) (large) Sample 149-900A-14R-5, 142 cm, XP (10) and Ph (11). **12, 13.** *Umbilicosphaera sibogae foliosa* (Kamptner) Okada and McIntyre, Sample 149-900A-14R-6, 112 cm, XP (12) and Ph (13). 14, 15. *Umbilicosphaera cricota* (Gartner) Cohen and Reinhardt, Sample 149-900A-14R-7, 144 cm, XP (14) and Ph (15). **16, 17.** *Umbilicosphaera* sp., elliptical Lohmann, Sample 149-900A-16R-1, 133 cm, XP (16) and Ph (17). **18-23.** *Coronocyclus nitescens* (Kamptner) Bramlette and Wilcoxon. (18, 19) (thick) Sample 149-900A-25R-1, 79 cm, XP (18) and Ph (19). (20, 21) Sample 149-900A-25R-1, 79 cm, XP (20) and Ph (21). (22, 23) (elliptical) Sample 149-900A-23R-3, 101 cm, XP (22) and Ph (23). **24-27.** *Coronocyclus* aff. *C. prionion* (Deflandre and Fert) Stradner in Stradner and Edward. (24, 25) Sample 149-900A-23R-3, 101 cm, XP (24) and Ph (25). (26, 27) Sample 149-900A-15R-3, 30 cm, XP (26) and Ph (27).

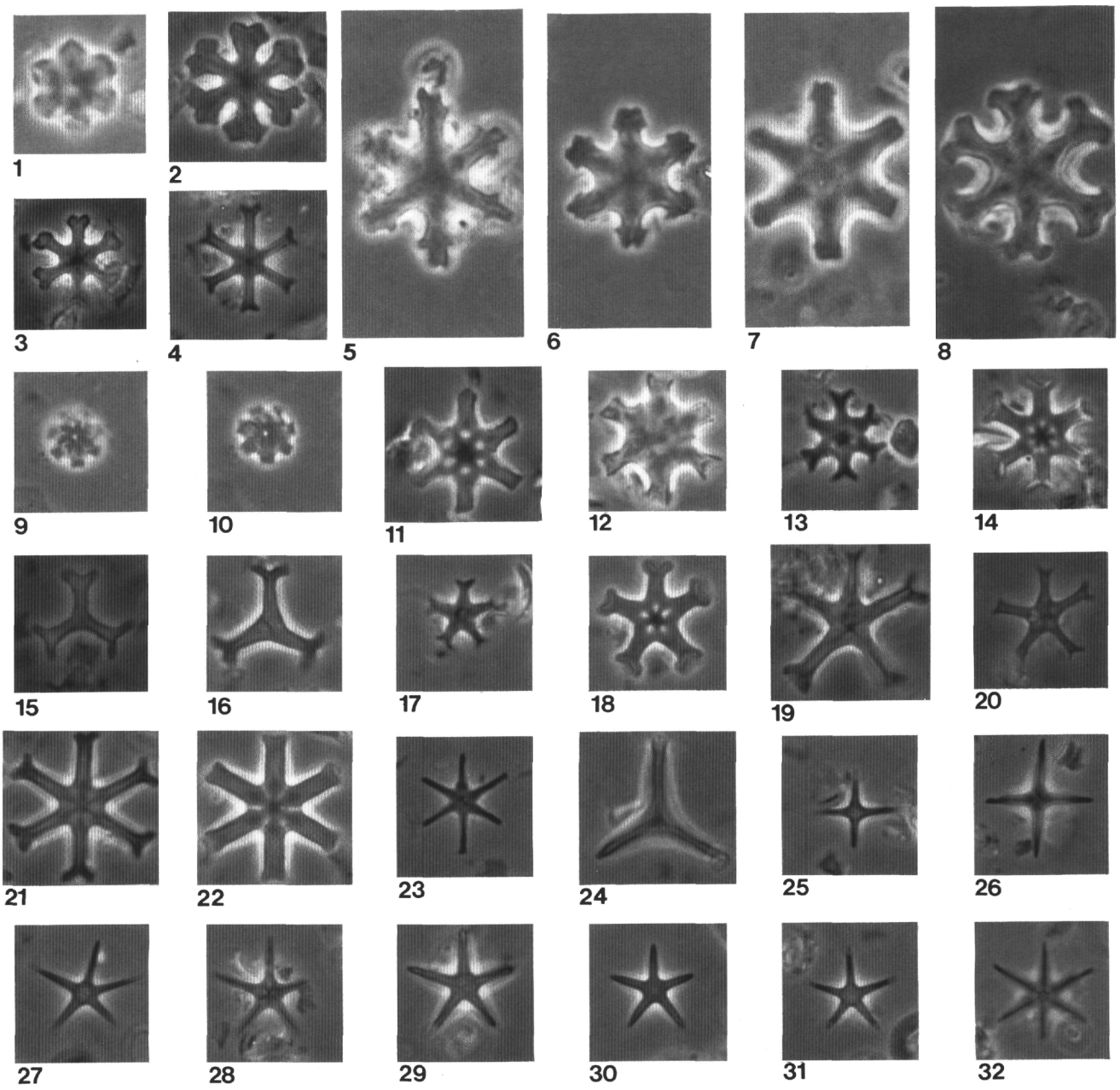

Plate 6. All micrographs are in phase contrast light. **1.** *Discoaster obtusus* Gartner, Sample 149-900A-23R-1, 80 cm. **2.** *Discoaster deflandrei* Bramlette and Riedel (5 ray), Sample 149-900A-20R-4, 90 cm. **3.** *Discoaster aulakos* Gartner, Sample 149-900A-27R-3, 33 cm. **4.** *Discoaster extensus* Hay, Sample 149-900A-20R-5, 64 cm. **5, 6.** *Discoaster deflandrei* var. *nodosus* new variation. (5) Sample 149-898A-25R-1, 105 cm. (6) Sample 149-898A-26R-2, 63 cm. **7.** *Discoaster druggii* Bramlette and Wilcoxon, Sample 149-898A-22R-5, 86 cm. **8.** *Discoaster variabilis* Martini and Bramlette, Sample 149-900A-20R-5, 64 cm. **9, 10.** *Discoaster micros* (Theodoridis) n. comb. (9) (high focus), Sample 149-900A-13R-CC. (10) (low focus). **11.** *Discoaster musicus* Stradner, Sample 149-900A 20R-5, 64 cm. **12.** *Discoaster kugleri* Martini and Bramlette, Sample 149-898A-18R-5, 134 cm. **13.** *Discoaster bollii* Martini and Bramlette, (small), Sample 149-900A-16R-2, 71 cm. **14-19, 21.** *Discoaster variabilis* Martini and Bramlette. (14) (bright tips), Sample 149-900A-14R-7, 44 cm. (15) (3 ray), Sample 900A-14R-5, 142 cm. (16) (3 ray), Sample 149-900A-12R-2, 106 cm. (17) (5 ray), Sample 149-900A-16R-2, 71 cm. (18) (5 ray), Sample 149-900A-14R-6, 66 cm. (19) (5 ray asymmetric), Sample 149-900A-16R-2, 71 cm. (21) (6 ray), Sample 149-900A-12R-1, 48 cm. **20.** *Discoaster prepentaradiatus* Bukry and Percival, Sample 149-900A-12R-1, 48 cm. **22.** *Discoaster surculus* Martini and Bramlette, (early form), Sample 149-900A-12R-1, 112 cm. **23.** *Discoaster braarudii* Bukry, Sample 149-900A-16R-1, 133 cm. **24, 32.** *Discoaster broweri* (Tan) emend. Bramlette and Riedel. (24) (3 ray), Sample 149-900A-14R-7, 144 cm. (32) Sample 149-900A-14R-7, 44 cm. **25, 26.** *Discoaster tamalis* Kamptner. (25) Sample 149-900A-15R-4, 43 cm. (26) Sample 149-900A-15R-1, 16 cm. **27.** *Discoaster asymmetricus* Gartner, Sample 149-900A-14R-6, 112 cm. **28.** *Discoaster* cf. *D. bellus* Sample 149-900A-16R-1, 133 cm. **29, 30.** *Discoaster bellus* Bukry and Percival. (29) Sample 149-900A-15R-1, 87 cm. (30) Sample 149-900A-15R-4, 43 cm. **31.** *Discoaster quinqueramus* var. A. Sample 149-900A-15R-4, 43cm.

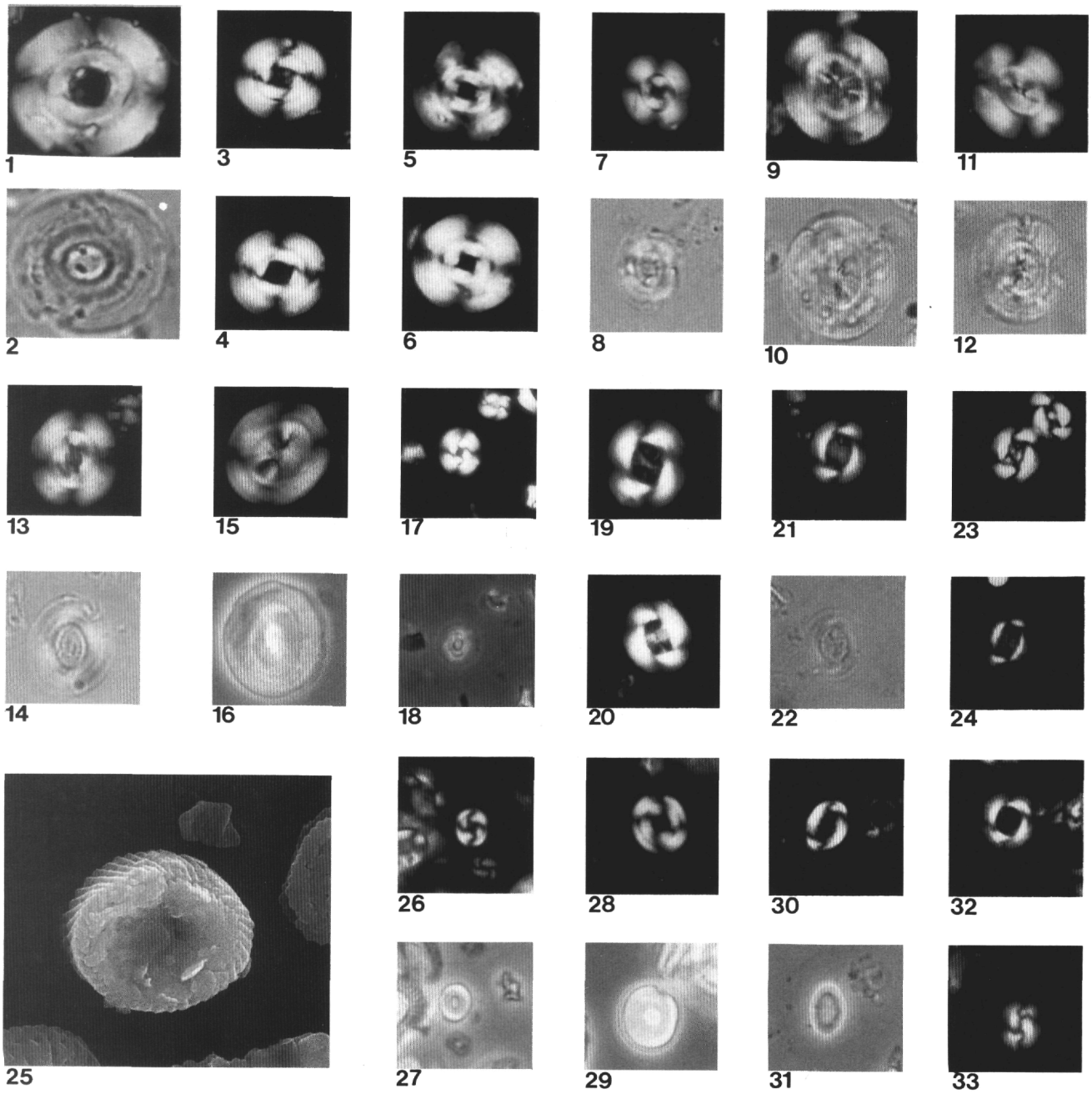

Plate 7. **1, 2.** *Reticulofenestra umbilicus* (Levin) Martini and Ritzkowski, Sample 149-900A-53R-1, 141 cm, XP (1) and PL (2). **3, 4.** *Reticulofenestra circus* n. sp. (3) Holotype, Sample 149-900A-50R-5, 6 cm, XP. (4) XP. **5, 6.** *Cyclicargolithus abisectus* (Muller) Wise, Sample 149-900A-44R-1, 131 cm. (5) XP. (6) XP. **7, 8.** *Cyclicargolithus floridanus* (Roth and Hay) Bukry, Sample 149-900A-39R-1, 78 cm, XP (7) and Ph (8). **9, 10.** *Reticulofenestra stavensis* (Levin and Joerger) Varol, Sample 149-900A-39R-1, 24 cm, XP (9) and Ph (10). **11, 12.** *Reticulofenestra bisecta bisecta* (Hay, Mohler, and Wade) Roth, (<10.0 µm), Sample 149-900A-39R-1, 24 cm, XP (11) and Ph (12). **13, 14.** *Reticulofenestra bisecta* (Hay, Mohler, and Wade) *Roth, filewiczii,* Wise and Wiegand, Sample 149-900A-39R-1, 24 cm, XP (13) and Ph (14). **15, 16.** *Bicolomnus ovatus* Wei and Wise, Sample 149-900A-39R-3, 109 cm, XP (15) and Ph (16). 17, 18. *Reticulofenestra haqii* Backman, Sample 149-900A-30R-2, 41 cm, XP (17) and Ph (18). **19, 20.** *Reticulofenestra lockerii* Müller. (19) Sample 149-900A-26R-2, 136 cm, XP. (20) Sample 149-900A-32R-2, 100 cm, XP. **21, 22.** *Reticulofenestra moguntina* Martini, Sample 149-900A-39R-1, 24 cm, XP (21) and Ph (22). **23**. *Reticulofenestra daviesi* (Haq) Haq, Sample 149-900A-48R-5, 103 cm, XP. **24.** *Reticulofenestra hampdenensis* Edwards, Sample 149-900A-39R-3, 109 cm, XP. **25-29.** *Pyrocyclus orangensis* (Bukry) Backman. (25-27)^{TR}, Sample 149-900A-29R-1, 122 cm. (25) Proximal view, ×8000. (26, 27) XP and Ph. (28, 29) (large), Sample 149-900A-39R-3, 109 cm, XP (28) and Ph (29). **30, 31.** *Pyrocyclus hermosus* Roth and Hay, Sample 149-900A-12R-2, 106 cm, XP (30) and Ph (31). **32.** *Crenalithus doronicoides* (Black and Burns) Roth, Sample 149-900A-12R-1, 48 cm, XP. **33.** *Reticulofenestra producta* (Kamptner) Wei and Thierstein, Sample 149-900A-12R-1, 48 cm, XP.

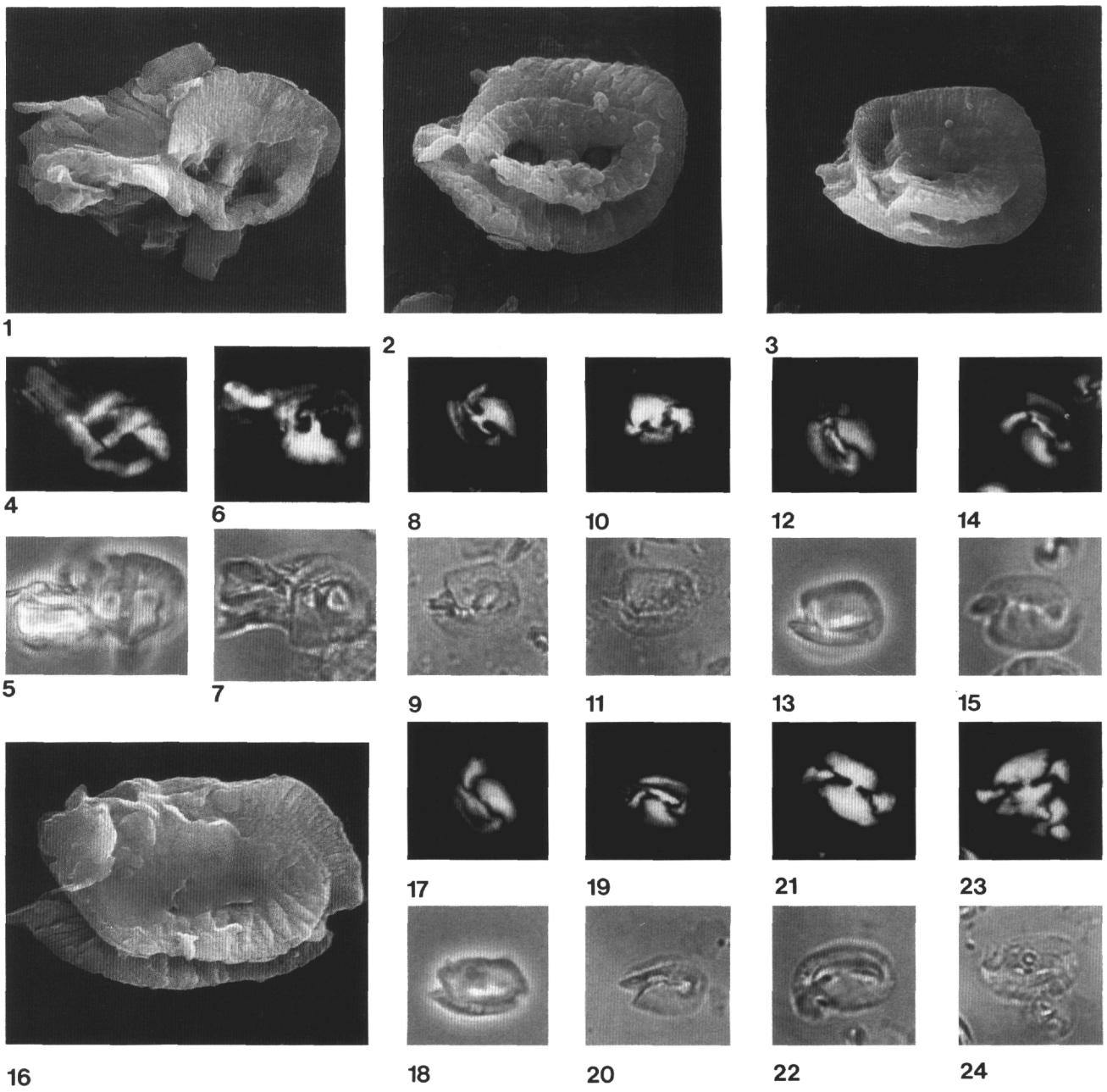

Plate 8. **1, 2, 4-11.** *Helicosphaera recta* Haq. (1, 4, 5)[TR], (long flange), Sample 149-900A-39R-3, 109 cm. (1) Proximal view, ×3000. (4, 5) XP and Ph. (6, 7) (long flange), Sample 149-900A-39R-3, 109 cm, XP (6) and PL (7). (2) Proximal view, ×4000, Sample 149-900A-51R-6, 47 cm. (8, 9) Sample 149-900A-44R-1, 131 cm, XP and PL. (10, 11) Sample 149-900A-44R-1, 131 cm, XP (10) and PL (11). **3, 12-15.** *Helicosphaera perch-nielseniae* Haq. (3, 12, 13)[TR], Sample 149-900A-39R-3, 109 cm. (3) Proximal view, ×4000. (12, 13) XP and Ph. (14, 15) XP, and PL. **16-20.** *Helicosphaera obliqua* Bramlette and Wilcoxon. (16-18)[TR], Sample 149-900A-39R-3, 109 cm. (16) Proximal view, ×6000. (17, 18) XP and Ph. (19, 20) Sample 149-900A-39R-3, 109 cm, XP (19) and PL (20). **21-24.** *Helicosphaera* aff. *H. carteri* (Wallich) Kamptner. (21, 22) Sample 149-900A-50R-5, 16 cm, XP (21) and PL (22). (23, 24) Sample 149-900A-50R-5, 16 cm, XP (23) and PL (24).

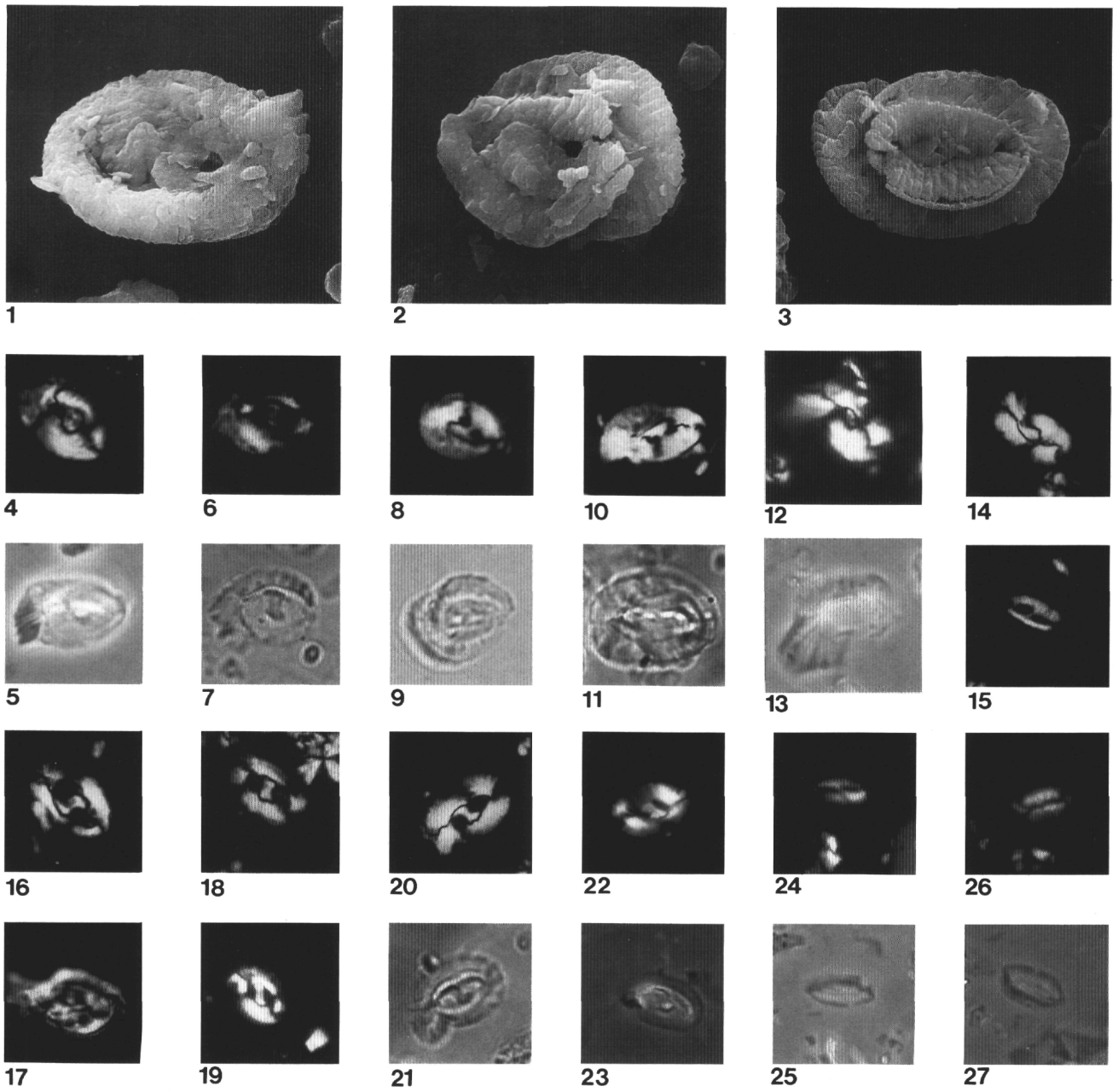

Plate 9. **1, 4-7.** *Helicosphaera wilcoxonii* Gartner. (1, 4, 5)[TR], Sample 149-900A-51R-6, 47 cm. (1) Distal view, ×4000. (4, 5) XP and Ph. (6, 7) Sample 149-900A-52R-6, 14 cm, XP (6) and PL (7). **2, 8-11.** *Helicosphaera compacta* Bramlette and Wilcoxon. (2, 8, 9)[TR], Sample 149-900A-51R-6, 47 cm. (2) Proximal view, ×4000. (8, 9) XP and PL. (10, 11) Sample 149-900A-52R-6, 14 cm, XP (10) and PL (11). **3, 12-14.** *Helicosphaera euphratis* Haq. (3) Proximal view, ×5000, Sample 900A-51R-6, 47 cm. (12, 13) (large flange) Sample 149-898A-24R-4, 121 cm, XP (12) and Ph (13). (14) Sample 149-897C-7R-2, 122 cm, XP. **15, 24-27.** *Helicosphaera elongata* Theodoridis. (15)Sample 149-900A-44R-1, 131 cm, XP. (24, 25) Sample 149-900A-33R-5, 129 cm, XP (24) and Ph (25). (26, 27) Sample 149-900A-34R-2, 83 cm, XP (26) and Ph (27). **16.** *Helicosphaera bramlettei* Muller, Sample 149-900A-51R-5, 120 cm, XP. **17.** *Helicosphaera reticulata* Bramlette and Wilcoxon, Sample 149-900A-33R-4, 91 cm, XP. **18.** *Helicosphaera truempyi* Biolzi and Perch-Nielsen, Sample 149-899B-7R-2, 122 cm, XP. **19.** *Helicosphaera gartneri* Theodoridis, Sample 149-900A-27R-3, 33 cm, XP. **20-23.** *Helicosphaera intermedia* Martini. (20, 21) Sample 149-898A-32R-3, 34 cm, XP (20) and PL (21). (22, 23) Sample 149-900A-32R-3, 7 cm, XP (22) and Ph (22).

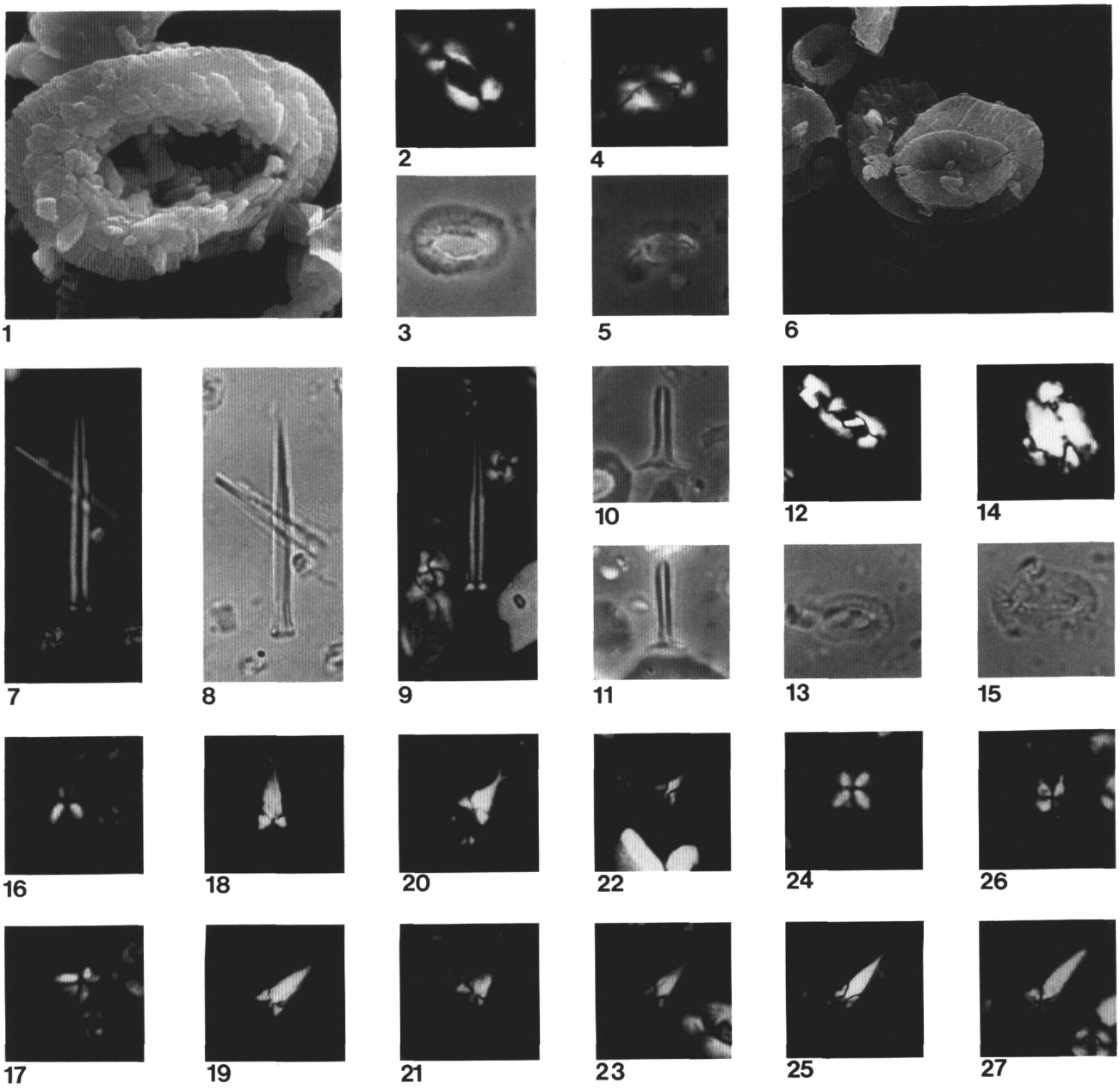

Plate 10. **1-3.** *Helicosphaera ampliaperta* Bramlette and Wilcoxon. 1. Distal view, ×6000, Sample 149-900A-22R-1, 122 cm. (2, 3) Sample 149-898A-20R-1, 72 cm, XP (2) and Ph (3). **4-6.** *Helicosphaera paleocarteri* Theodoridis. (6) Proximal view, ×4000, Sample 149-900A-22R-1, 122 cm. (4, 5)Sample 149-900A-25R-1, 79 cm, XP (4) and Ph (5). **7-9.** *Blackites tenuis* (Bramlette and Sullivan) Bybell. 7, 8. Sample 149-900A-53R-1, 141 cm, XP (7) and Ph (8). 9. Sample 149-900A-53R-2, 45 cm, XP. **10, 11.** *Rhabdosphaera procera* Martini, Sample 149-900A-38R-2, 57 cm, Ph (10) and Ph (11). **12, 13.** *Helicosphaera limasera* n. sp., Holotype, Sample 897C-47R-6, 6 cm, XP (12) and PL (13). **14, 15.** *Helicosphaera* aff. *H. carteri* (Wallich) Kamptner, Sample 149-897C-47R-6, 6 cm, XP (14) and PL (15). **16, 17.** *Sphenolithus orphanknollensis* Perch-Nielsen, Sample 149-900A-53R-6, 86 cm, XP, 0° (16) and XP, 45° (17). **18-21.** *Sphenolithus distentus* (Martini) Bramlette and Wilcoxon. (18, 19) Sample 149-897C-45R-4, 109 cm, XP, 0° (18) and XP, 45° (19). (20) Sample 149-900A-49R-4, 99 cm, XP, 45°. (21) Sample 149-900A-49R-3, 113 cm, XP, 45°. **22, 23, 25.** *Sphenolithus ciperoensis* Bramlette and Wilcoxon. (22) Sample 149-900A-44R-1, 131 cm, XP, 45°. (23) Sample 149-900A-44R-1, 131 cm, XP, 45°. (25) Sample 149-899B-9R-5, 21 cm, XP, 45°. **24, 26**, 27. *Sphenolithus calyculus* Bukry, Sample 149-900A-36R-1, 56 cm. (24) XP, 0°. (26-27) XP, 0° and XP, 45°.

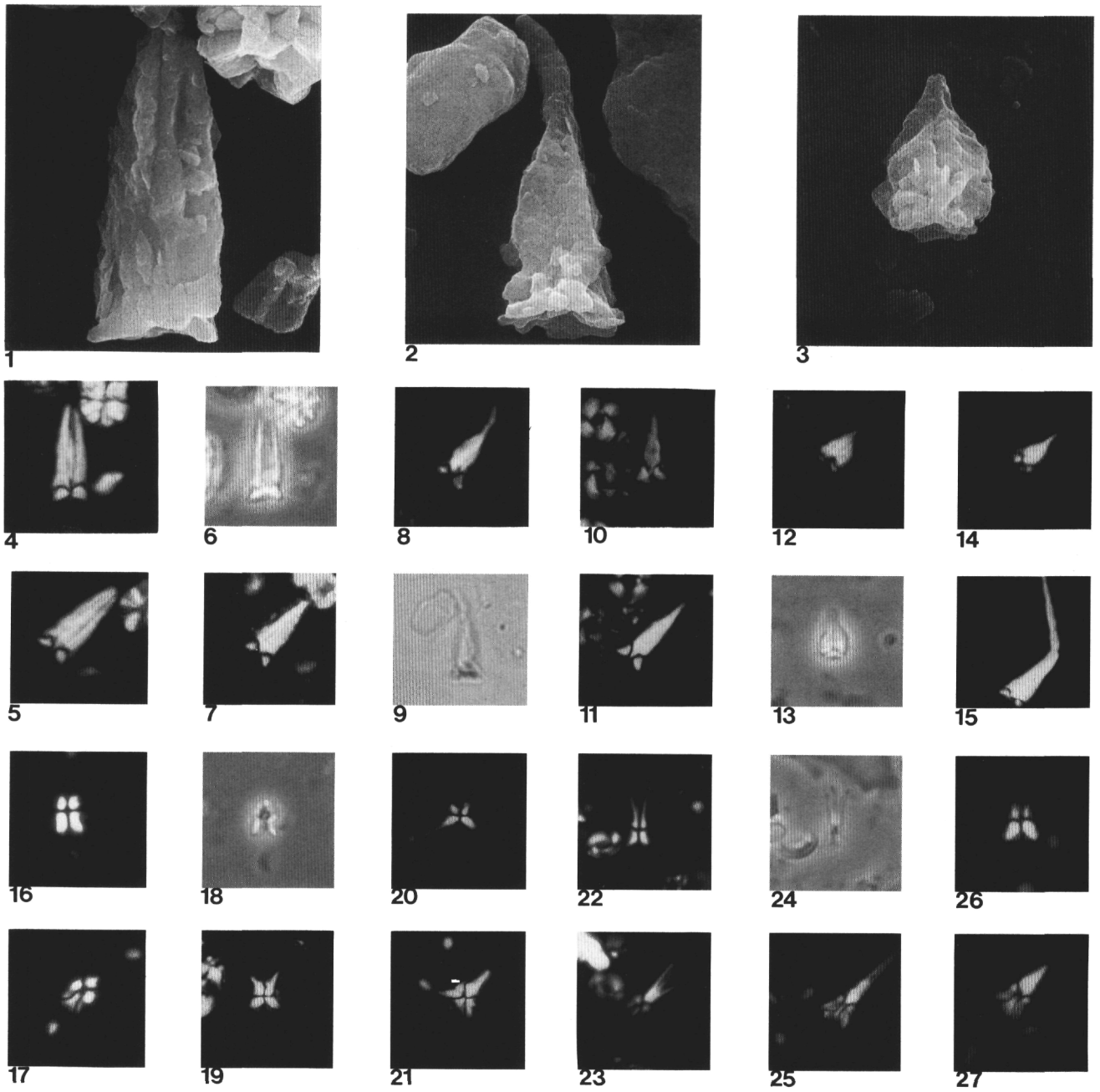

Plate 11. **1, 2, 4-11.** *Sphenolithus akropodus* n. sp. (1, 4-6)[TR], holotype, Sample 149-900A-51R-6, 47 cm. (1) ×6000. (4, 5) XP, 0° and XP, 45°. (6) Ph. (2, 8, 9)[TR], Sample 149-900A-51R-6, 47 cm. (2) ×6000. (8, 9) XP, 45° and Ph. (7) Sample 149-897C-49R-3, 123 cm; XP, 45°. (10, 11) Sample 149-900A-51R-6, 47 cm; XP, 0° and XP, 45°. **3, 12-15.** *Sphenolithus predistentus* Bramlette and Wilcoxon. (3, 12, 13)[TR], Sample 149-900A-51R-6, 47 cm. (3) ×6000. (12, 13) XP, 45° and Ph. (14) Sample 149-900A-50R-5, 16 cm; XP, 45°. (15) Sample 149-900A-50R-5, 16 cm; XP, 45°. **16-18.** *Sphenolithus aubryae* n. sp., holotype, Sample 149-900A-29R-6, 23 cm; XP, 0° (16); XP, 45° (17); and Ph (18) **19.** *Sphenolithus capricornutus* Bukry and Percival, Sample 149-898A-28R-1, 99 cm; XP, 0°. **20, 21.** *Sphenolithus delphix* Bukry, Sample 149-898A-28R-1, 99 cm; XP, 0° (20) and XP, 45° (21). **22-24.** *Sphenolithus cometa* n. sp., holotype, Sample 149-898A-24R-5, 24 cm; XP, 0° (22), XP, 45° (23), and Ph (24). **25-27.** *Sphenolithus belemnos* Bramlette and Wilcoxon, Sample 149-900A-24R-5 44 cm (25) XP, 45°. (26, 27) XP, 0° and XP, 45°.

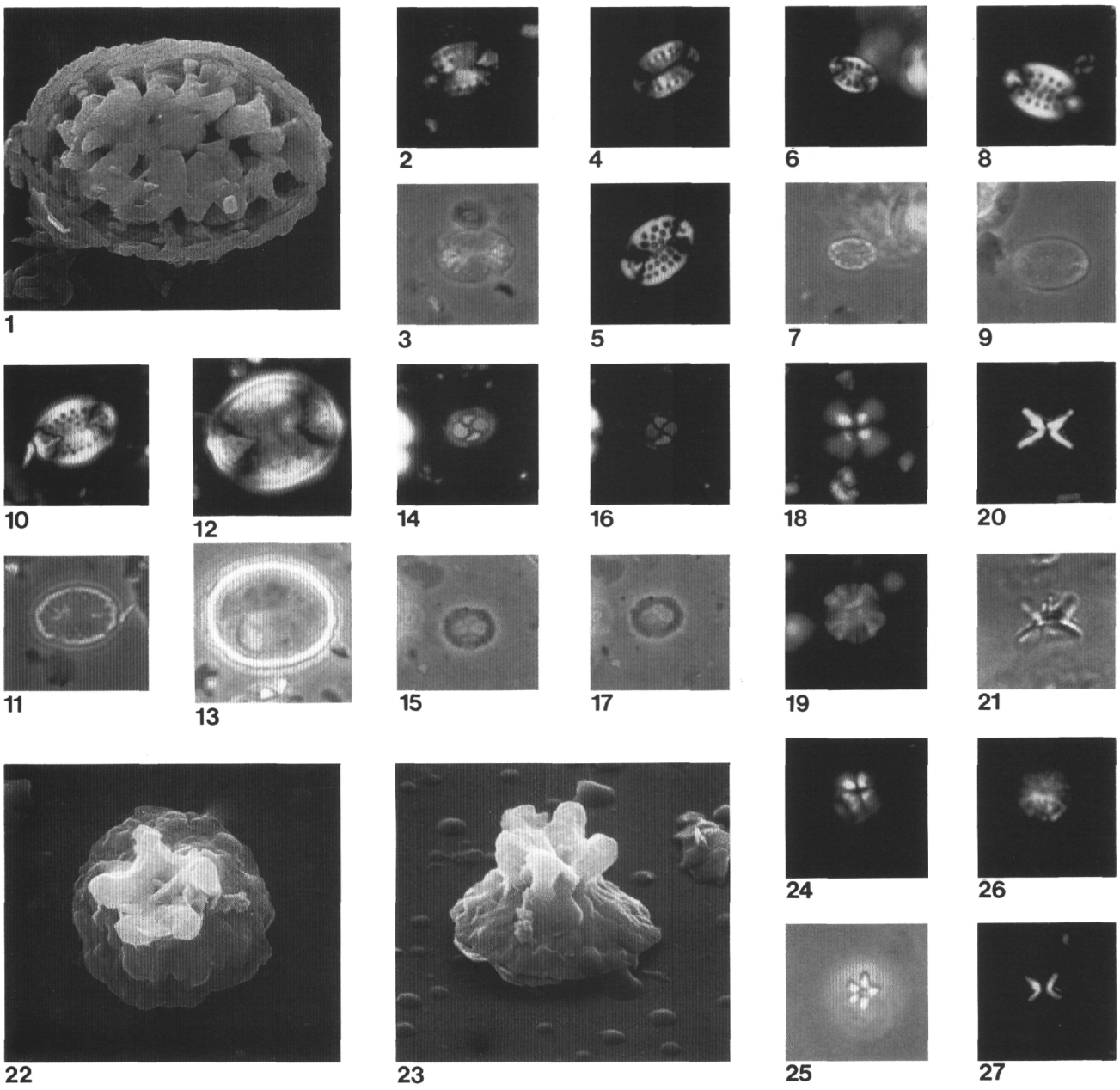

Plate 12. **1-4.** *Pontosphaera longiforaminis* (Baldi-Beke) n. comb. (1) Distal view, ×6000, Sample 149-900A-22R-1, 122 cm. (2, 3) Sample 149-900A-38R-2, 57 cm, XP (2) and Ph (3). (4) Sample 149-900A-32R-2, 100 cm, XP. **5-9.** *Pontosphaera multipora* (Kamptner) Roth. (5) Sample 149-899B-7R-2, 122 cm, XP. (6, 7) (1 cycle of perforations) Sample 149-900A-23R-3, 101 cm, XP (6) and Ph (7). (8, 9) (2 cycles of perforations) Sample 149-900A-34R-2, 83 cm, XP (8) and Ph (9). **10, 11.** *Pontosphaera callosa* (Martini) Varol, Sample 149-900A-25R-1, 79 cm, XP (10) and Ph (11). **12, 13.** *Pontosphaera anisotrema* (Kamptner) Backman, Sample 149-900A-23R-3, 101 cm, XP (12) and Ph (13). **14-17.** *Tetralithoides symeonidesii* Theodoridis. (14, 15) Sample 149-900A-38R-5, 47 cm, XP (14) and Ph (15). (16, 17) Sample 149-900A-38R-5, 47 cm, XP (16) and Ph (17). **18-27.** *Ilselithina fusa* Roth. (18-19) Sample 149-900A-38R-2, 57 cm, XP, high focus (18) and XP, low focus (19). (20, 21) Side view, Sample 149-900A-39R-3, 109 cm, XP (20) and Ph (21). (22-26)[TR], Sample 149-900A-33R-5, 129 cm. (22) Distal view, ×6000. (23) Distal oblique view, ×6000. (24, 25, 26) XP, high focus (24), XP, low focus (26), and Ph (25). (27) Side view, Sample 149-900A-53R-4, 91 cm, XP.

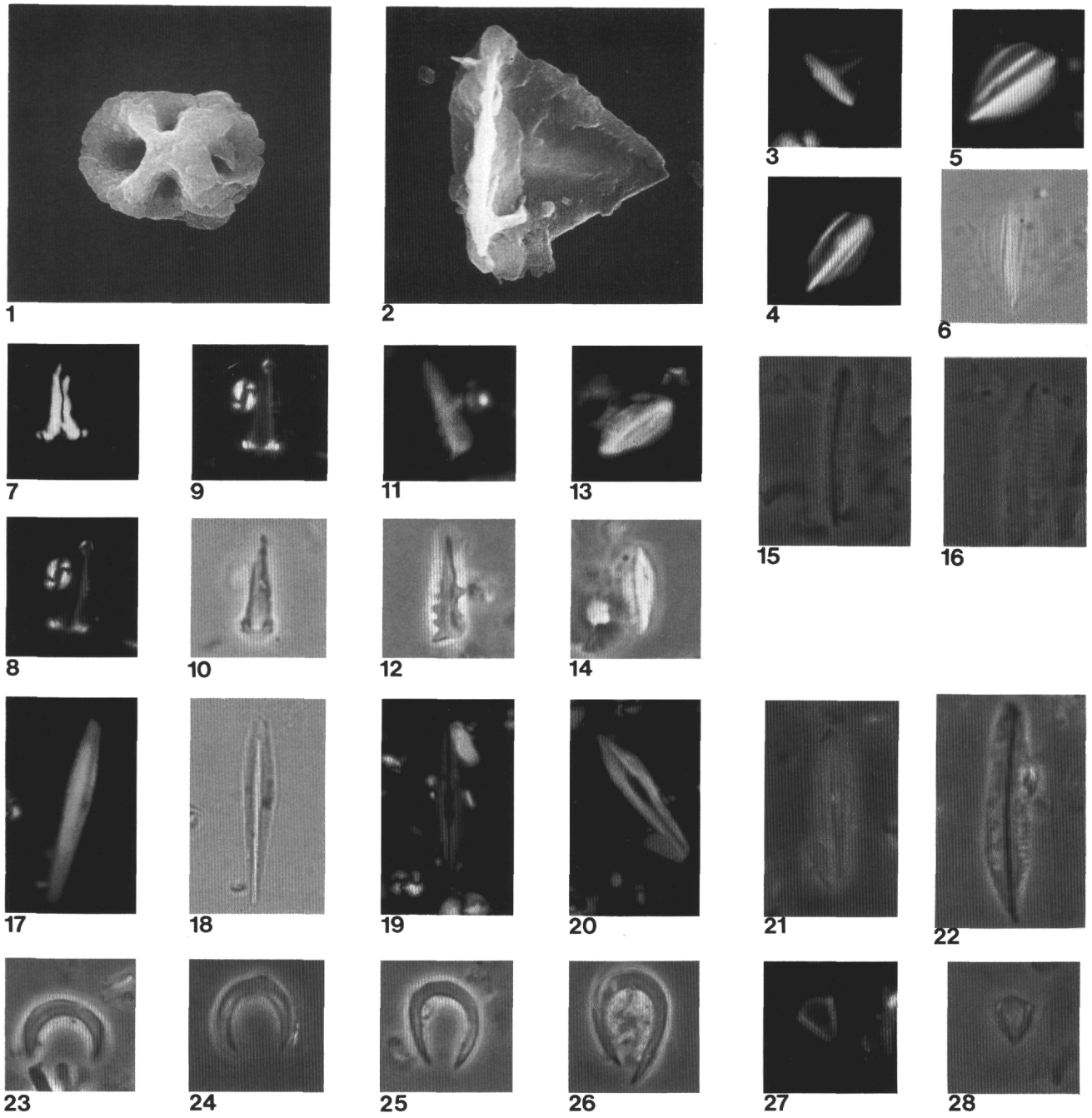

Plate 13. **1, 7.** *Zygrhablithus bijugatus* (Deflandre) Deflandre. (1) Top view, ×6000, Sample 149-900A-39R-3, 109 cm. (7) Sample 149-900A-53R-4, 11 cm, XP. **2, 3.**[TR] *Triquetrorhabdulus milowii* Bukry, Sample 149-900A-29R-1, 122 cm. (2) Side view, ×6000. (3) XP. **4-6.** *Triquetrorhabdulus challengeri* Perch-Nielsen. (4) Sample 149-898A-29R-3, 65 cm, XP. (5, 6) Sample 149-898A-25R-CC, 60 cm, XP (5) and Ph (6). **8-10.** *Zygrhablithus* sp. 1, Sample 149-898A-26R-1, 102 cm. (8) XP, low focus. (9) XP, high focus. (10) Ph. **11, 12.** *Triquetrorhabdulus serratus* (Bramlette and Wilcoxon) Olafsson, Sample 149-898A-22R-5, 86 cm, XP (11) and Ph (12). **13, 14.** *Triquetrorhabdulus rioi* Olafsson, XP, Sample 149-898A-19R-1, 106 cm, and Ph. **15, 16, 22.** *Triquetrorhabdulus rugosus* Bramlette and Wilcoxon. (15-16) Sample 149-900A-14R-5, 142 cm, XP (15) and Ph (16). (22) Sample 149-900A-15R-1, 87 cm, Ph. **17-21.** *Triquetrorhabdulus carinatus* Martini. (17, 18) Sample 149-898A-27R-5, 26 cm, XP (17) and Ph (18). (19-21) Sample 149-900A-12R-4, 15 cm; XP, 0° (19), XP, 45° (20), and Ph 21). **23, 24.** *Amaurolithus primus* (Bukry and Percival) Gartner and Bukry. (23) Sample 149-900A-12R-1, 112 cm, Ph. (24) Sample 149-900A-11R-CC, Ph. **25, 26.** *Amaurolithus delicatus* Gartner and Bukry. (25) Sample 149-900A-12R-1, 112 cm, Ph. (26) Sample 149-900A-12R-1, 48 cm, Ph. **27, 28.** *Minylitha convallis* Bukry, Sample 149-900A-14R-5, 142 cm, XP (27) and Ph (28).

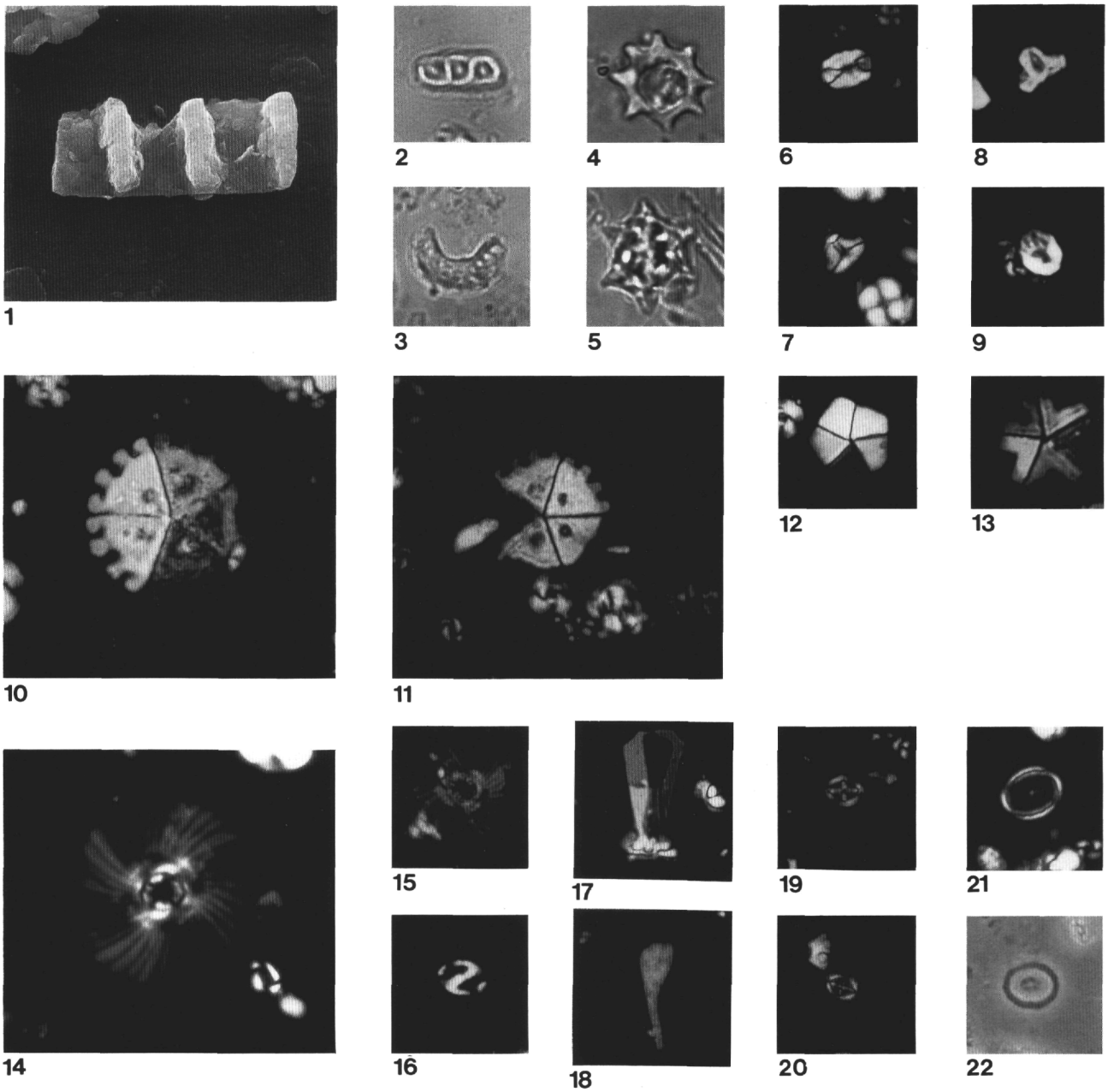

Plate 14. **1, 2.** *Isthmolithus recurvus* Martini. (1) Side view, ×6000, Sample 149-900A-51R-6, 47 cm. (2) Sample 149-900A-53R-1, 141 cm, PL. **3.** *Peritrachelina joidesa* Bukry and Bramlette, Sample 149-900A-52R-6, 14 cm, PL. **4.** *Corannulus germanicus* Stradner, Sample 149-900A-53R-1, 141 cm, PL. **5.** *Lithostromation operosum* (Deflandre) Bybell, Sample 149-900A-53R-1, 141 cm, PL. **6, 7.** *Lanternithus minutus* Stradner. (6) Sample 149-900A-53R-1, 141 cm, XP. (7) Sample 149-900A-53R-4, 91 cm, XP. **8, 9.** *Orthozygus aureus* (Stradner) Bramlette and Wilcoxon. (8) Sample 149-900A-53R-4, 91 cm, XP. (9) Sample 149-900A-44R-1, 131 cm, XP. **10, 11.** *Pemma papillata* Martini, Sample 149-900A-53R-2, 45 cm. (10) XP. (11) XP. **12.** *Braarudosphaera bigelowii* (Gran and Braarud) Deflandre, Sample 149-900A-53R-2, 45 cm, XP. **13.** *Micrantholithus aequalis* Sullivan, Sample 149-900A-53R-1, 141 cm, XP. **14, 15.** *Pedinocyclus larvalis* (Bukry and Bramlette) Loeblich and Tappan. (14) Sample 149-900A-53R-4, 91 cm, XP, ×2500. (15) Sample 149-900A-53R-6, 86 cm, XP. **16.** *Transversopontis obliquipons* (Deflandre) Hay, Mohler, and Wade, Sample 149-900A-53R-4, 91 cm, XP. **17-20.** *Bramletteius serraculoides* Gartner. (17) Sample 149-900A-53R-4, 91 cm, XP. (18) Sample 149-900A-53R-4, 91 cm, XP. (19) Sample 149-900A-53R-6, 86 cm; XP, 0°. (20) Sample 149-900A-53R-1, 141 cm; XP, 45°. **21, 22.** *Syracosphaera lamina* n. sp., holotype, ×1700, Sample 149-900A-27R-2, 72 cm, XP (21) and Ph (22).